Supplementary material to the EMEP Status Report 1/2017
Date: August 2017

METEOROLOGISK INSTITUTT
Norwegian Meteorological Institute

EMEP MSC-W model performance for acidifying and eutrophying components, photo-oxidants and particulate matter in 2015

EMEP/MSC-W:
Michael Gauss, Svetlana Tsyro and Hilde Fagerli

EMEP/CCC:
Anne-Gunn Hjellbrekke, Wenche Aas and Sverre Solberg

Supplementary material to EMEP Status Report 1/2017

Contents

CHAPTER 1

Introduction

This report is a supplement to the EMEP Status Report 1/2017 and presents a more detailed evaluation of the EMEP MSC-W model. This report is available from the EMEP website (www.emep.int).

The EMEP MSC-W model is evaluated with respect to acidifying and eutrophying components, photo-oxidants and particulate matter. Model results for 2015 are validated against measurements that have been collected from the EMEP monitoring network for 2015.

This year we present results from EMEP MSC-W model version rv4.15, which is slightly different from model version rv4.9, which was used for last year's evaluation. As last year, the meteorological input data are based on data from the ECMWF-IFS model. Recent changes in the EMEP MSC-W model code are described in Simpson et al. (2017). However, the most important novelty this year is the increase in resolution on which the model has been run, i.e. 0.1 x 0.1 degrees on a regular longitude-latitude grid (compared to 50 km x 50 km on a polar stereographic grid used until last year). This puts much stronger requirements not only on the parameterizations in the model itself, but also on the quality of the input data, such as emissions and meteorology. A more detailed account of model performance on different resolutions is given in (Solberg et al. 2017).

Tables of model skill and time series plots are presented in this report for different chemical species at individual EMEP measurement stations, along with scatter-plots and maps covering the EMEP domain.

As in previous evaluation reports, data from some measurement stations have been excluded from this evaluation for either of the following reasons:

- Problems have been identified in regard to the measurements (during Quality Control by EMEP-CCC).
- The measurement site is located in a mountain area, and the difference between its height above sea level and the mean elevation in the respective EMEP MSC-W model grid cell is larger than 500m.

The agreement between model results and observations depends on a combination of several factors - the measurement accuracy (sampling and analysis), the representativeness of the

measurement sites, the adequacy of emissions, and the model performance. Thus, any model underestimation or overestimation in the evaluation presented in the following chapters only implies that the modelled values are different from the observations, but is not necessarily an indication of model deficiency.

Chapter 2 deals with acidifiying and eutrophying components (sulphur and nitrogen species), Chapter 3 with photo-oxidants (ozone and nitrogen dioxide), and Chapter 4 with particulate matter.

References

D. Simpson, R. Bergström, H. Imhof, and P. Wind. Updates to the emep/msc-w model, 2016-2017. In *Transboundary particulate matter, photo-oxidants, acidifying and eutrophying components. EMEP Status Report 1/2017*. The Norwegian Meteorological Institute, Oslo, Norway, 2017.

S. Solberg, H. Fagerli, and S. Tsyro. Emep msc-w model runs using the emep emissions in fine resolution - comparison to observations. In *Transboundary particulate matter, photo-oxidants, acidifying and eutrophying components. EMEP Status Report 1/2017*. The Norwegian Meteorological Institute, Oslo, Norway, 2017.

CHAPTER 2

Acidifying and eutrophying components

In this chapter the EMEP MSC-W model is evaluated with respect to acidifying and eutrophying components. Section 2.1 includes an overview table of the model performance and scatter plots for acidifying and eutrophying components. In Section 2.2 we present time series plots for all EMEP stations with measurements in year 2015, while Section 2.3 contains combined maps of modelled and measured air concentrations and of concentrations in precipitation for selected species in 2015.

2.1 Scatter plots and tables

Evaluations of the EMEP MSC-W model performance for acidifying and eutrophying components have been presented earlier in numerous EMEP publications (e.g. Gauss et al. 2016, Gauss et al. 2015, Fagerli and Hjellbrekke 2008, Fagerli and Aas 2008).

In addition, an overview study of how the model performance has changed over the years was presented in Chapter 3 of EMEP Status Report 1/2013 (Simpson et al. 2013). The main conclusions of that study were:

- Year-to-year variations in evaluations of model performance can be large when all EMEP mearusements available are used. This is mainly caused by the varying number of measurement sies available from year to year. Futhermore, changes in instrumentation, protocols and personnel may influence the quality of measurements.
- Model performance varies strongly among pollutants.
- Model performance is (as expected) generally better for secondary than for primary pollutants;
- A more systematic evaluation is needed, with all inputs and observations held constant while the model version is changed, in order to identify key factors behind changes in model performance (benchmarking);

Component	N_{stat}	Obs.	Mod.	Bias (%)	RMSE	Corr.	IOA
NO_2 (μg(N) m^{-3})	65	1.88	1.29	-32	1.32	0.69	0.78
SO_2 (μg(S) m^{-3})	54	0.34	0.38	10	0.36	0.47	0.65
SO_4^{2-}, sea salt corrected (μg(S) m^{-3})	26	0.37	0.26	-29	0.19	0.86	0.83
SO_4^{2-}, including sea salt (μg(S) m^{-3})	33	0.44	0.37	-16	0.16	0.83	0.86
NO_3^- (μg(N) m^{-3})	20	0.28	0.35	26	0.19	0.79	0.81
HNO_3 (μg(N) m^{-3})	14	0.26	0.11	-60	0.52	0.09	0.26
NO_3^-+HNO_3 (μg(N) m^{-3})	38	0.47	0.56	18	0.15	0.90	0.91
NH_3 (μg(N) m^{-3})	16	0.58	0.72	25	0.38	0.90	0.90
NH_4^+ (μg(N) m^{-3})	19	0.56	0.50	-10	0.26	0.70	0.83
NH_3+NH_4^+ (μg(N) m^{-3})	32	1.27	1.53	21	1.07	0.74	0.79
SO_4^{2-} wd (μg(S)m^{-2})	51	8994	8026	-11	123	0.67	0.76
SO_4^{2-} cp (μg(S)l^{-1})	51	0.26	0.20	-23	0.15	0.75	0.80
NH_4^+ wd (μg(N)m^{-2})	51	13858	13586	-2	196	0.46	0.68
NH_4^+ cp (μg(N)l^{-1})	51	0.40	0.37	-7	0.21	0.50	0.71
NO_3^- wd (μg(N)m^{-2})	52	10312	9995	-3	122	0.65	0.81
NO_3^- cp (μg(N)l^{-1})	52	0.28	0.26	-8	0.11	0.72	0.83
precipitation (mm)	53	42324	46557	10	223	0.89	0.93

Table 2.1: Comparison of model results and observations for 2015. Annual averages over all EMEP sites with measurements. N_{stat}= number of stations, wd=wet deposition, cp= concentration in precipitation, Corr. = spatial correlation coefficient, RMSE = root mean square error, IOA = index of agreement.

Table 2.1 shows for each component the number of stations where measurements were available and data coverage criteria were satisfied (N_{stat}), measured yearly average over all stations (Obs), modelled yearly average over all stations (Mod), bias ($\frac{Mod-Obs}{Obs} \times 100\%$), correlation between observation and model for station yearly averages (Corr), root mean square error, Rmse ($\sqrt{\frac{1}{n}\sum_{i=1}^{n}(m_i - o_i)^2}$ where m_i and o_i are modelled and measured concentration at monitoring station *i*), and index of agreement (Willmott 1981, 1982). The index of agreement is calculated as follows: IOA= $1 - \frac{\sum_{i=1}^{N_{stat}}(m_i - o_i)^2}{\sum_{i=1}^{N_{stat}}(|m_i - Obs| + |o_i - Obs|)^2}$). It varies between 0 (theoretical minimum) and 1 (perfect agreement between observed and predicted values) and gives the degree to which model predictions are error free.

The scatter plots in Figures 2.1–2.3 are based on yearly averages of observed data at EMEP stations with measurements in 2015. The lines on the scatter plots display deviations in the scatter of 30% ('30% line') and 50% ('50% line') relative bias, respectively. Relative bias is defined here as $\frac{Mod-Obs}{0.5\,(Mod+Obs)} \times 100\%$, where 'Mod' refers to yearly averaged modelled concentrations, while 'Obs' refers to yearly averaged measured concentrations.

Sulphur dioxide in air

SO_2 has, on annual average, a slightly positive bias (10%) compared to measurements in 2015. In 2012, several modifications to reduce the overestimation during the cold season were implemented (Fagerli et al. 2012). One of these was improved seasonal variation of the emissions implying a 10% displacement per decade from winter to summer in the model (Simpson et al. 2012) to better account for the fact that nowadays a larger part of emissions is released during the summer time with increasing use of air condition, and more importantly, the growth of telecommunications and computer hardware use.

Figure 2.1(a) shows largest overestimations for SO_2 occurring at stations ES06, RU18, and IS02, and large underestimations at AT05, EE09, NO42 and some Spanish sites.

Sulphate in air

Figures 2.1(b)–2.1(c) show EMEP model results compared to measurements for, respectively, sea salt-corrected sulphate, and sulphate including sea salt. For comparisons with measurements including sea salt, 7% of the modelled sea salt[1] have been added to modelled suphate. The modelled and observed sulphate levels are in somewhat better agreement when sea salt sulphate is included, in particular the bias is smaller in this year's evaluation, but the correlation is slightly better for for sea salt corrected sulphate than for sulphate without sea salt (0.86 vs. 0.83). Both correlations are better than in last year's evaluation.

In 2012 a change in the scheme for the oxidation of SO_2 to SO_4^{2-} was implemented in the EMEP model (Fagerli et al. 2012, Simpson et al. 2012) resulting in higher oxidation rate and, consequently, less underestimation of sulphate concentrations in air. But the underestimation remains, as visible from the scatter plots.

Time series for sulphate in air are shown in Figures 2.12–2.18.

Nitrate and nitric acid in air

Measurements of airborne nitrate are expected to have a rather large uncertainty due to the very different physical characteristics of the compounds making up total nitrate. Whilst nitric acid is a spatially variable volatile gas with fast dry deposition, particulate nitrate dry deposits only slowly and hence concentrations are more determined by long range transport.

In Figure 2.2 we show scatter plots for total nitrate, particulate nitrate and nitric acid in air. Time series for total nitrate in air are shown in Figures 2.20–2.23.

Normally, the results for nitrate aerosol and nitric acid are somewhat worse than for total nitrate, because the monitoring data quality for these components are in general not as good as for total nitrate. The reason for this is that the individual concentrations of nitrate and nitric acid are biased when using the common filter-pack method. This has also been shown in the evaluation of the EMEP model performance for nitrogen compounds using intensive measurement data from two sampling periods, June 2006 and January 2007 (Fagerli and Aas 2008).

In this year's model results, HNO_3 is underestimated by 60%, while NO_3^- is overestimated by 26%. The sum of NO_3^-+HNO_3 is overestimated by 18%. The spatial correlation is 0.79 for nitrate aerosol (Corr = 0.81), slightly better for the sum of aerosol and gas (Corr = 0.90), but very low for nitric acid (Corr = 0.09). The correlation for the sum of aerosol and gas is

[1] Sea salt is assumed to consist of approximately 7% sulphate.

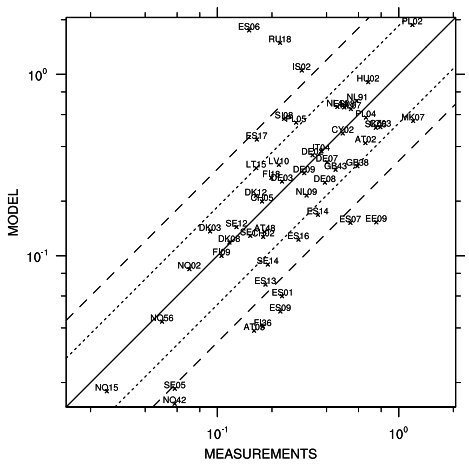

(a) SO_2

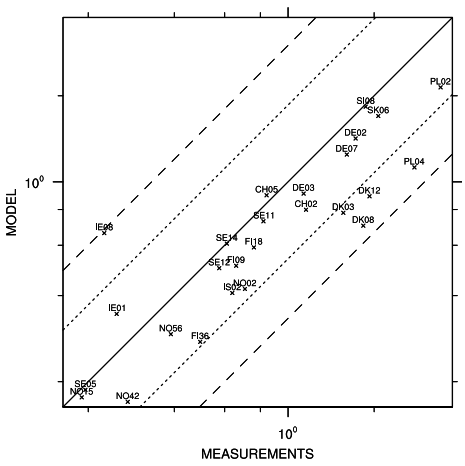

(b) SO_4^{2-}, measurements corrected for sea salt

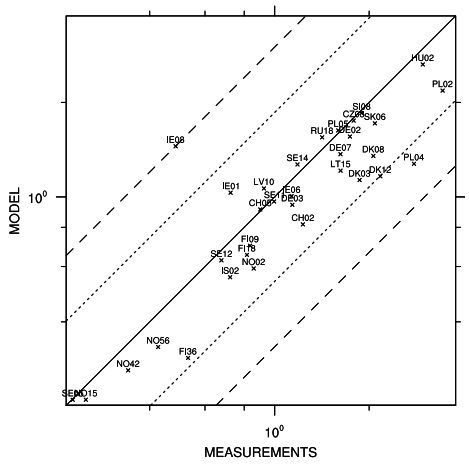

(c) SO_4^{2-}, including sea salt SO_4^{2-}

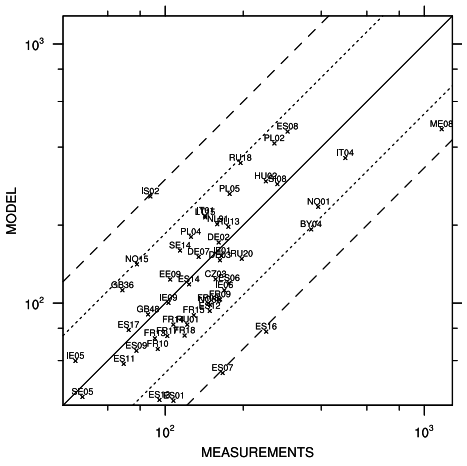

(d) SO_4^{2-} wet dep.

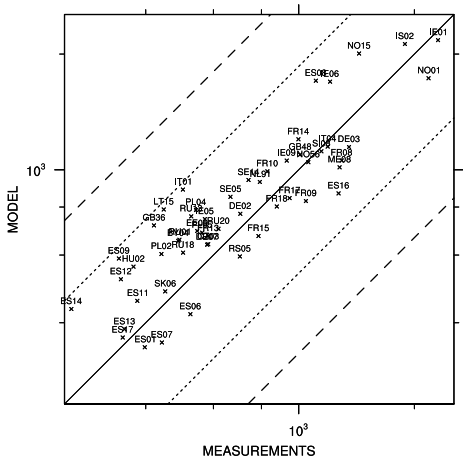

(e) Precipitation

Figure 2.1: Scatter plots of model results versus observations of a) sulphur dioxide [μg(S) m^{-3}], b+c) sulphate [μg(S) m^{-3}], d) wet deposition of sulphur [μg(S)m^{-2}], and e) precipitation [mm]. For sulphate concentrations, panel (b) shows a comparison of model results to sea salt corrected sulphate measurements, while panel (c) shows model results of sulphate plus 7 % sea salt in comparison to non-corrected measurement data.

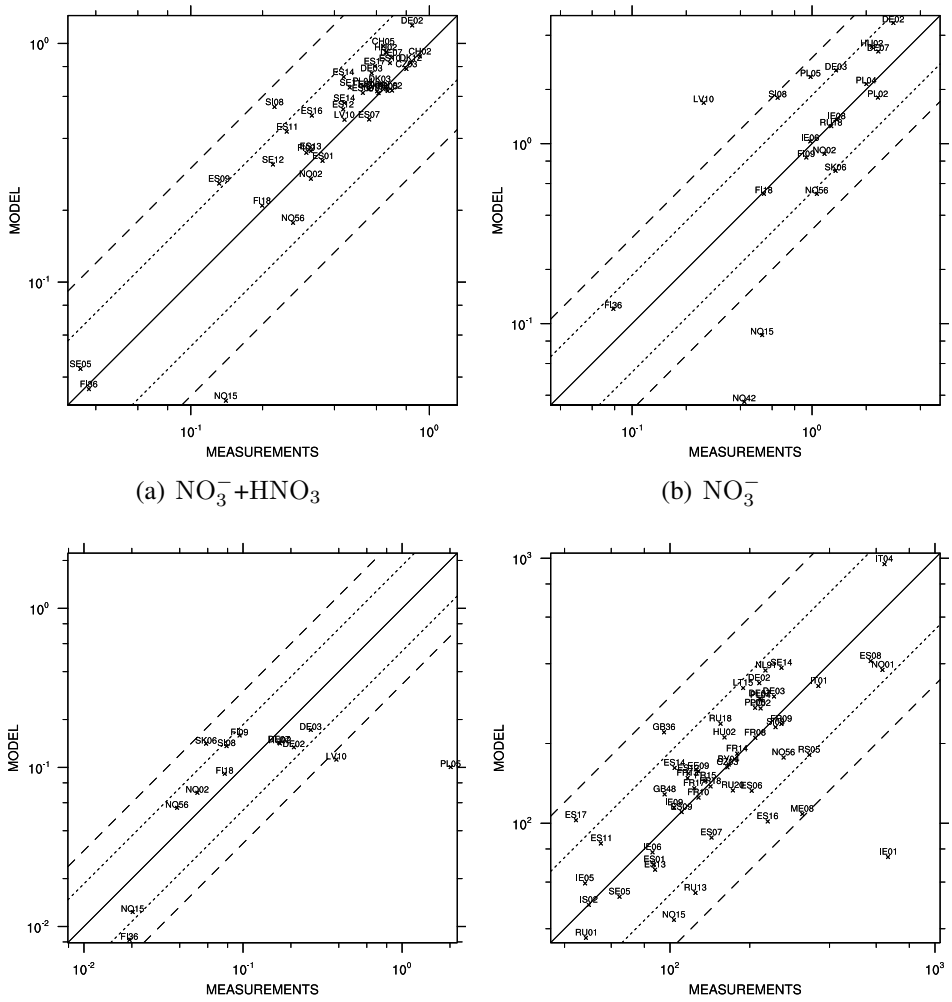

(a) NO_3^-+HNO_3 (b) NO_3^-

(c) HNO_3 (d) NO_3^- wet dep.

Figure 2.2: Scatter plots of modelled versus observed concentrations of total nitrate, nitrate aerosol, nitric acid [μg(N) m^{-3}] and wet deposition of oxidized nitrogen [μg(N)m^{-2}].

better this year than it was last year, while the other scores have become worse. However, one should keep in mind that the stations used in the comparison for the different components are not exactly the same, thus the results are only indicative and not strictly comparable.

Ammonia and ammonium aerosol in air

In order to evaluate the model performance for NH_x (NH_3+NH_4^+) properly, ammonia and ammonium should be studied separately. However, the number of measurements for 2014 where the gaseous and particle phase are analyzed both separately and at the same time is limited, e.g. NH_3 measurements are available only from 16 sites (although this is a increase by 3 stations since last year).

In earlier evaluations, individual results for NH_3 and NH_4^+ used to be somewhat worse than for total reduced nitrogen (NH_x), because the monitoring data quantity and quality for these components are in general not as good as for NH_3+NH_4^+.

In this year's evaluation, the RMSE for the sum is higher than for the individual components, and the correlation is lower than for NH_3 individually.

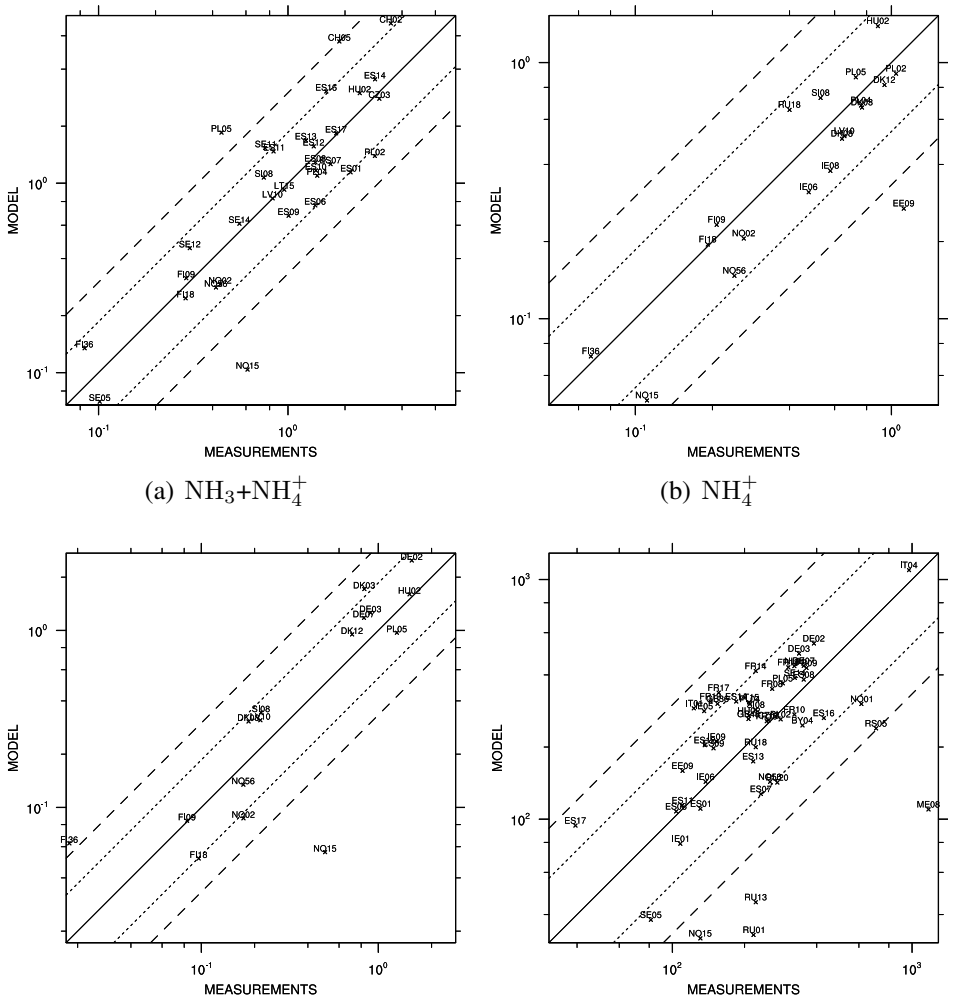

(a) NH_3+NH_4^+ (b) NH_4^+

(c) NH_3 (d) NH_4^+ wet dep.

Figure 2.3: Scatter plots of modelled versus observed concentrations of total ammonium+ammonia, aerosol ammonium and ammonia in air [μg(N) m^{-3}] and wet deposition of reduced nitrogen [μg(N)m^{-2}].

The modelled yearly averages of the concentrations of ammonia, ammonium and the sum of ammonia and ammonium have biases of 25%, -10% and 21%, respectively, compared to the monitoring data. The spatial correlations for NH_3 is very high (0.90) and higher than last year, while the correlations for NH_4^+ and the sum are somwhat lower than last year (0.7 and 0.74, respectively).

Scatter plots for modelled versus measured concentrations for total ammonium+ammonia, aerosol ammonium and ammonia in air in 2015 are presented in Figures 2.3(a), 2.3(b) and 2.3(c), respectively, while time series for NH_3+NH_4^+ are shown in Figures 2.25–2.28.

Concentrations in precipitation / wet depositions

The ability of the model to predict concentrations in precipitations and wet depositions is limited by the accuracy of the precipitation fields used in the model. The precipitation field pattern is very patchy (e.g. influenced by local topographic effects), and the regional scale model is unable to resolve this sub grid scale distribution. A typical problem arises with small

scale showers. In reality precipitation is high in a small area of a given grid, but a large fraction of the grid should remain dry. Within the model, however, this precipitation is averaged out to cover the whole grid at a lower intensity. Thus, even though average precipitation amounts may be simulated well, the model experiences precipitation more often, but in lower amounts than in reality. On a shorter time scale, e.g on daily basis, this may lead to too high concentrations in precipitation for episodes when it rains only in a small part of the grid square. For a regional scale model it is more sensible to compare the bulk concentrations, i.e the sum of the wet deposited compounds divided by the sum of precipitation.

The correlation between model and measurements for concentrations in precipitation and wet depositions will to a large extent depend on the model precipitation field.

A scatter plot for modelled versus observed precipitation is shown in Figure 2.1(e). On average, the observed and modelled precipitation is similar (bias=10%) and the spatial correlation coefficient is high (0.89). This also contributes to the relatively good model performance in terms of reduced nitrogen and sulphur in precipitation (low biases and good correlations).

Scatter plots for modelled versus observed wet depositions of sulphur, oxidized nitrogen and reduced nitrogen are shown in Figures 2.1(d), 2.2(d) and 2.3(d), respectively. The overall performance is good, althoug some outliers are visible, e.g. IE01 for NO_3^- in precipitation.

Time series for wet deposition of sulphur, oxidized nitrogen and reduced nitrogen are shown in Figures 2.29–2.34, Figures 2.35–2.40 and Figures 2.41–2.46, respectively.

2.2 Time series

In this section we present time series plots for a selection of stations that have supplied data on acidifying and eutrophying components to EMEP CCC for 2015. The plots show daily model results and measurements, where available. Time series for sulphur dioxide in air are shown in Figures 2.4–2.11, for sulphate in air in Figures 2.12–2.19, for total nitrate in air in Figures 2.20–2.24 and for ammonia+ammonium in air in Figures 2.25–2.28. In addition, time series are shown for wet deposition of sulphur, oxidized nitrogen and reduced nitrogen in Figures 2.29–2.34, Figures 2.35–2.40 and Figures 2.41–2.46, respectively.

After communication with the providers of measurements (via CCC), specific comments about selected stations are added here for reference:

- NO15 (Tustervatn): measured sulphate in precipitation on 11 August was high, all data on this day were flagged invalid;
- ME08 (Zabljak):sulphate in precipitation had one high value on 20 July, which did not impact the deposition due to low precipitation amount, all data in this sample were deleted;
- CH01 (Jungfraujoch): High SO_2 concentrations on 8 December with air from North North East, with advection of air masses at high altitudes. A similar episode occurred in late 2015 as well;
- RU18 (Danki): Low SO_2 concentrations in comparison to the model, but no reasons have been identified for discarding these data;
- NO02 (Birkenes II): High SO_2 concentrations on 9 March due to advection from South-West. The peak is higher than what we usually see during LRT events in recent years, but no reasons have been identified for discarding these data;

- NO02 (Birkenes II): High sulphate concentrations in the period 13-20 October, with a peak on the 15th with also very high nitrate levels, due to air masses from South East;
- AM01 (Amberd): Very low measured SO_2 concentrations compared to the model, this is consistent with earlier years and the time variability is in better agreement. However, the data coverage for sulphur dioxide is relatively low (lower than 75%).

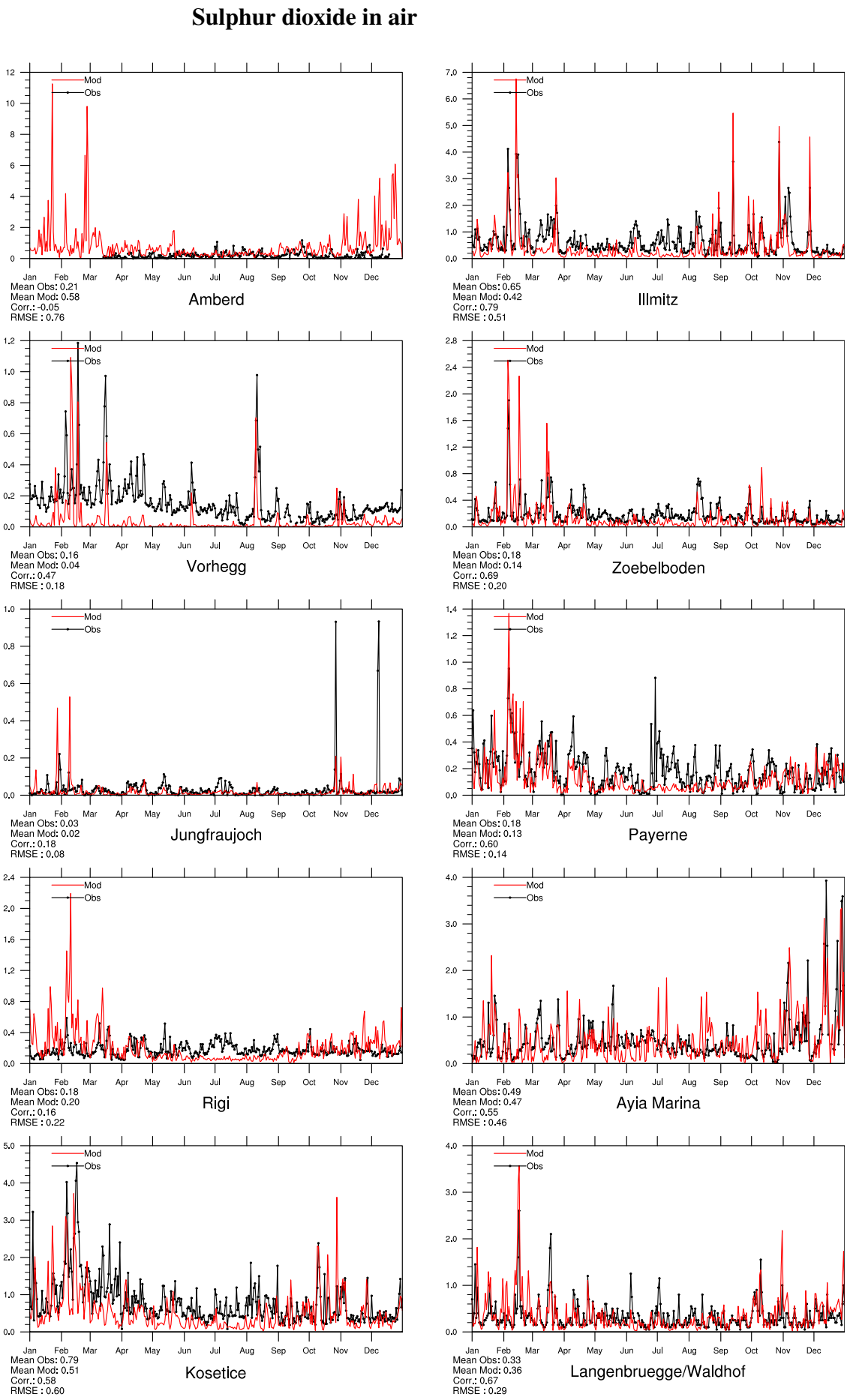

Figure 2.4: Comparison of model results and measurements (daily) for SO_2 in air [ugS] for stations that have measured SO_2 in 2015.

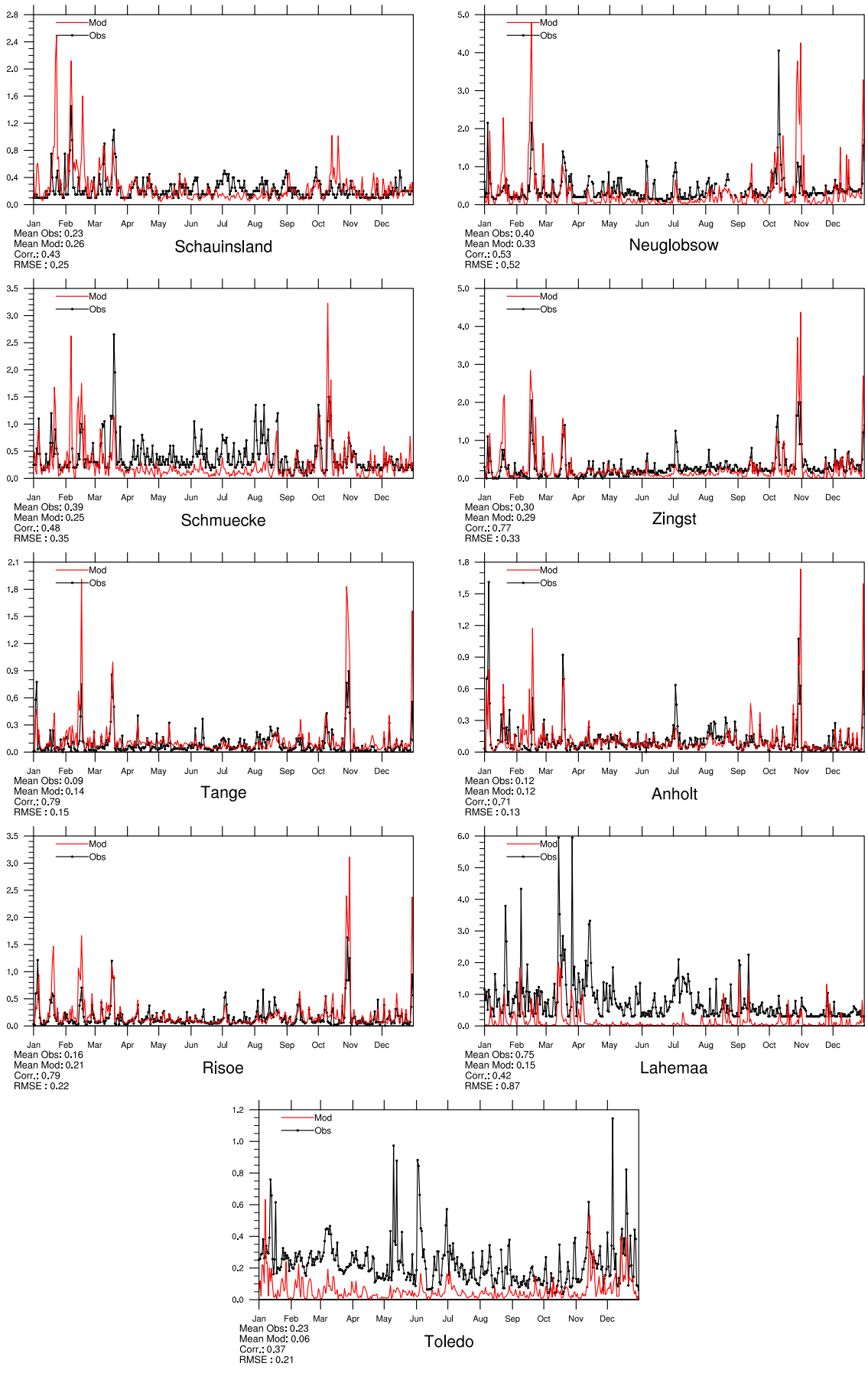

Figure 2.5: Comparison of model results and measurements (daily) for SO_2 in air [ugS] for stations that have measured SO_2 in 2015.

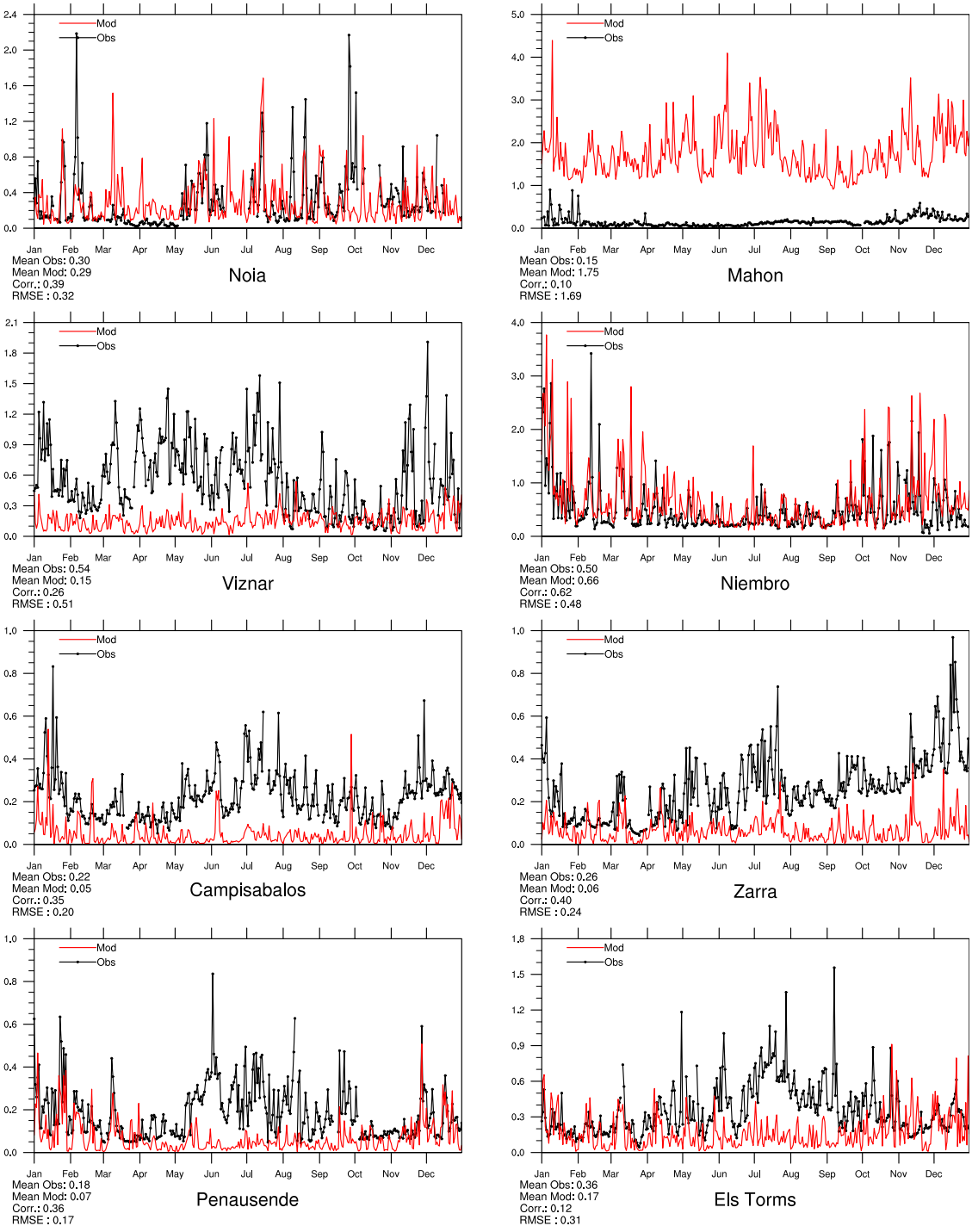

Figure 2.6: Comparison of model results and measurements (daily) for SO_2 in air [ugS] for stations that have measured SO_2 in 2015.

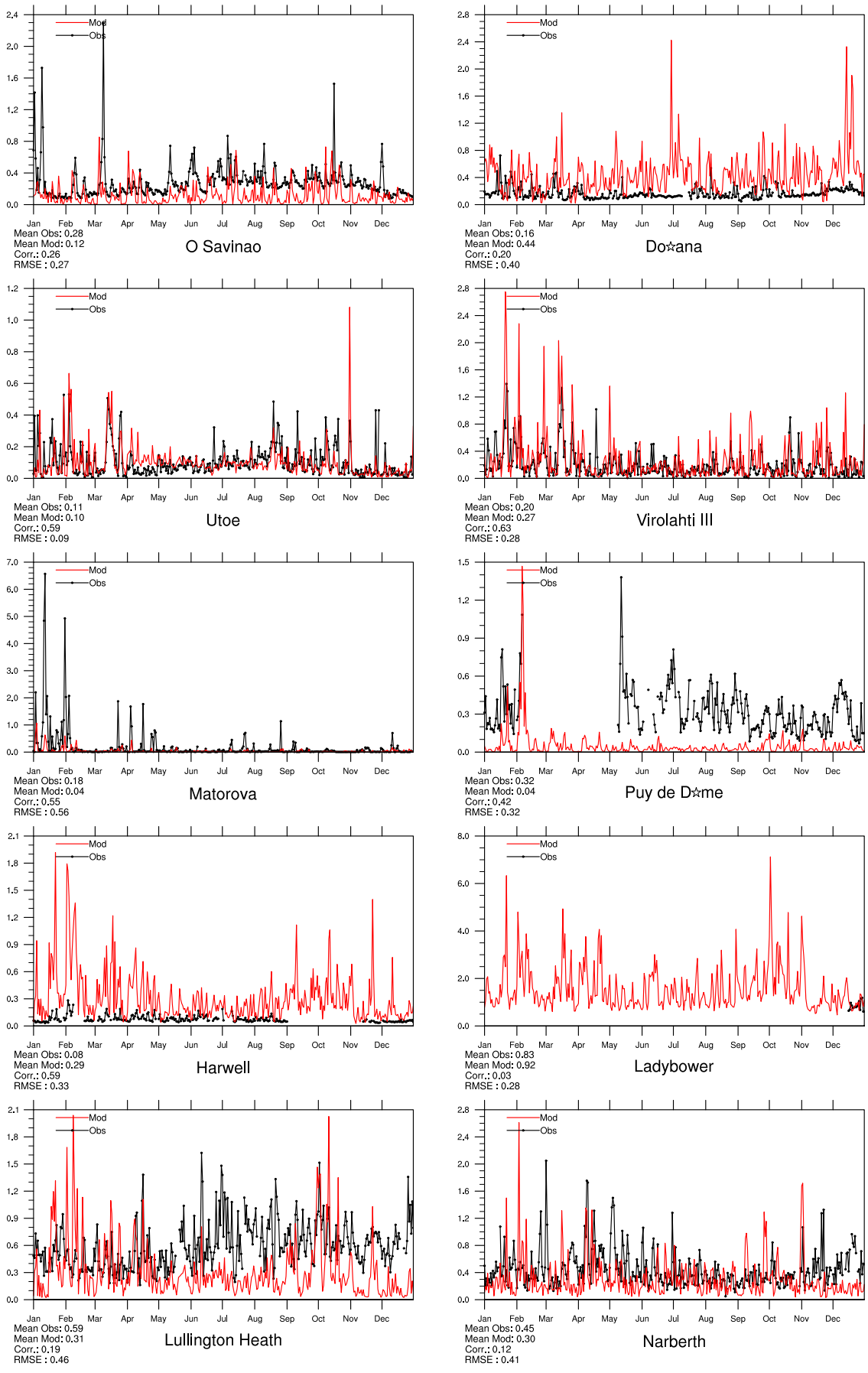

Figure 2.7: Comparison of model results and measurements (daily) for SO_2 in air [ugS] for stations that have measured SO_2 in 2015.

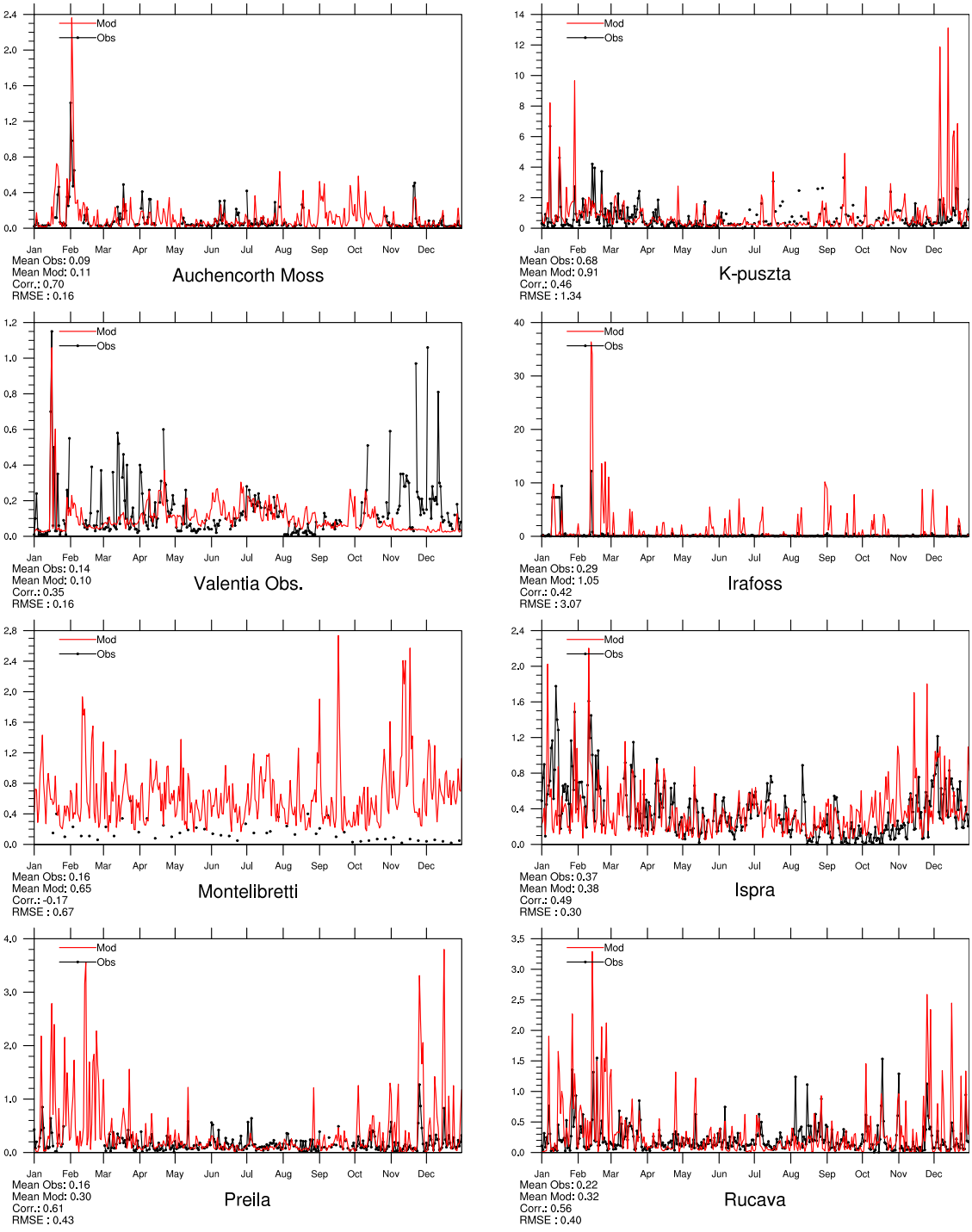

Figure 2.8: Comparison of model results and measurements (daily) for SO_2 in air [ugS] for stations that have measured SO_2 in 2015.

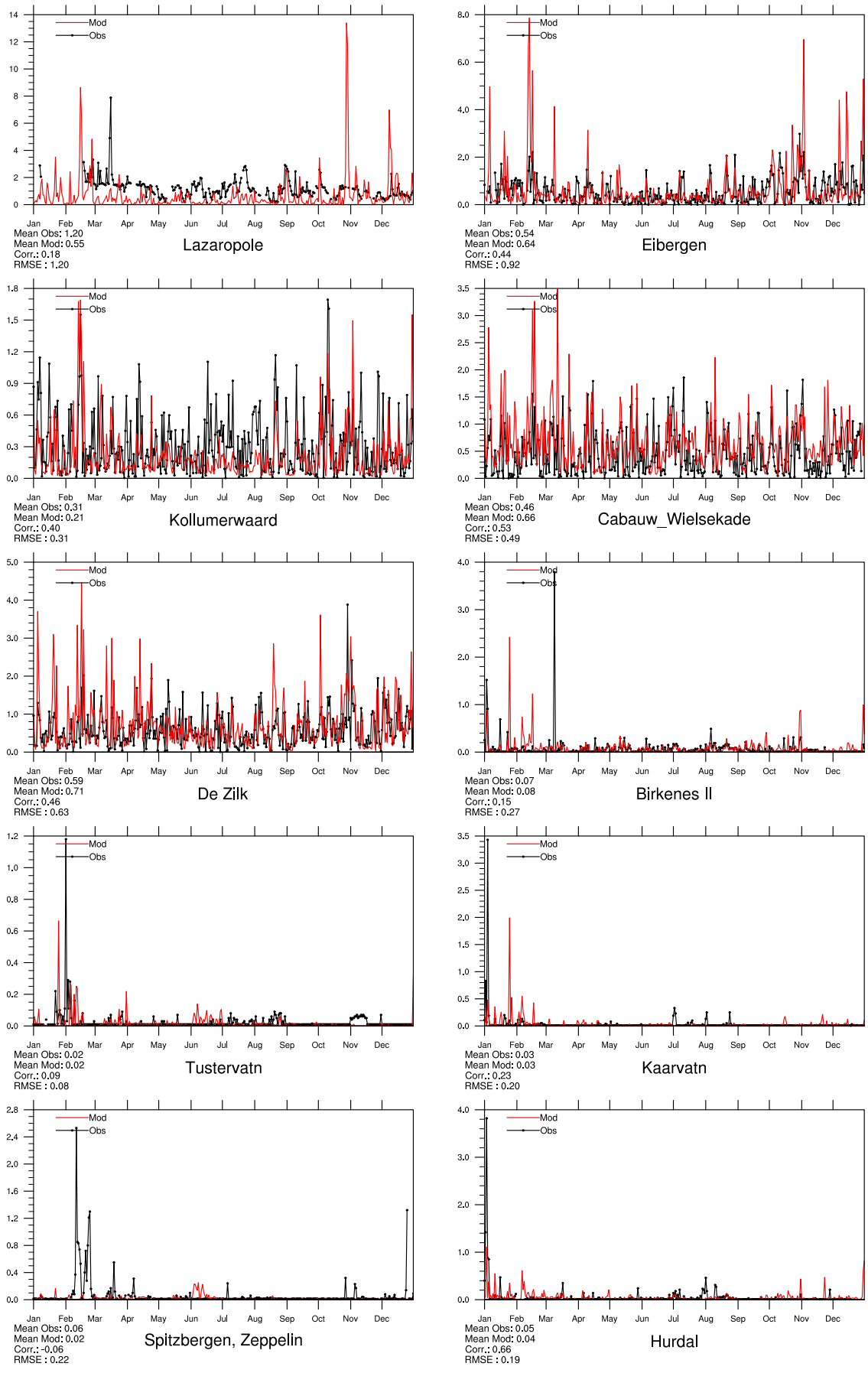

Figure 2.9: Comparison of model results and measurements (daily) for SO_2 in air [ugS] for stations that have measured SO_2 in 2015.

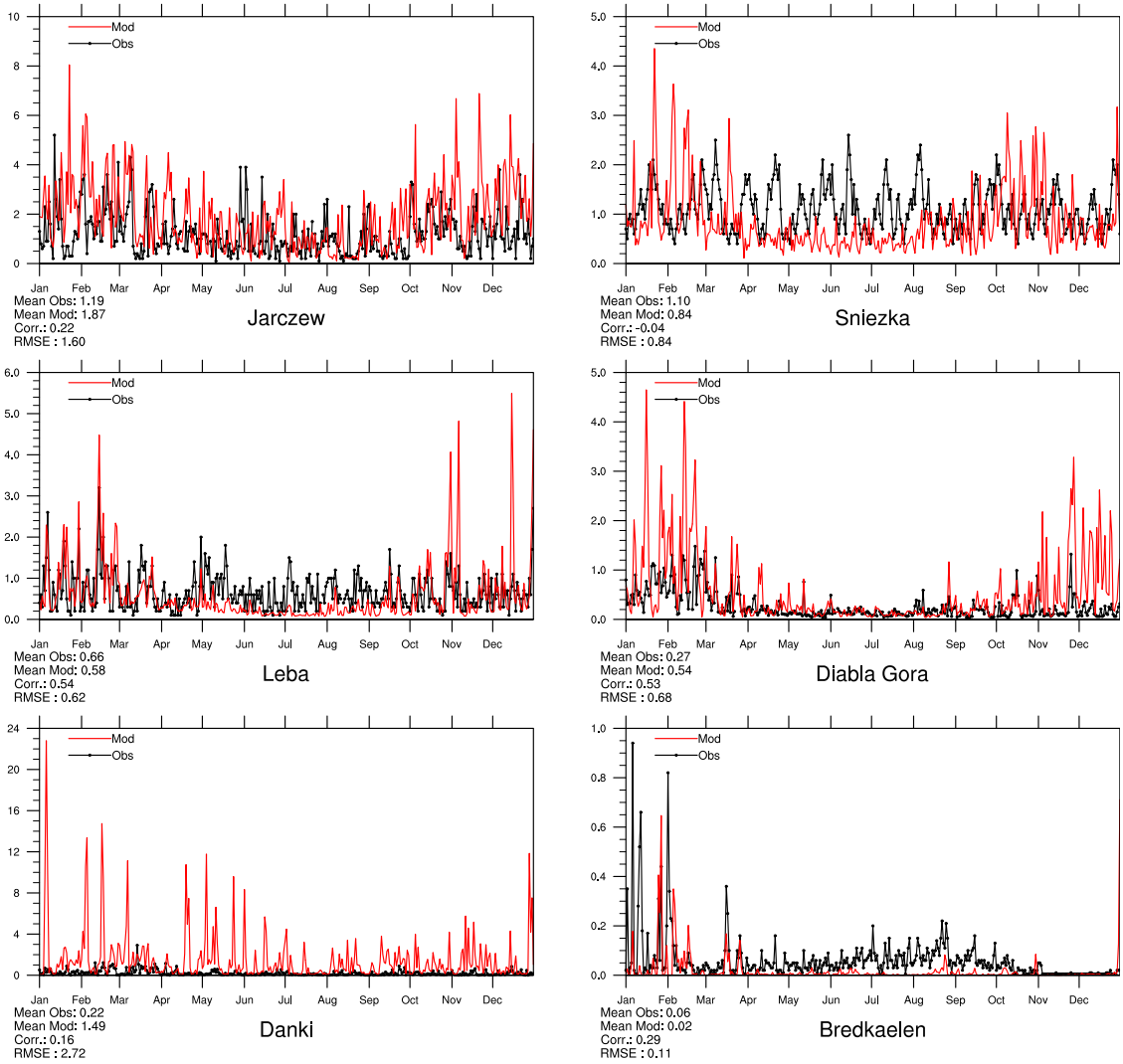

Figure 2.10: Comparison of model results and measurements (daily) for SO_2 in air [ugS] for stations that have measured SO_2 in 2015.

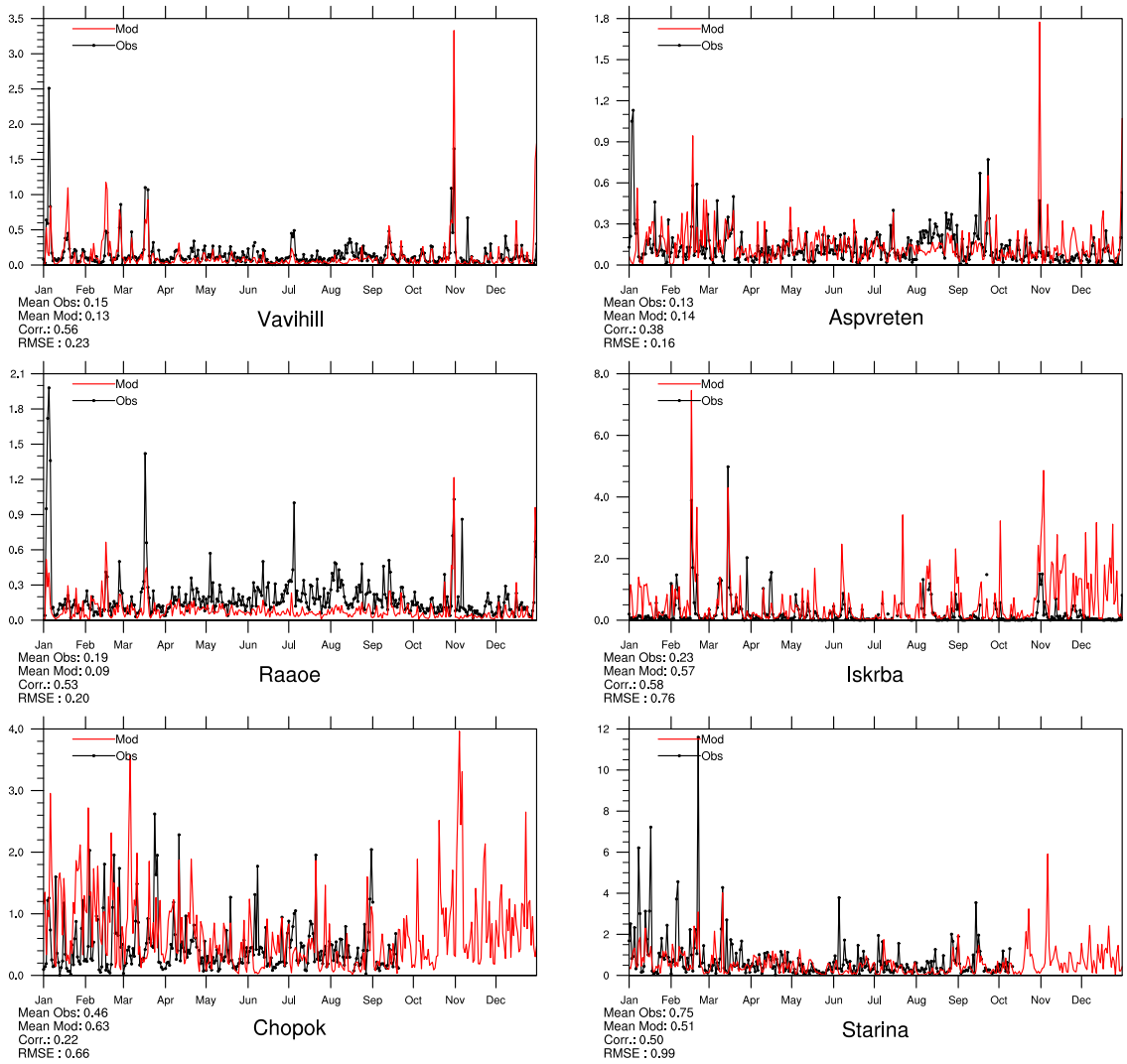

Figure 2.11: Comparison of model results and measurements (daily) for SO_2 in air [ugS] for stations that have measured SO_2 in 2015.

Sulphate in air – sea salt corrected

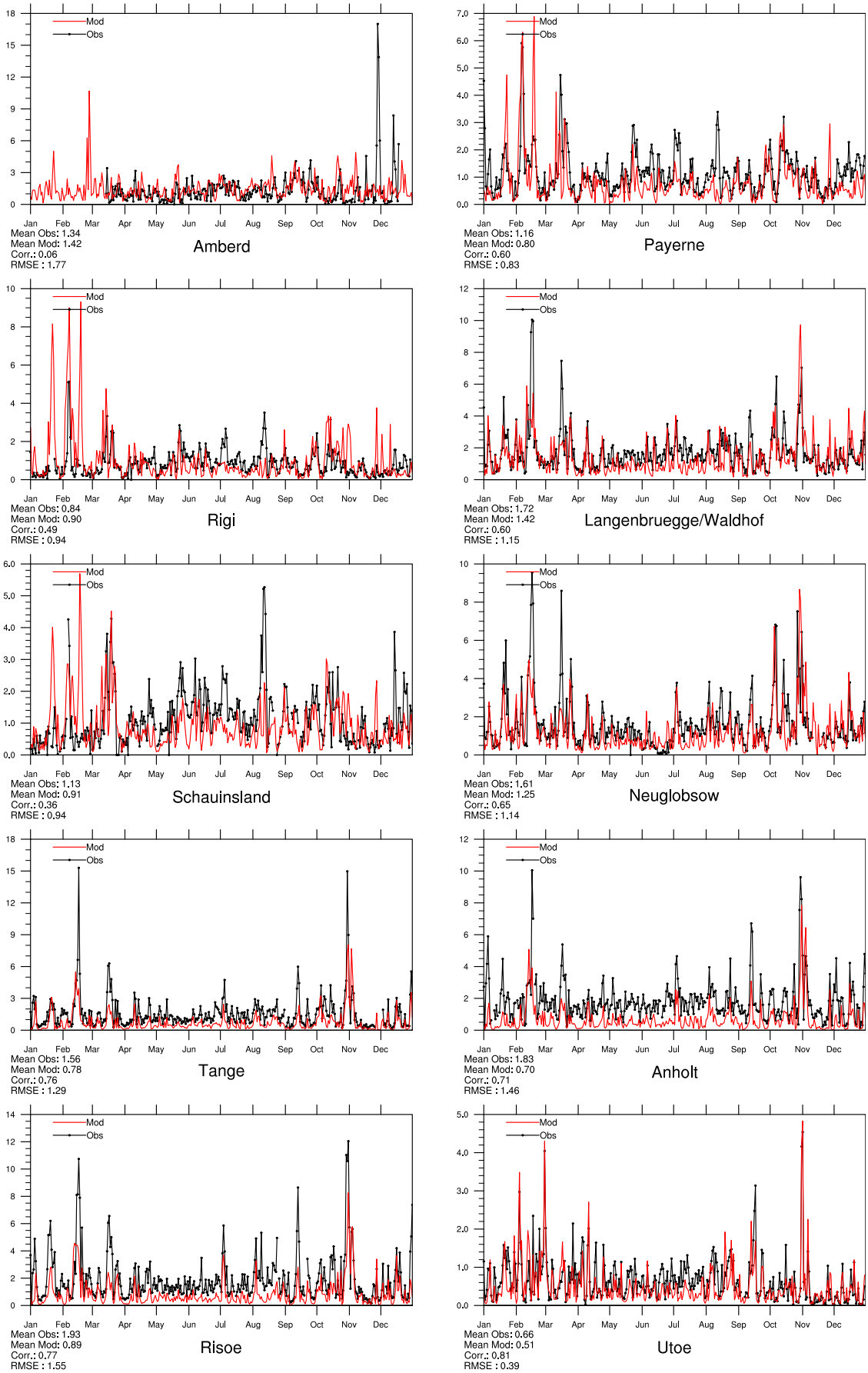

Figure 2.12: Comparison of model results and measurements (daily) for sea salt corrected sulphate in air [ugS] for stations that have measured sulphate in 2015.

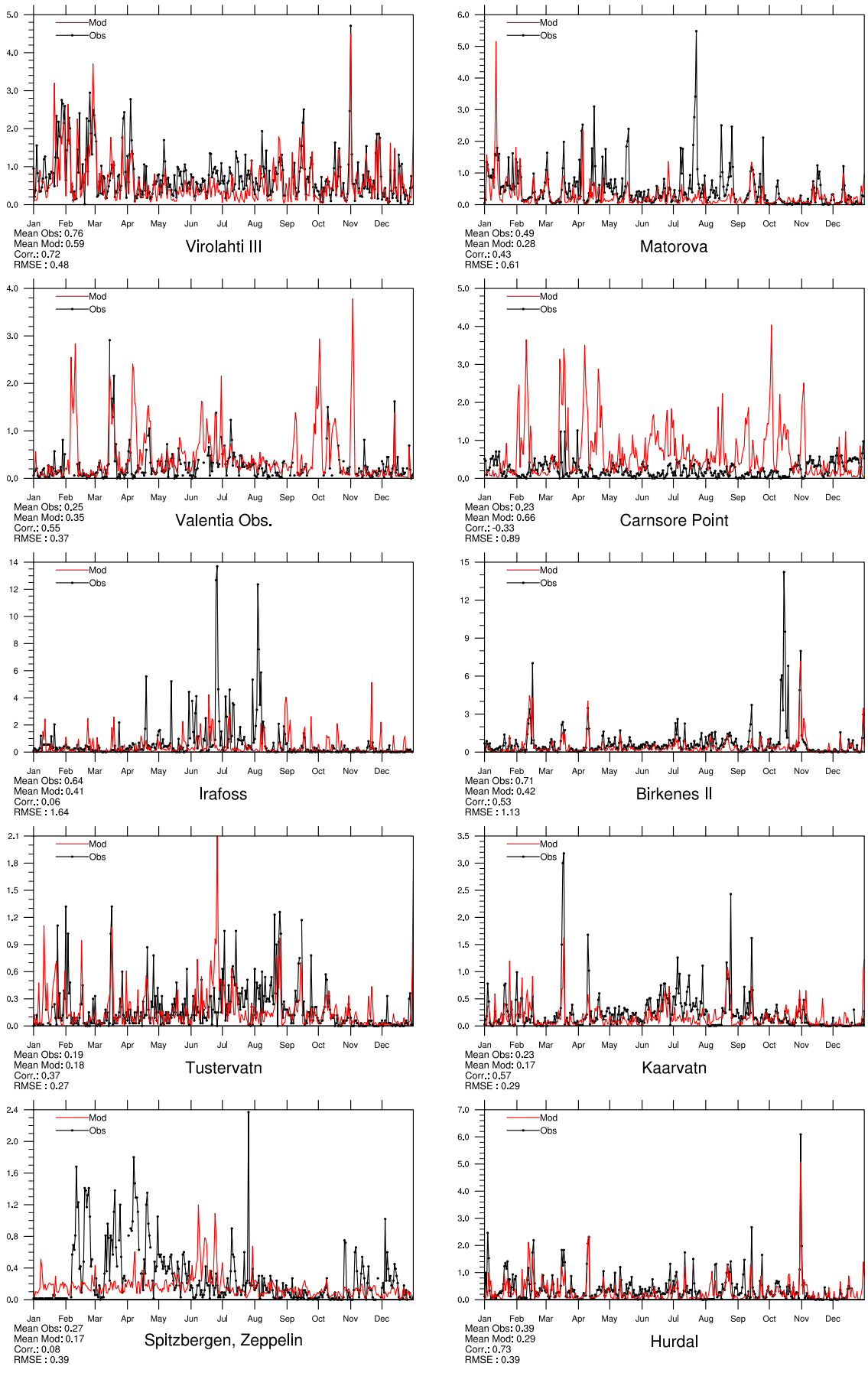

Figure 2.13: Comparison of model results and measurements (daily) for sea salt corrected sulphate in air [ugS] for stations that have measured sulphate in 2015.

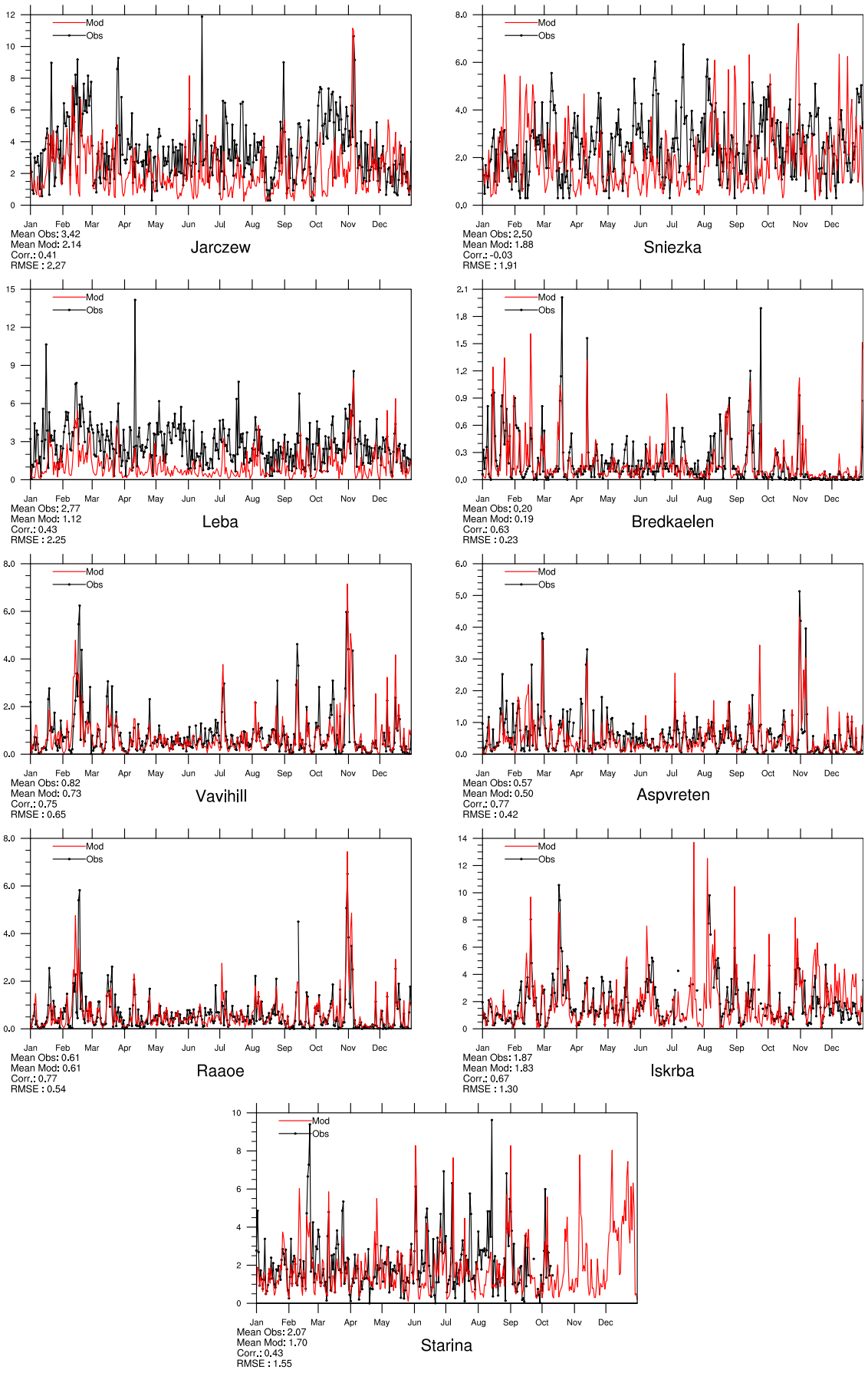

Figure 2.14: Comparison of model results and measurements (daily) for sea salt corrected sulphate in air [ugS] for stations that have measured sulphate in 2015.

Sulphate in air – sea salt included

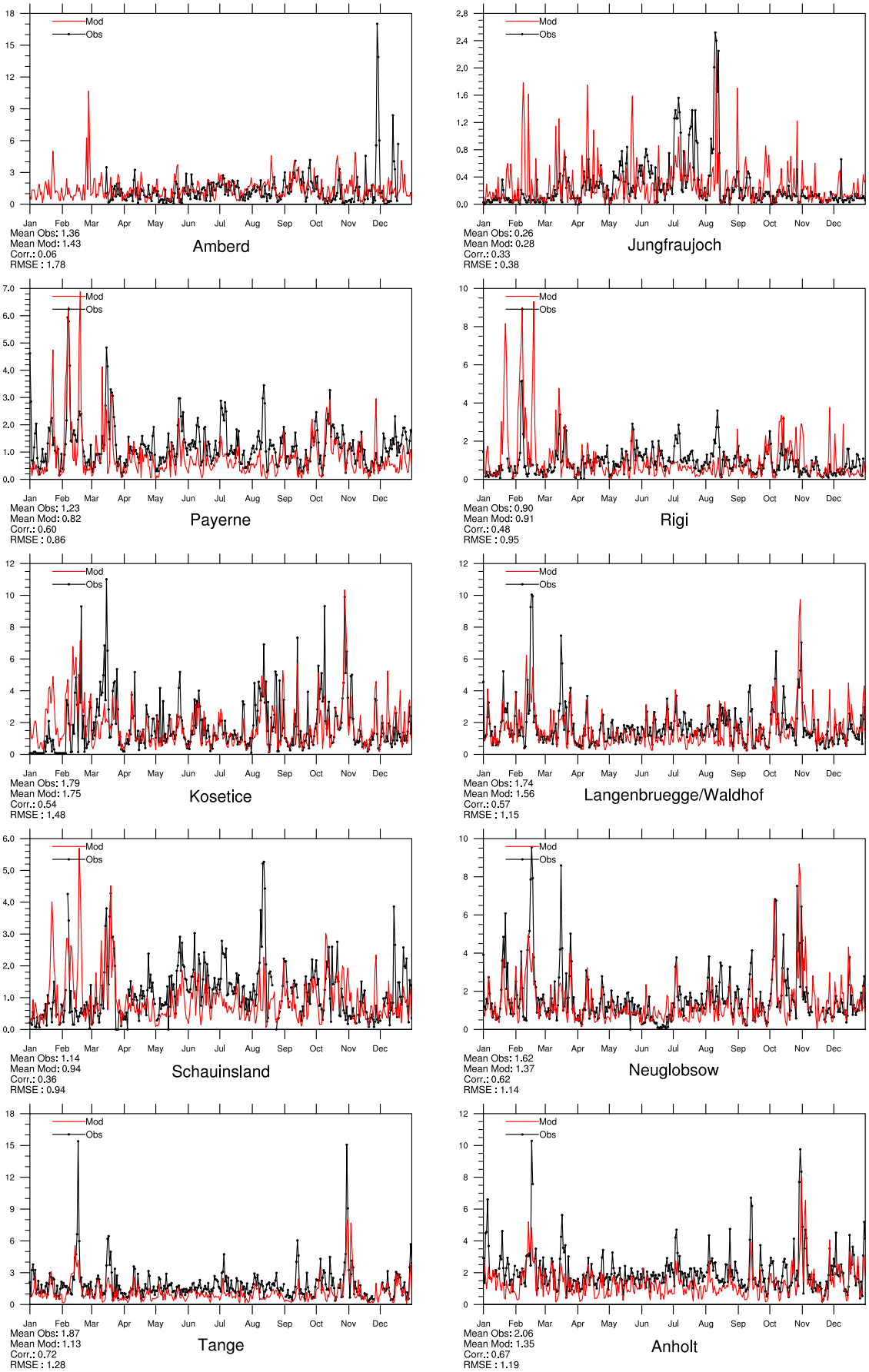

Figure 2.15: Comparison of model results and measurements (daily) for sulphate (including sea salt) in air [ugS] for stations that have measured sulphate in 2015.

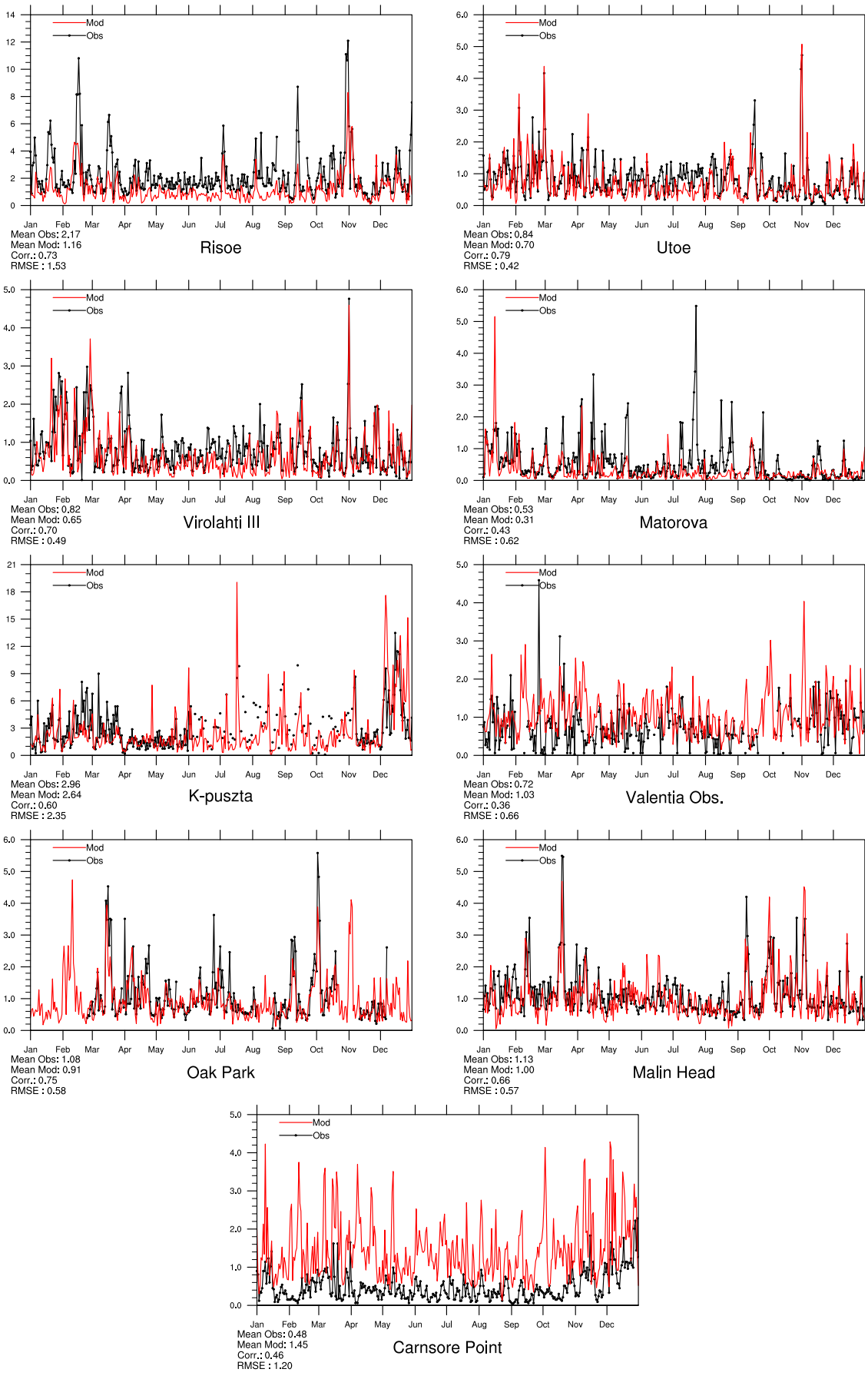

Figure 2.16: Comparison of model results and measurements (daily) for sulphate (including sea salt) in air [ugS] for stations that have measured sulphate in 2015.

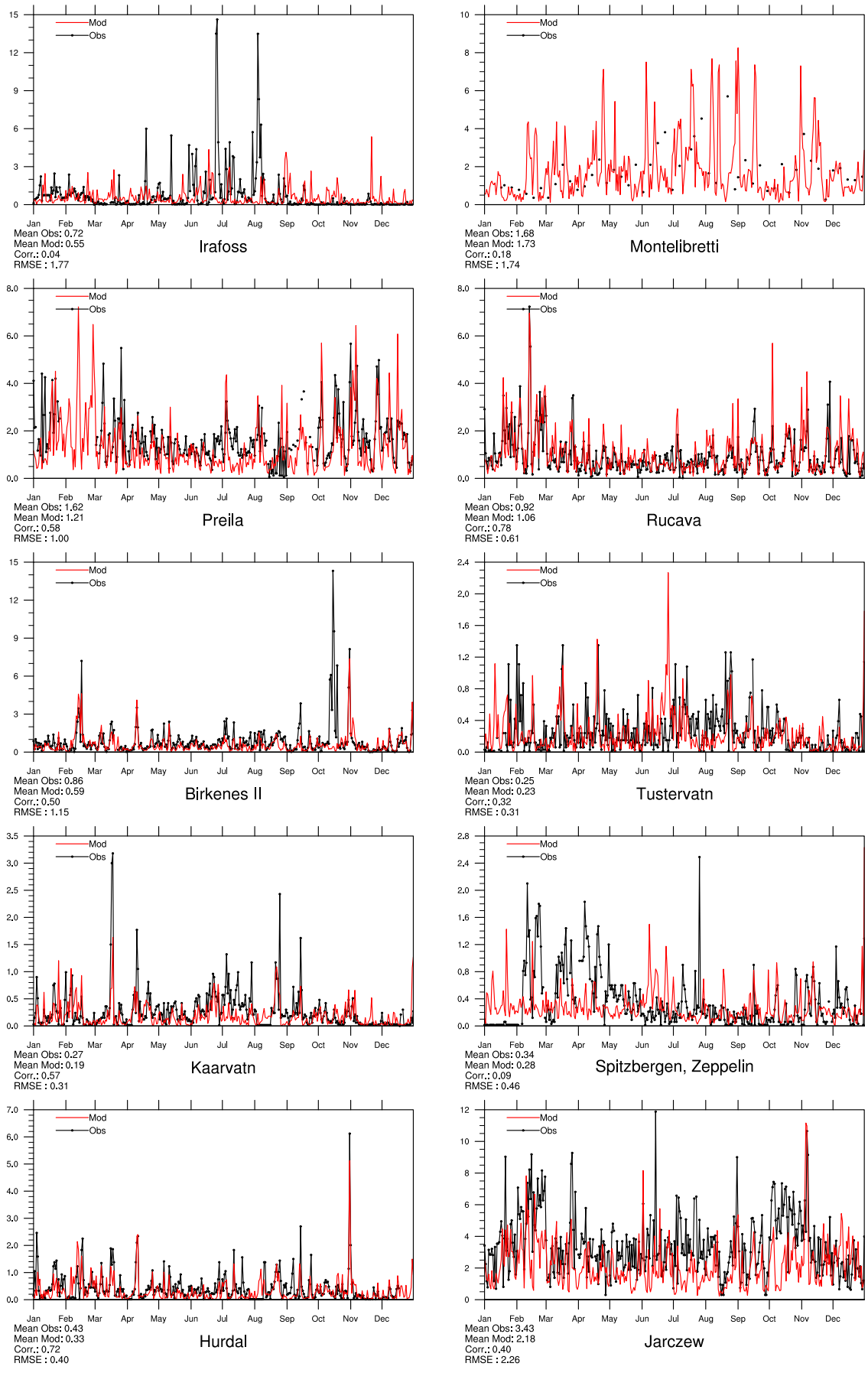

Figure 2.17: Comparison of model results and measurements (daily) for sulphate (including sea salt) in air [ugS] for stations that have measured sulphate in 2015.

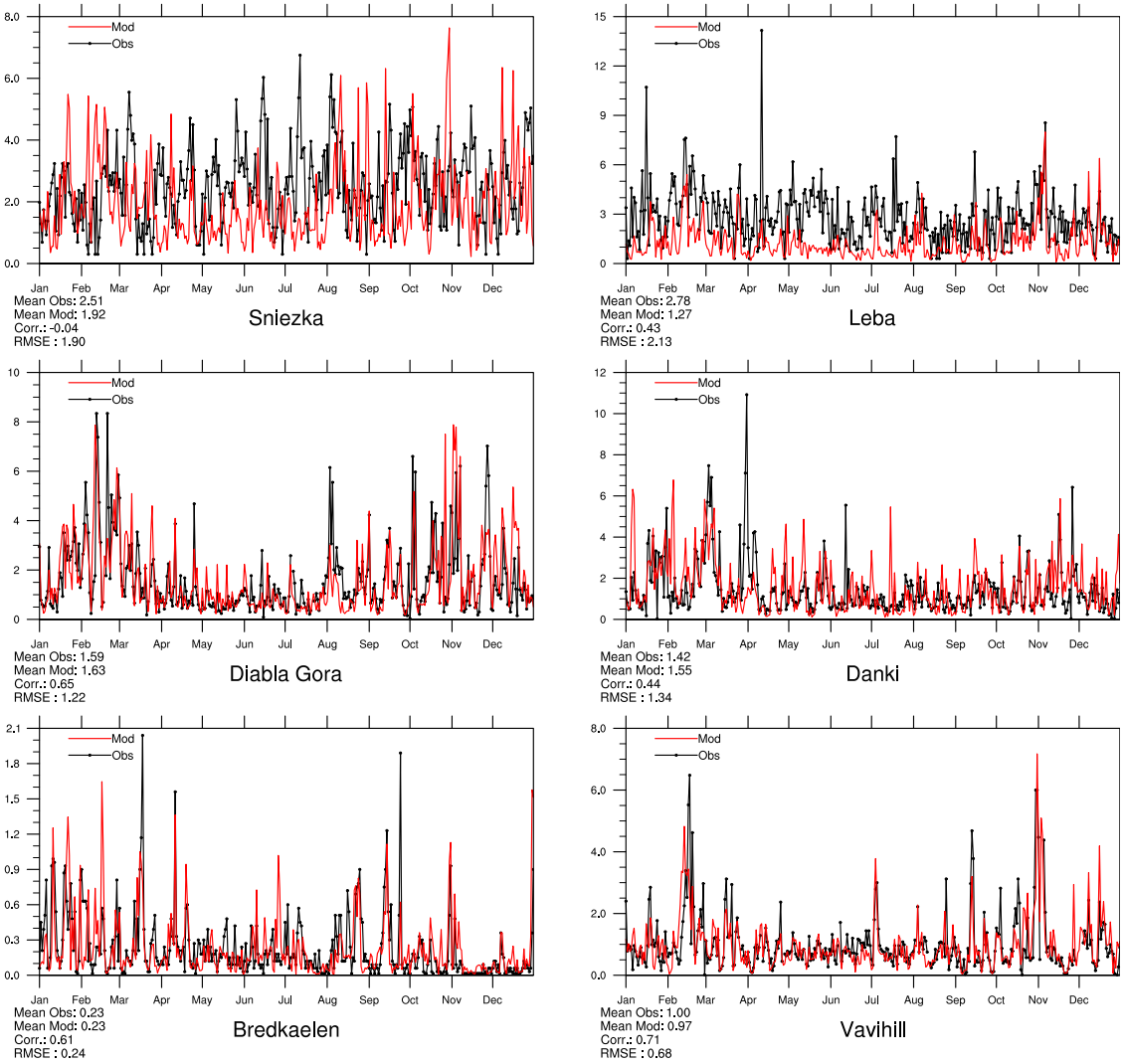

Figure 2.18: Comparison of model results and measurements (daily) for sulphate (including sea salt) in air [ugS] for stations that have measured sulphate in 2015.

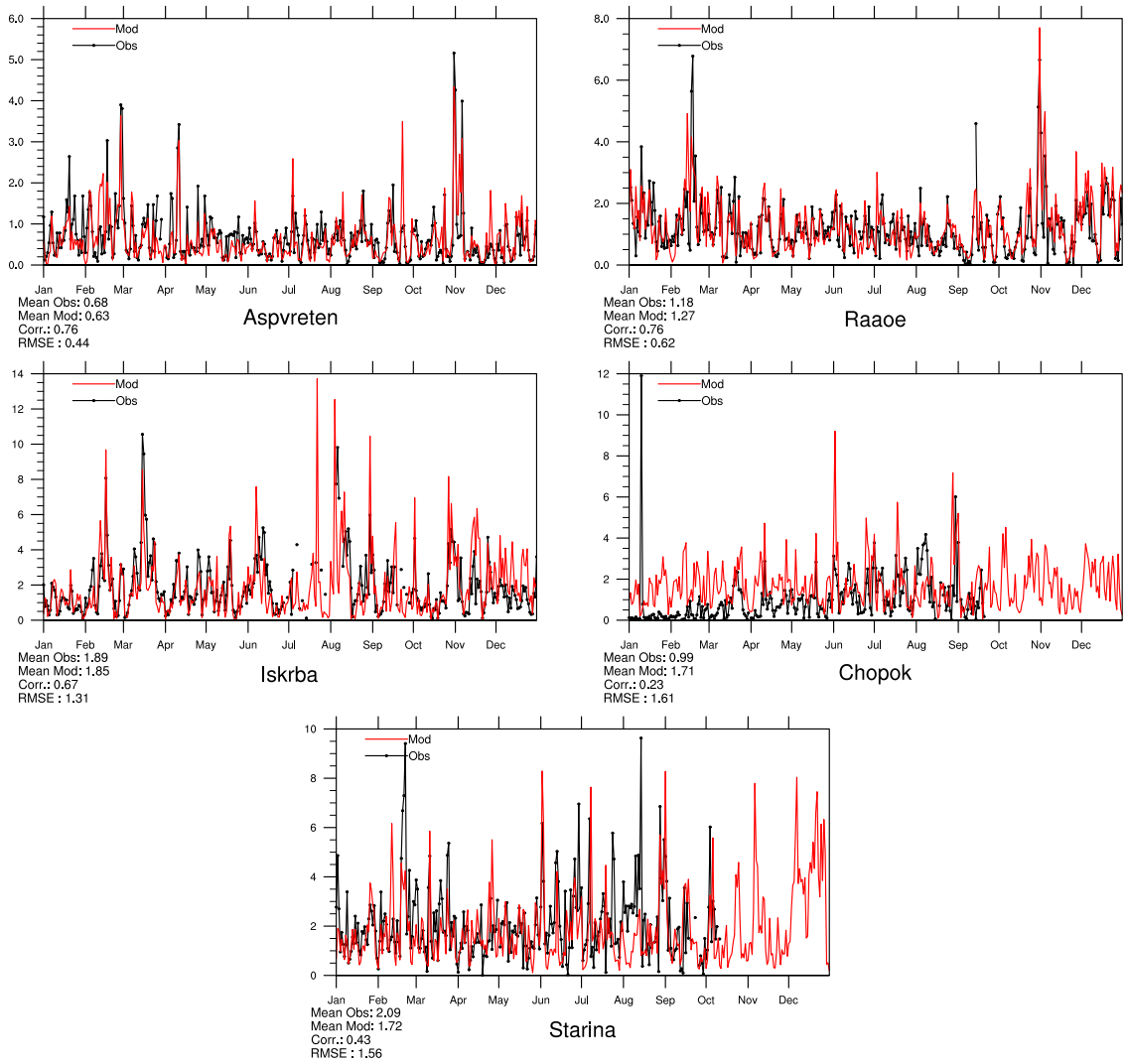

Figure 2.19: Comparison of model results and measurements (daily) for sulphate (including sea salt) in air [ugS] for stations that have measured sulphate in 2015.

Total nitrate in air

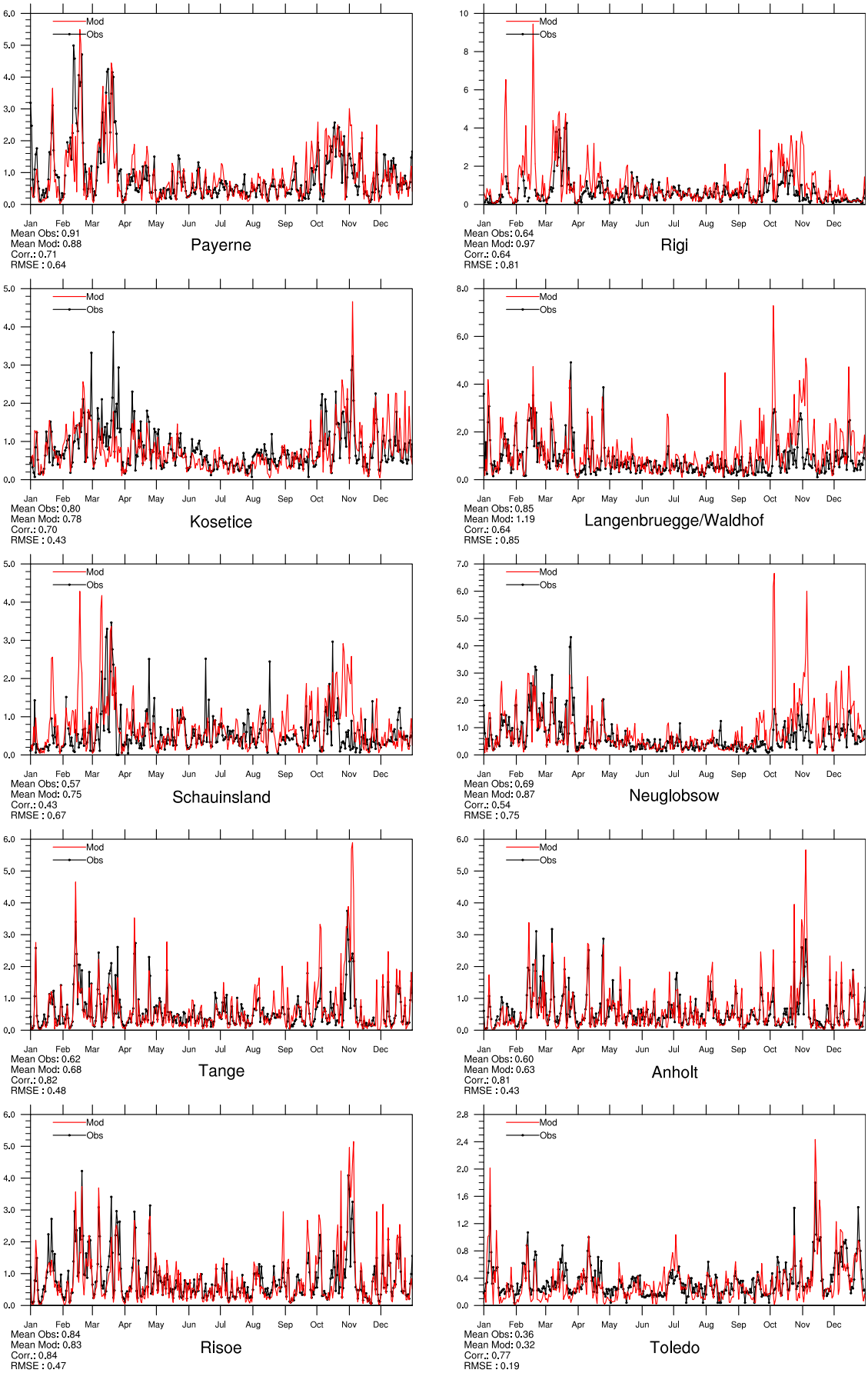

Figure 2.20: Comparison of model results and measurements (daily) total nitrate concentrations [μg(N) m^{-3}] for stations that have measured total nitrate in 2015.

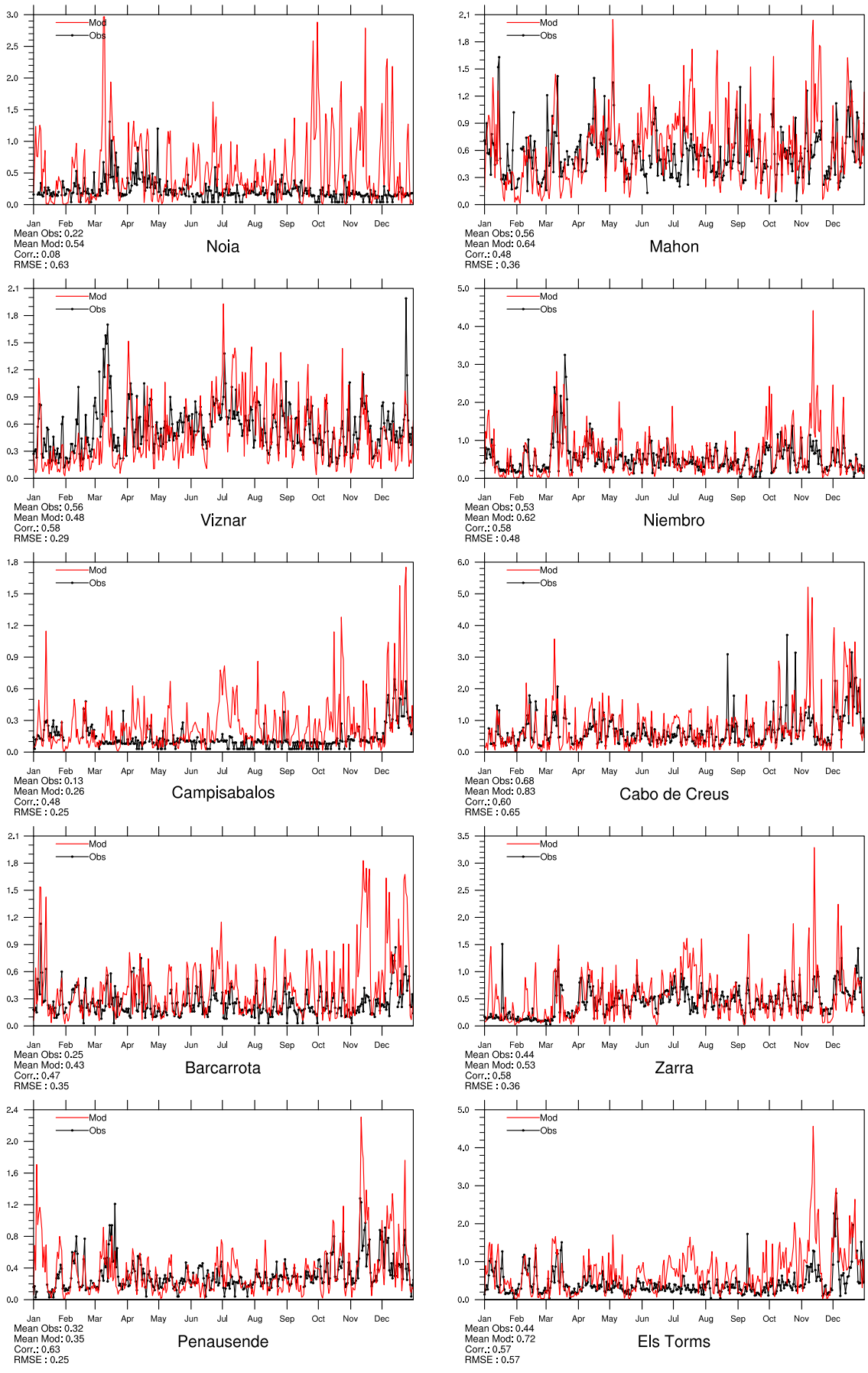

Figure 2.21: Comparison of model results and measurements (daily) total nitrate concentrations [μg(N) m^{-3}] for stations that have measured total nitrate in 2015.

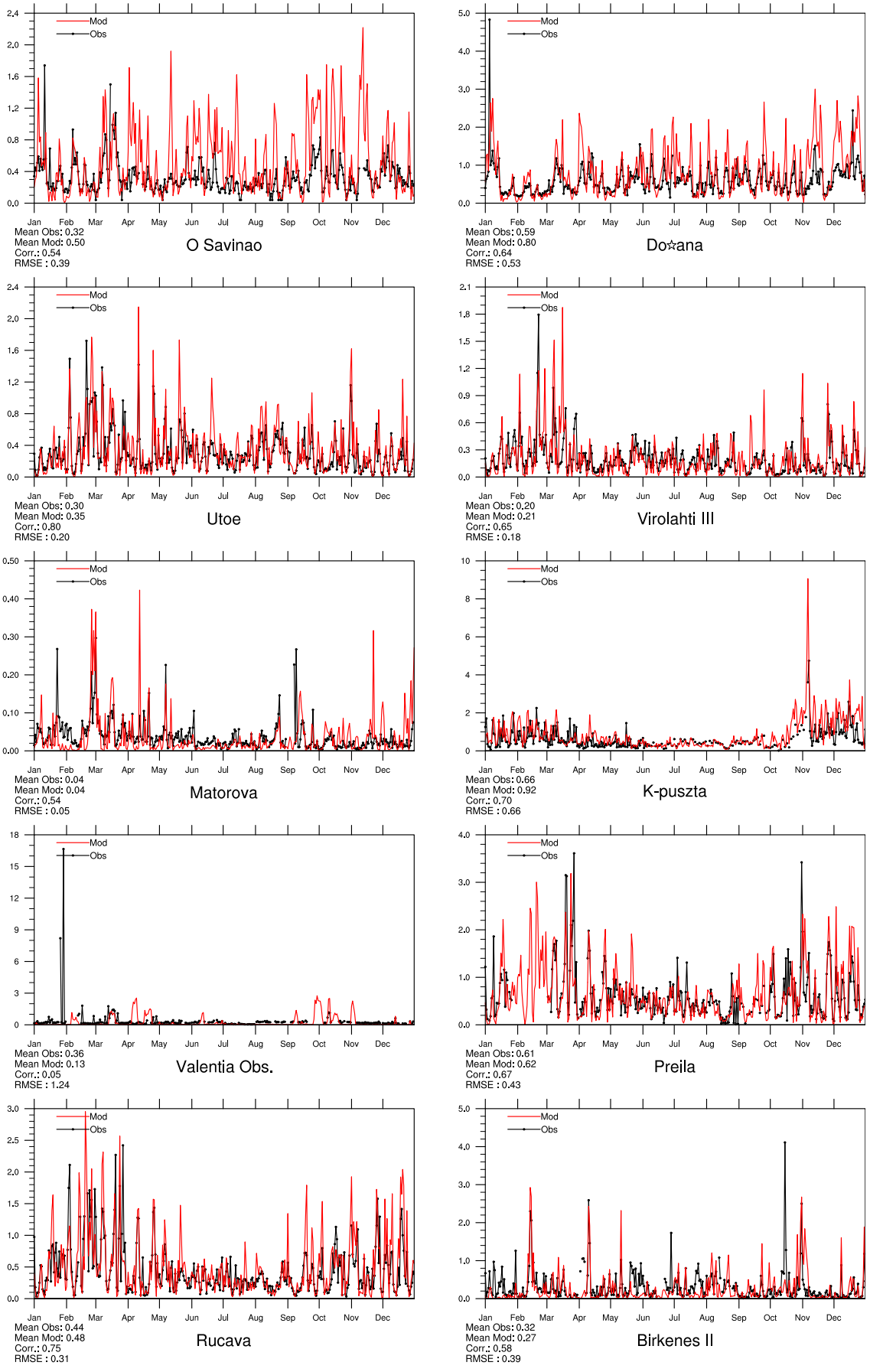

Figure 2.22: Comparison of model results and measurements (daily) total nitrate concentrations (μg(N) m^{-3}) for stations that have measured total nitrate in 2015.

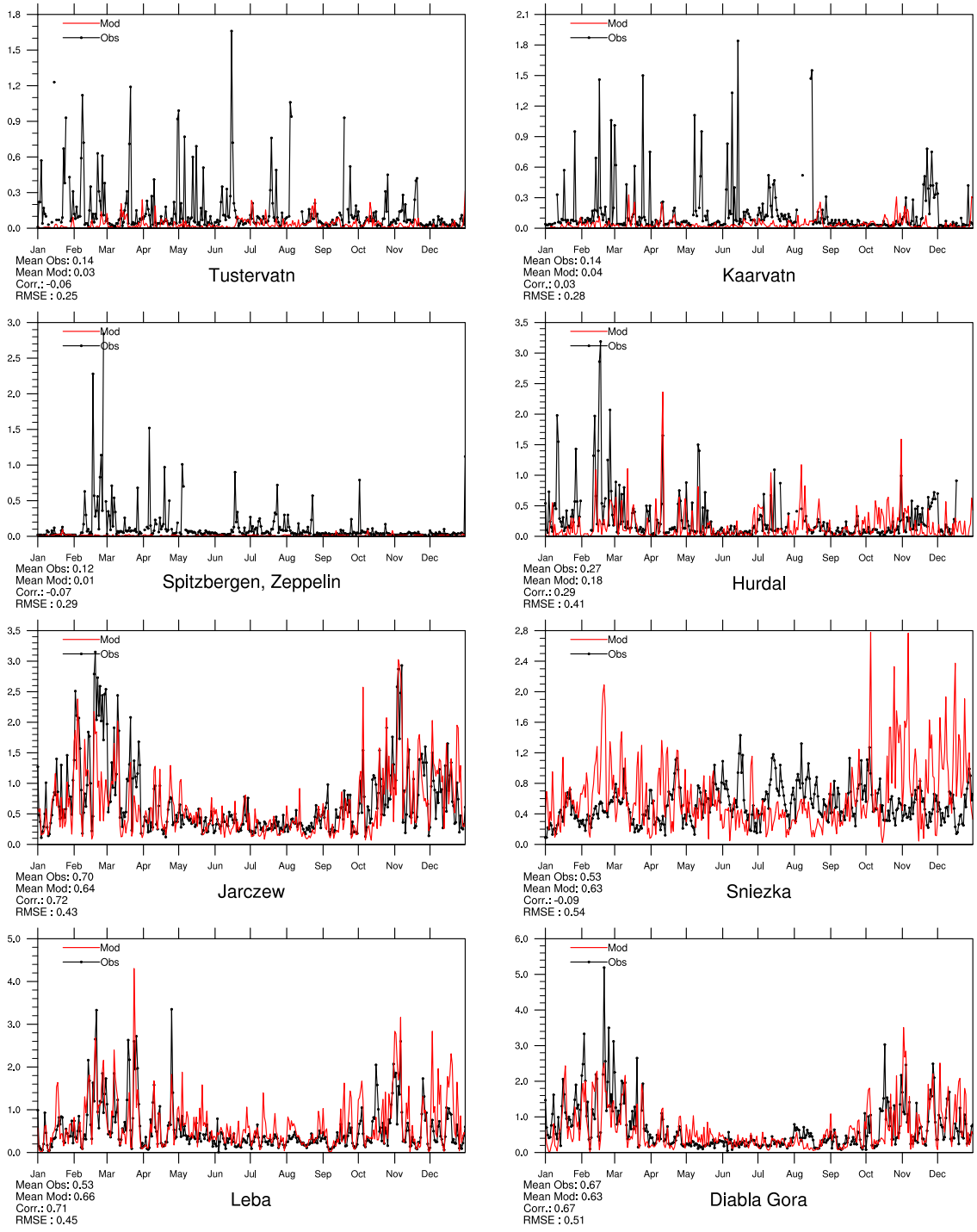

Figure 2.23: Comparison of model results and measurements (daily) total nitrate concentrations [μg(N) m^{-3}] for stations that have measured total nitrate in 2015.

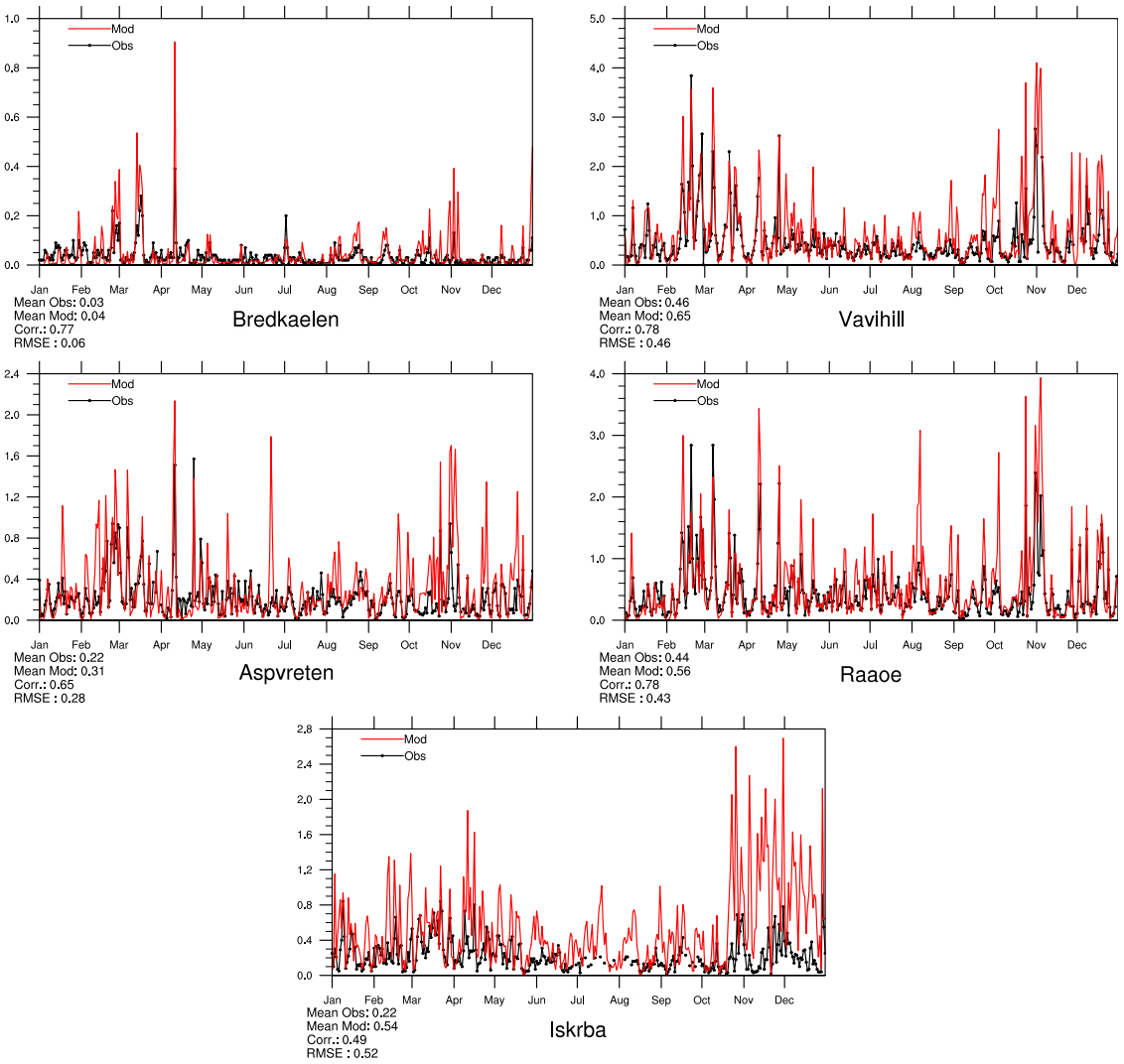

Figure 2.24: Comparison of model results and measurements (daily) total nitrate concentrations [μg(N) m^{-3}] for stations that have measured total nitrate in 2015.

Ammonia+ammonium in air

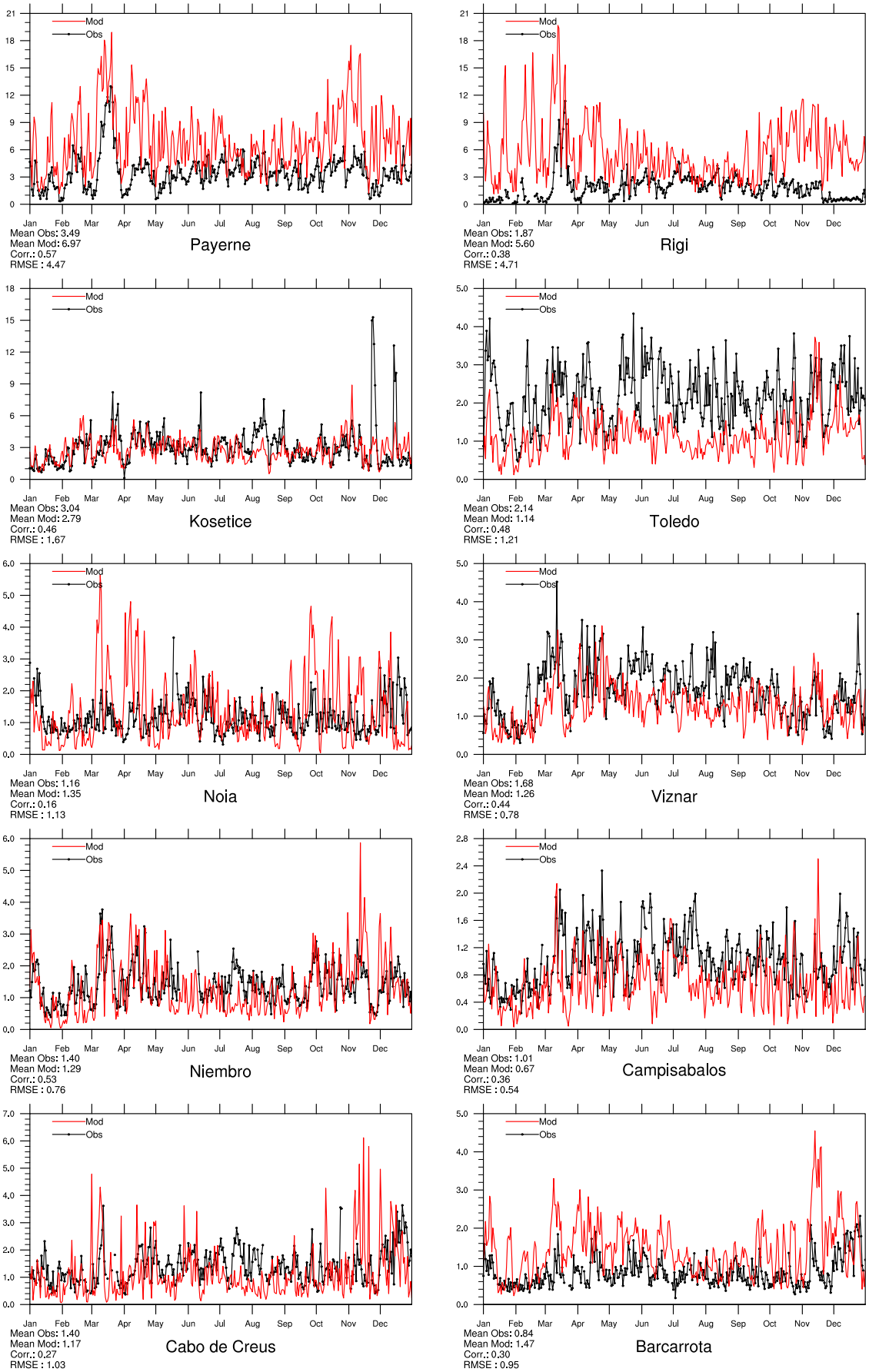

Figure 2.25: Comparison of model results and measurements (daily) total ammonium+ammonia concentrations [μg(N) m^{-3}] for stations that have measured total ammonium+ammonia in 2015.

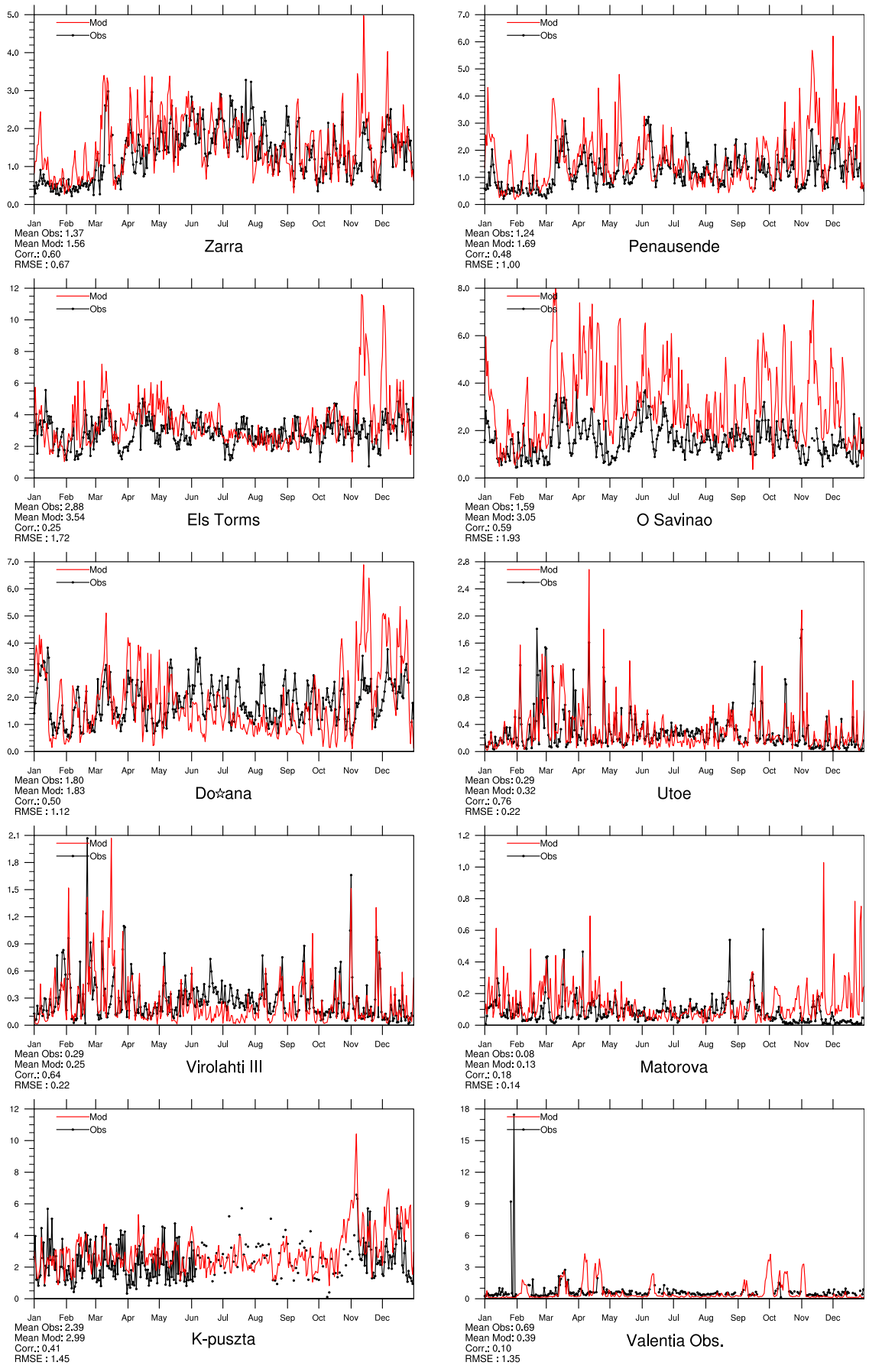

Figure 2.26: Comparison of model results and measurements (daily) total ammonium+ammonia concentrations [μg(N) m^{-3}] for stations that have measured total ammonium+ammonia in 2015.

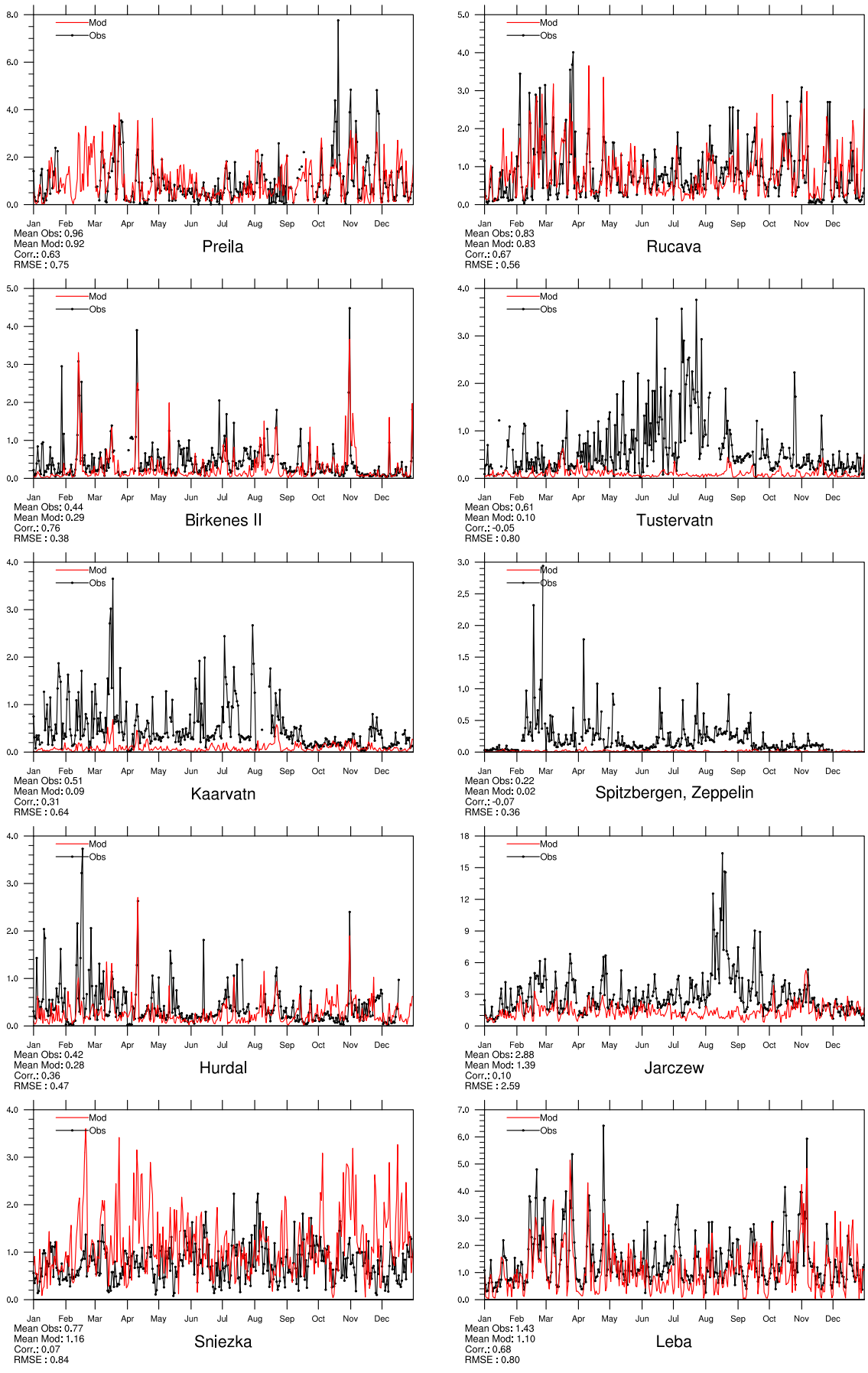

Figure 2.27: Comparison of model results and measurements (daily) total ammonium+ammonia concentrations [μg(N) m^{-3}] for stations that have measured total ammonium+ammonia in 2015.

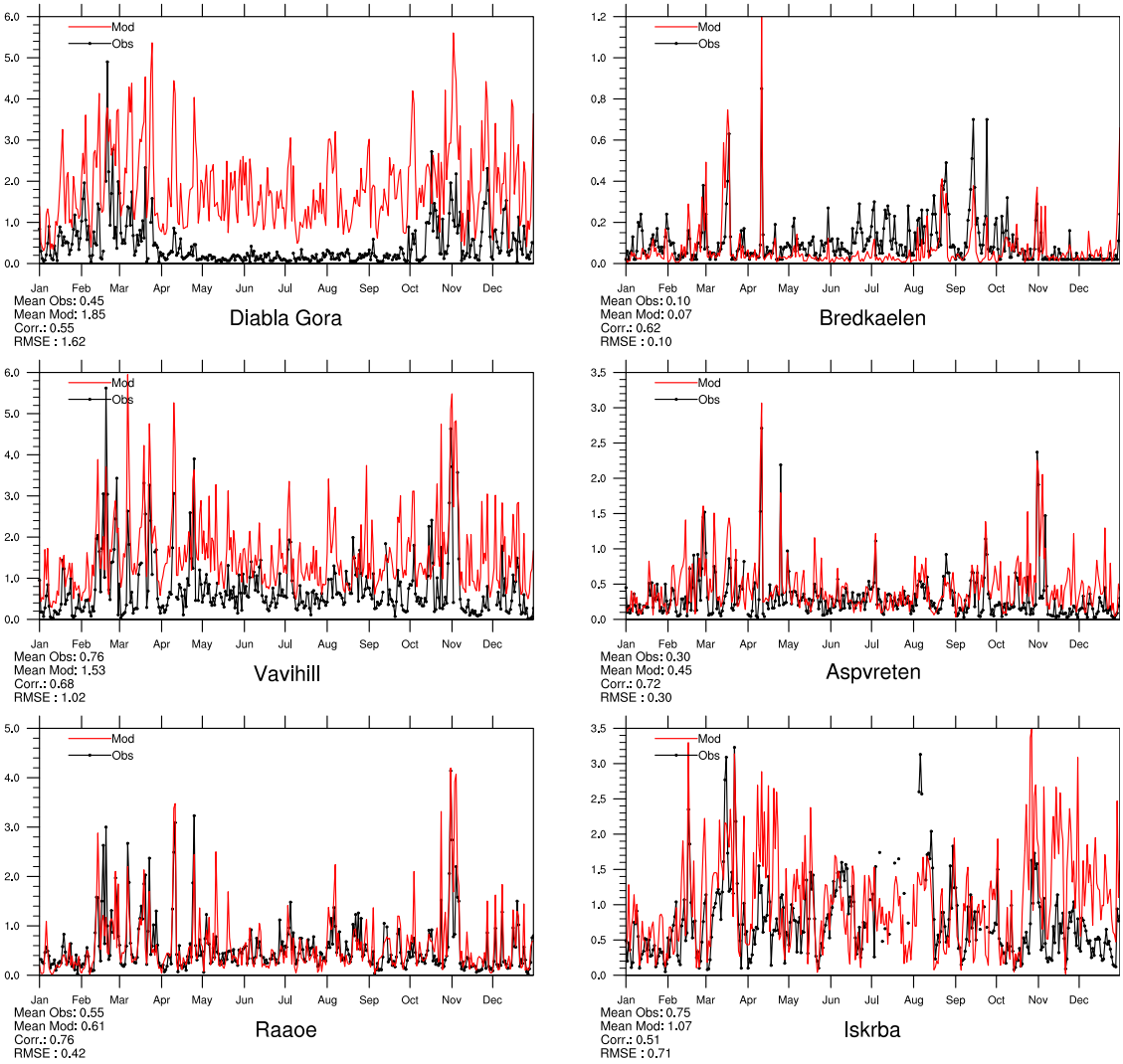

Figure 2.28: Comparison of model results and measurements (daily) total ammonium+ammonia concentrations [μg(N) m^{-3}] for stations that have measured total ammonium+ammonia in 2015.

Sulphur in precipitation

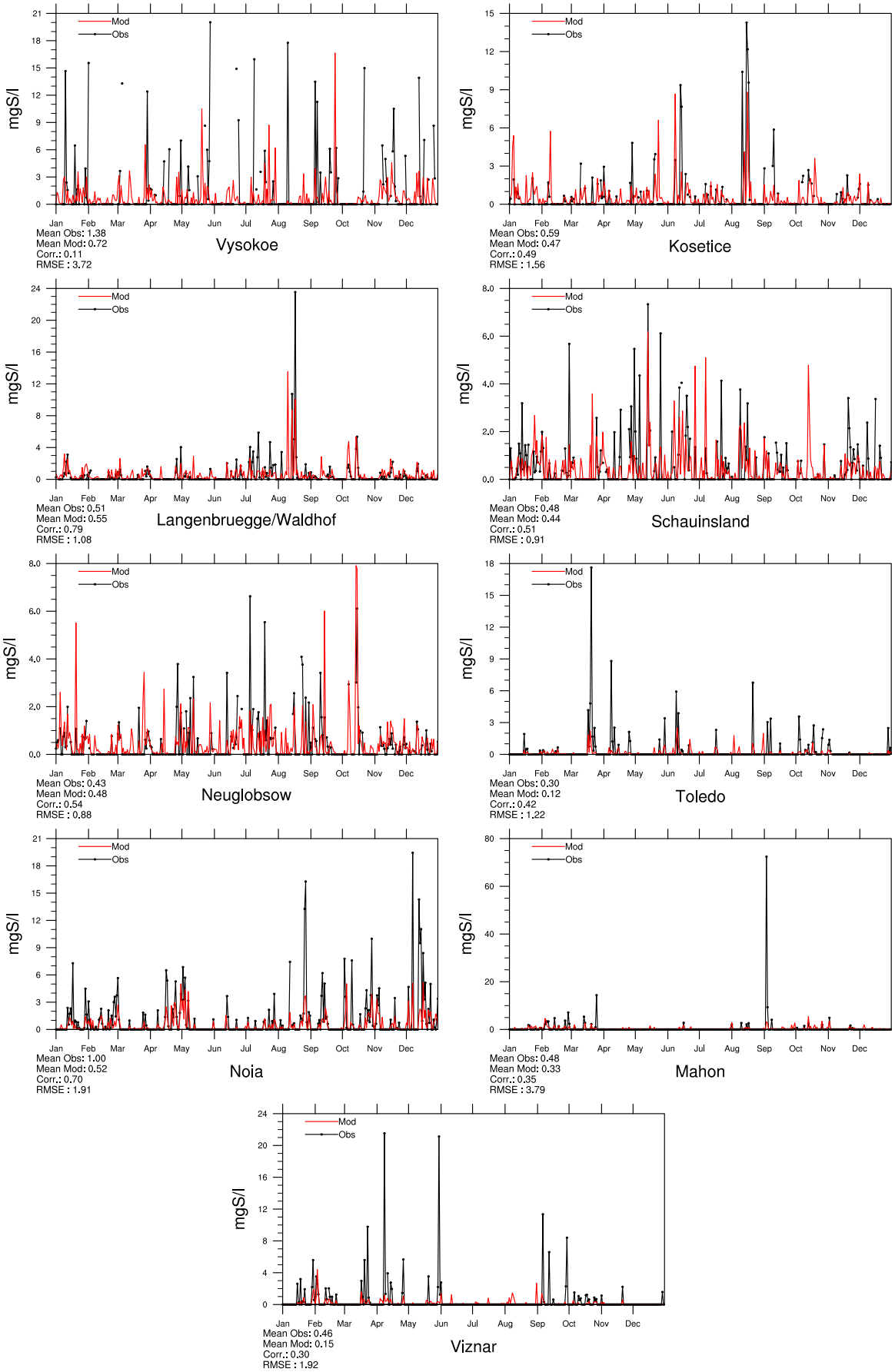

Figure 2.29: Comparison of model results and measurements (daily) for wet deposition of sulphur [mg(S)l^{-1}] in 2015.

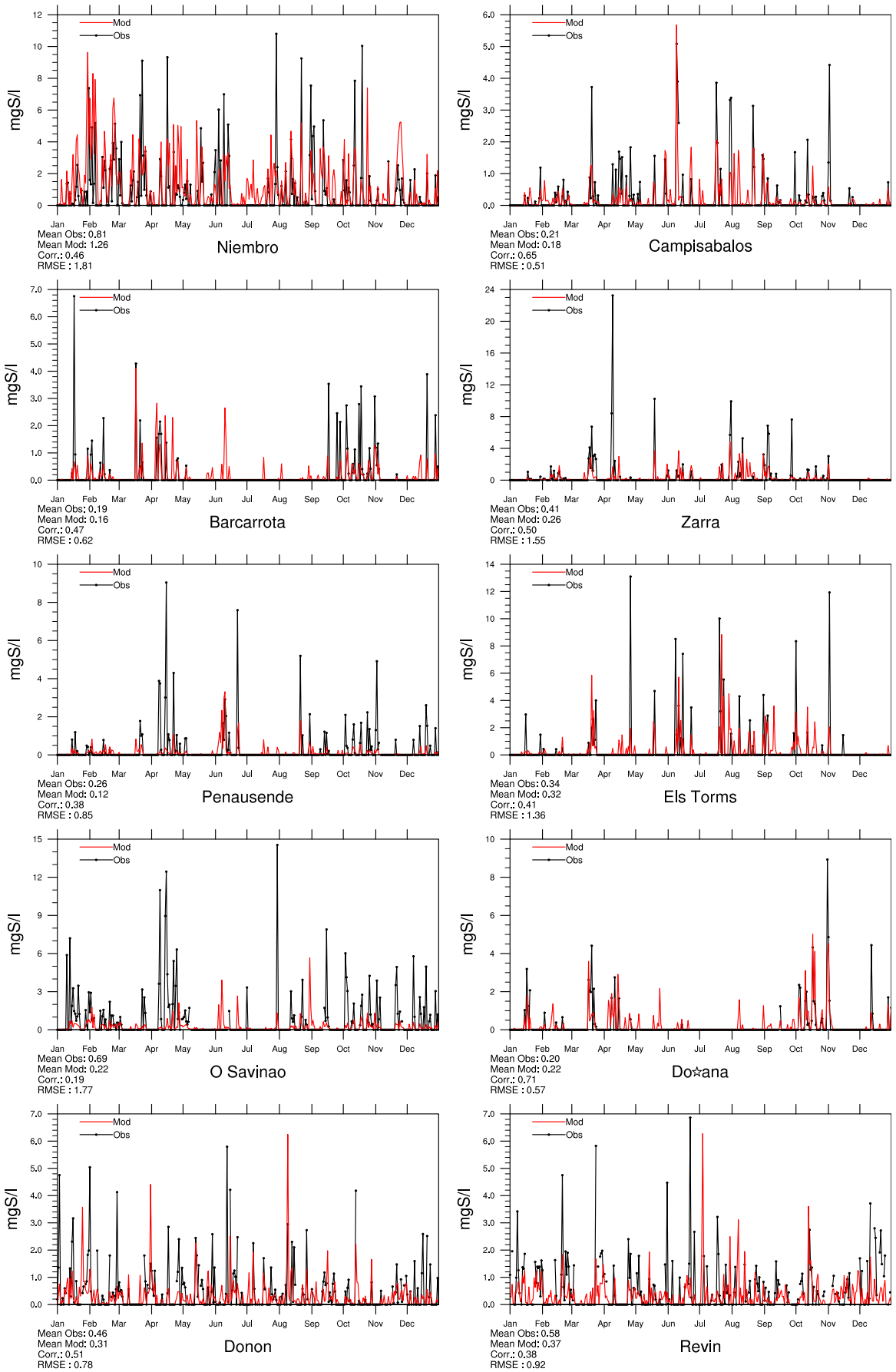

Figure 2.30: Comparison of model results and measurements (daily) for wet deposition of sulphur [mg(S)l^{-1}] in 2015.

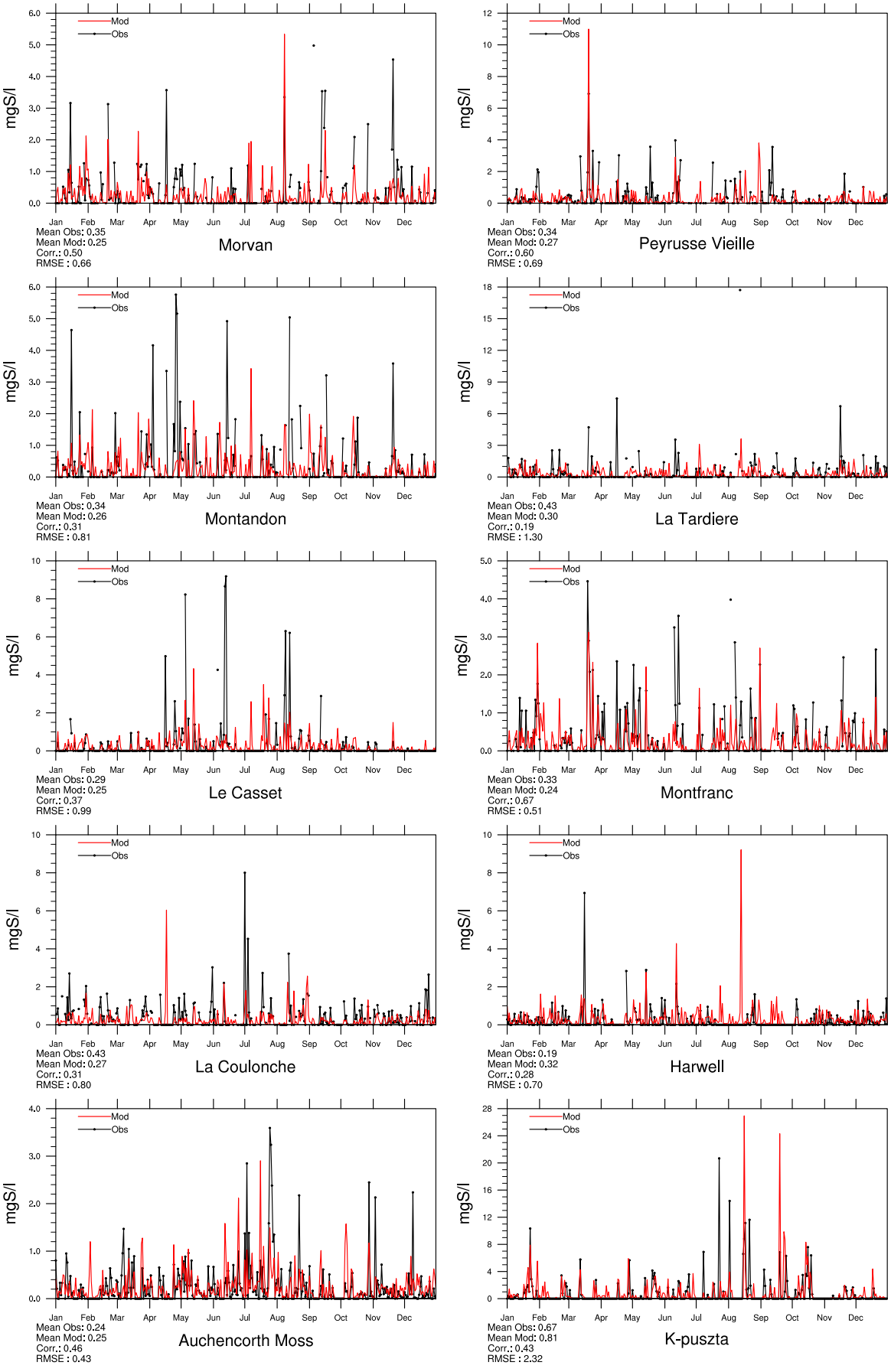

Figure 2.31: Comparison of model results and measurements (daily) for wet deposition of sulphur [mg(S)l^{-1}] in 2015.

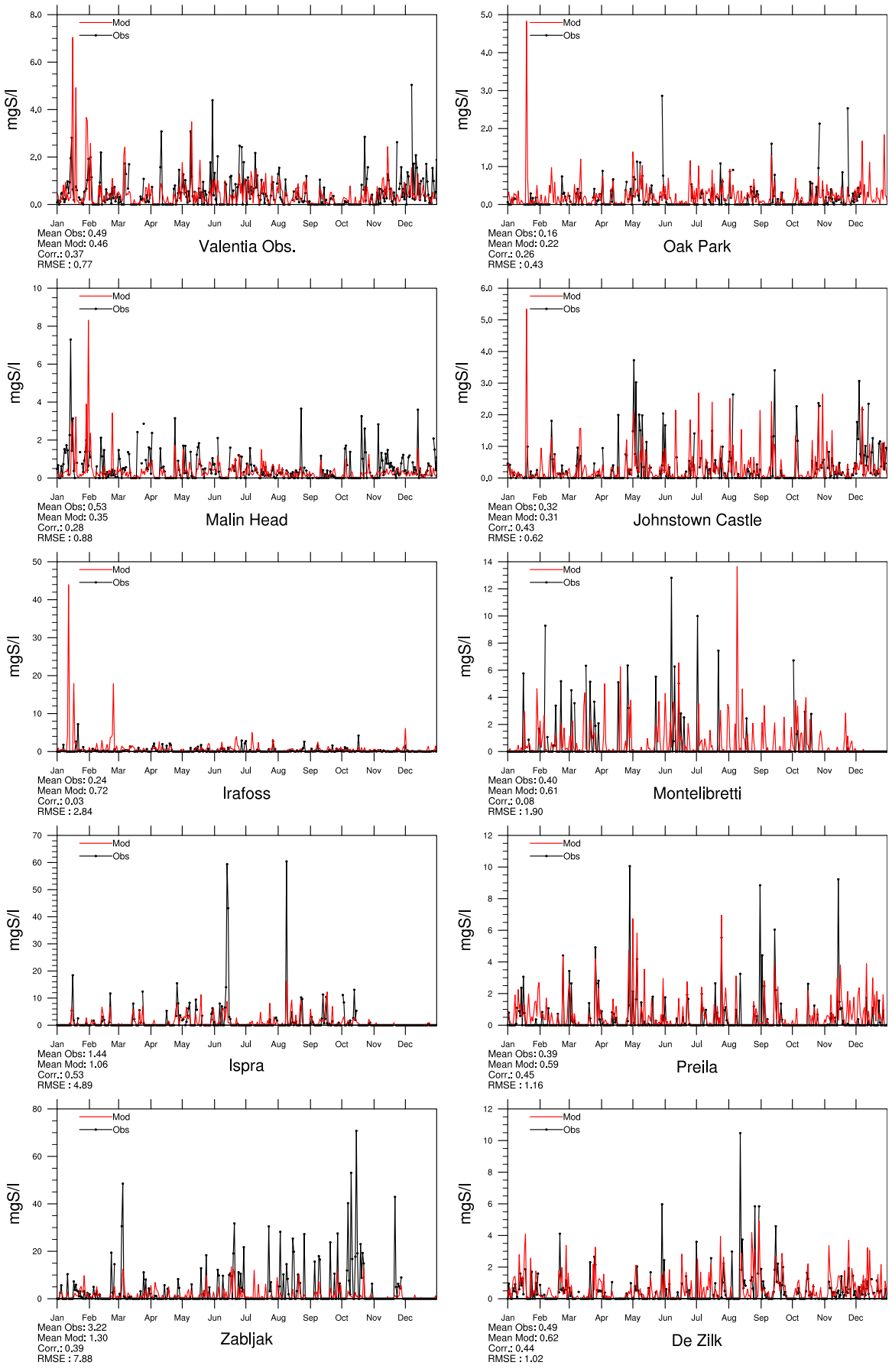

Figure 2.32: Comparison of model results and measurements (daily) for wet deposition of sulphur [mg(S)l^{-1}] in 2015.

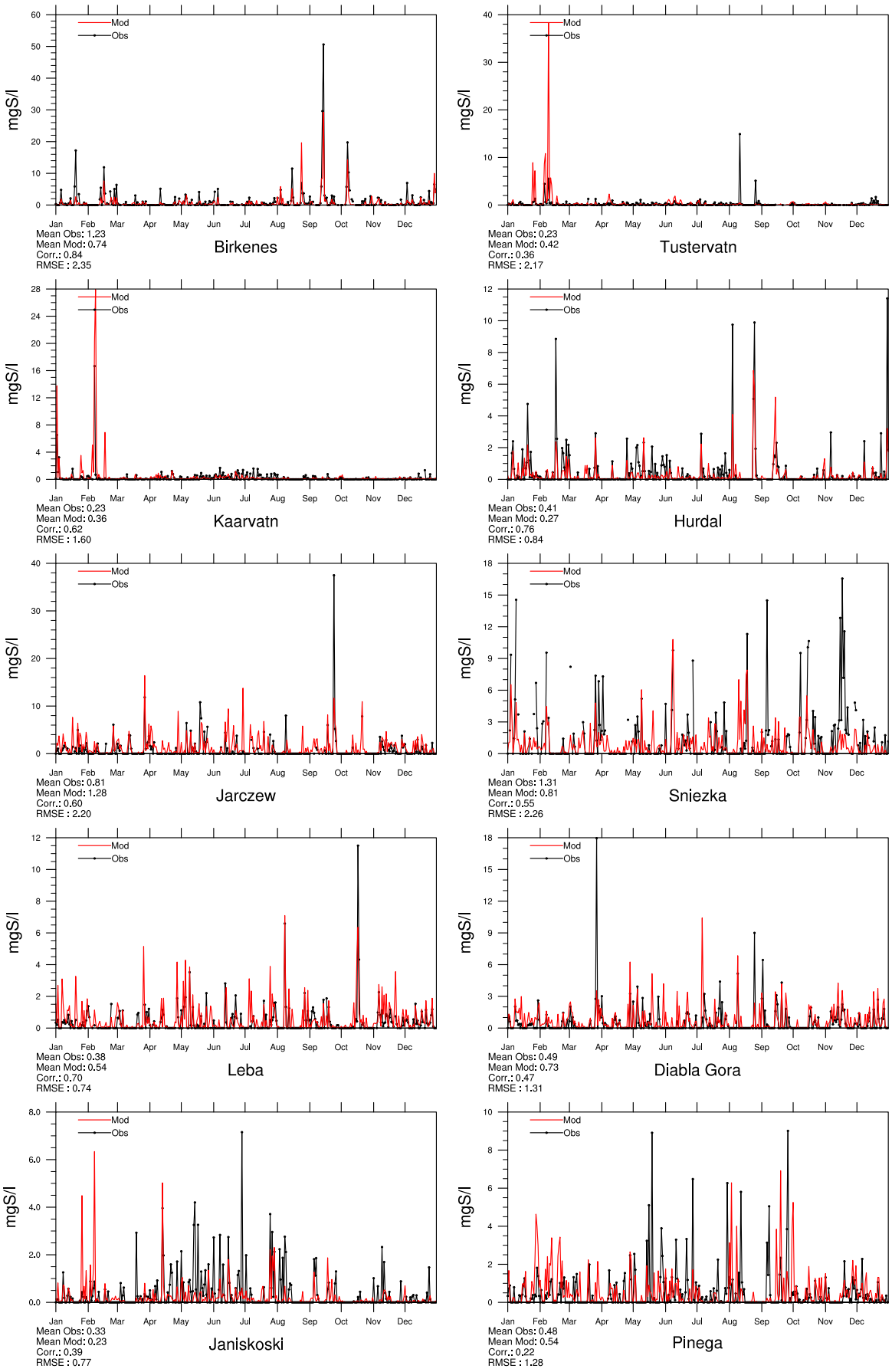

Figure 2.33: Comparison of model results and measurements (daily) for wet deposition of sulphur [mg(S)l^{-1}] in 2015.

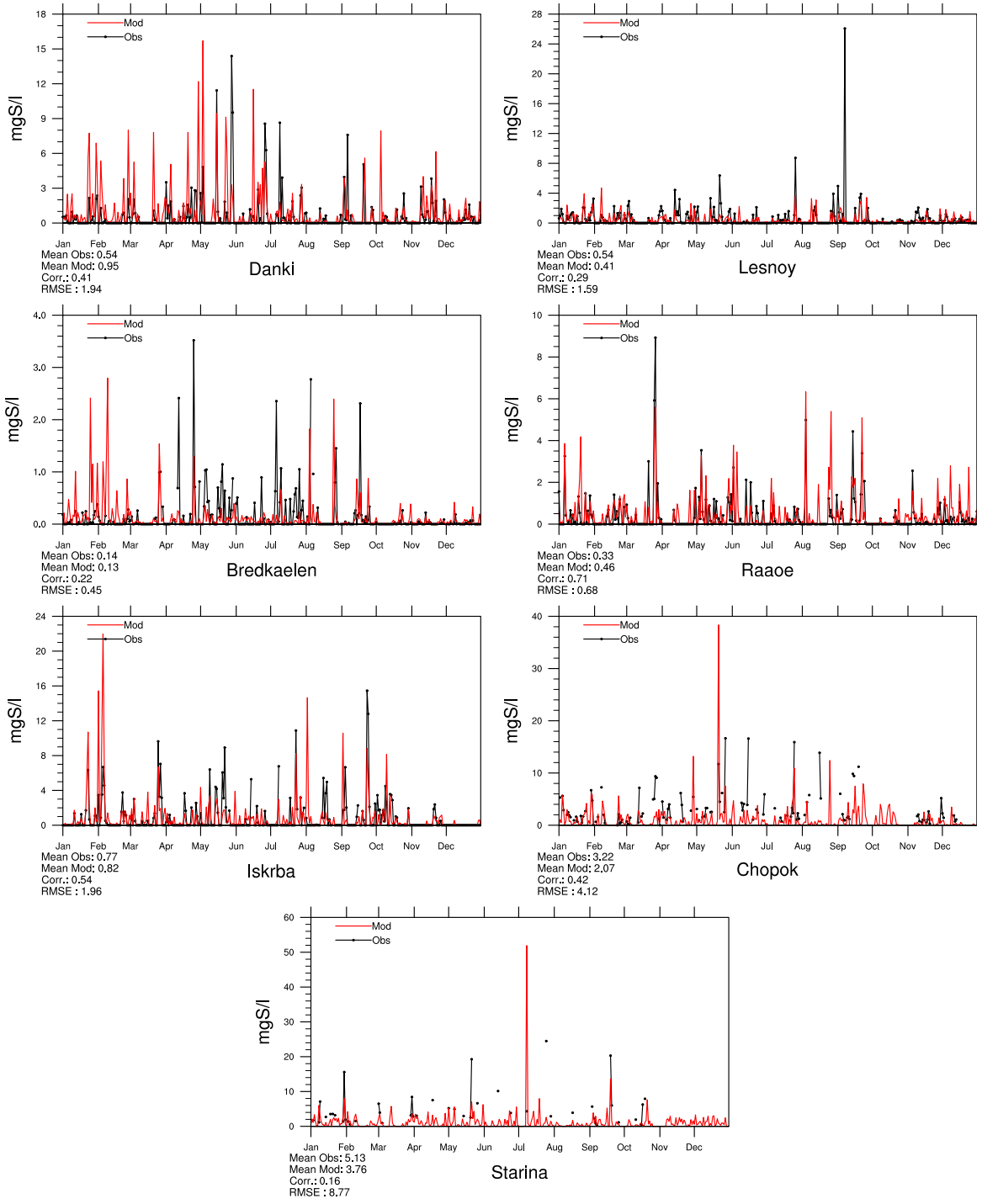

Figure 2.34: Comparison of model results and measurements (daily) for wet deposition of sulphur [mg(S)l^{-1}] in 2015.

Oxidized nitrogen in precipitation

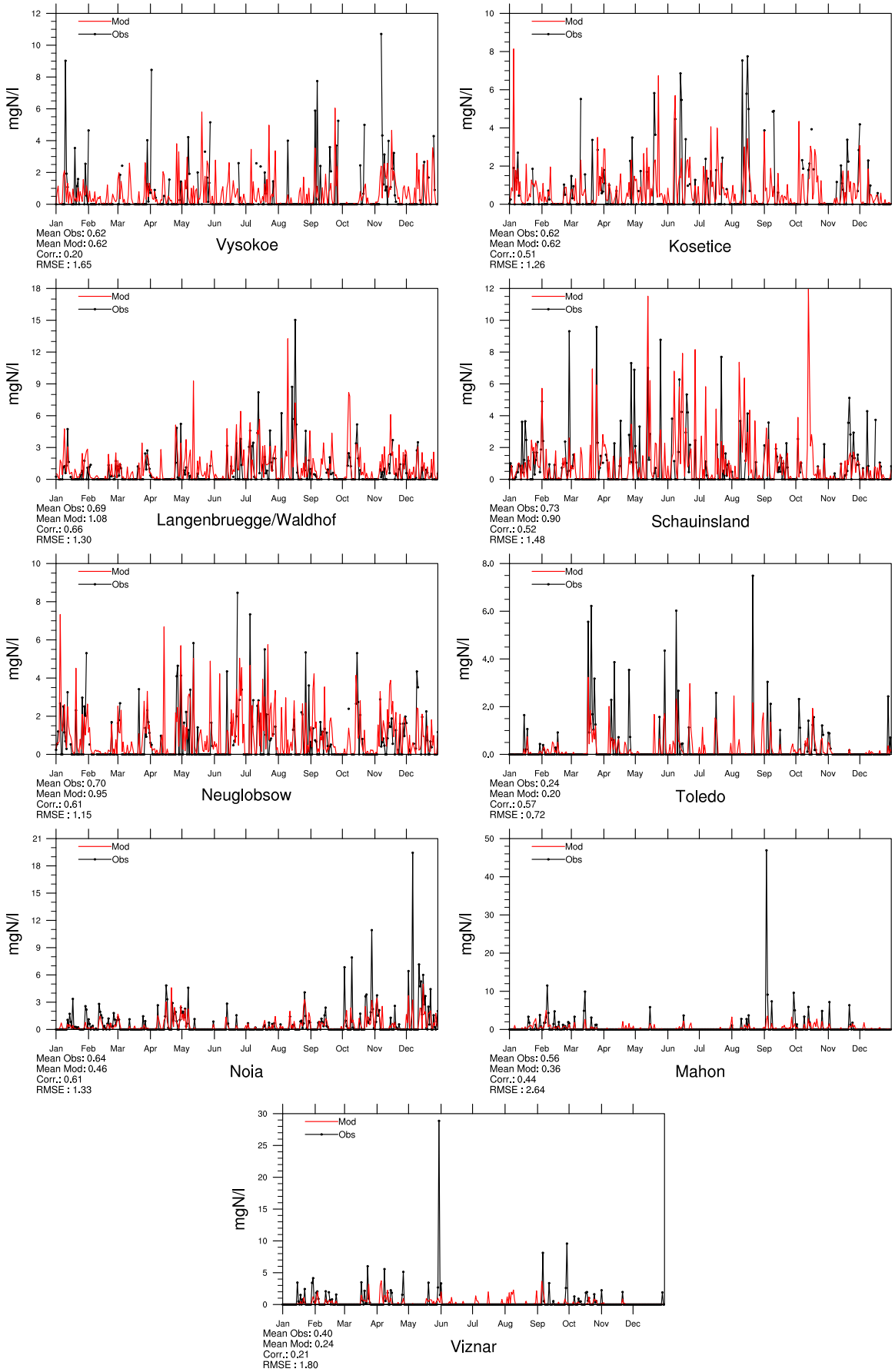

Figure 2.35: Comparison of model results and measurements (daily) for wet deposition of oxidized nitrogen [mg(N)l^{-1}] in 2015.

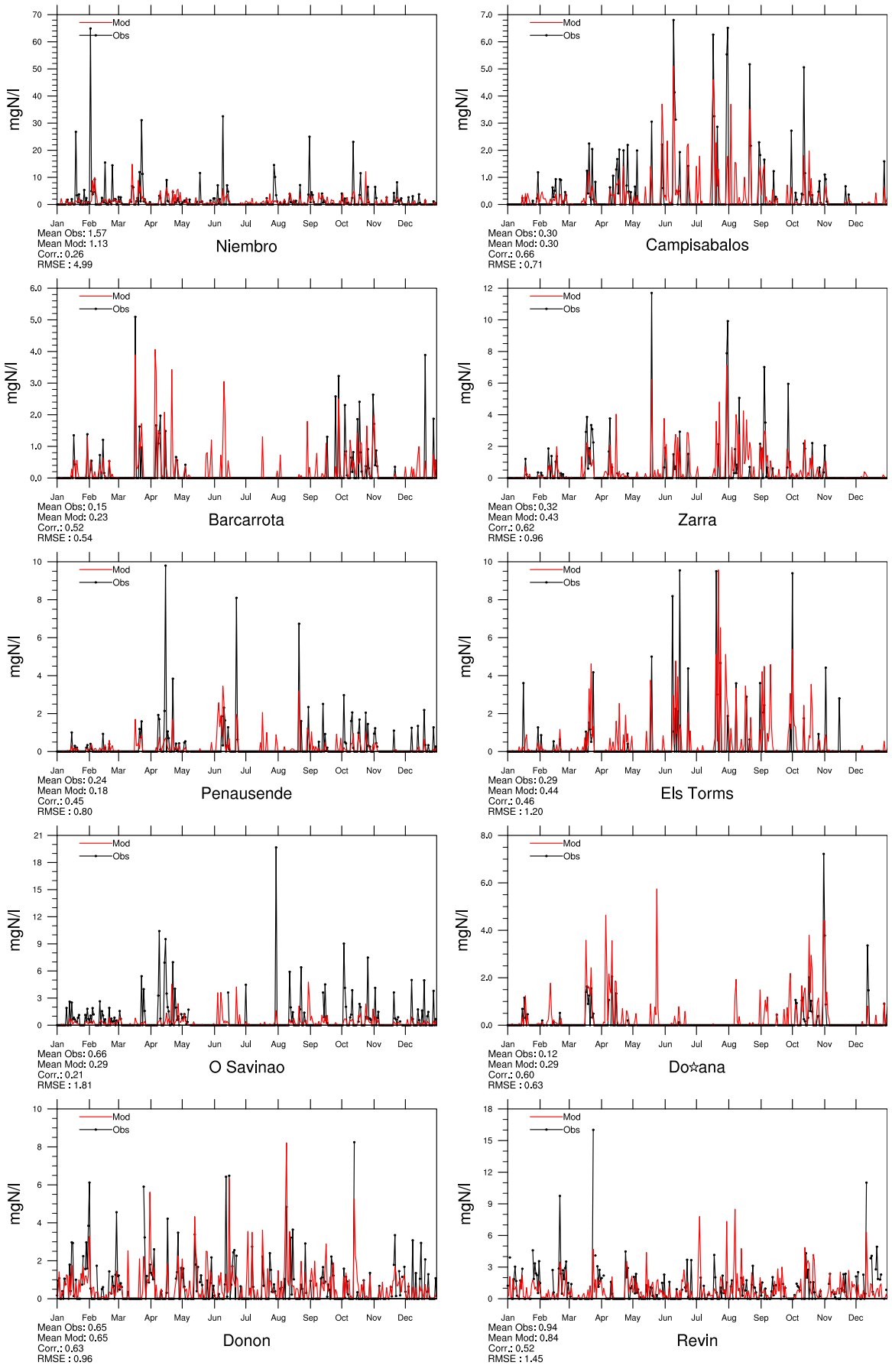

Figure 2.36: Comparison of model results and measurements (daily) for wet deposition of oxidized nitrogen [mg(N)l^{-1}] in 2015.

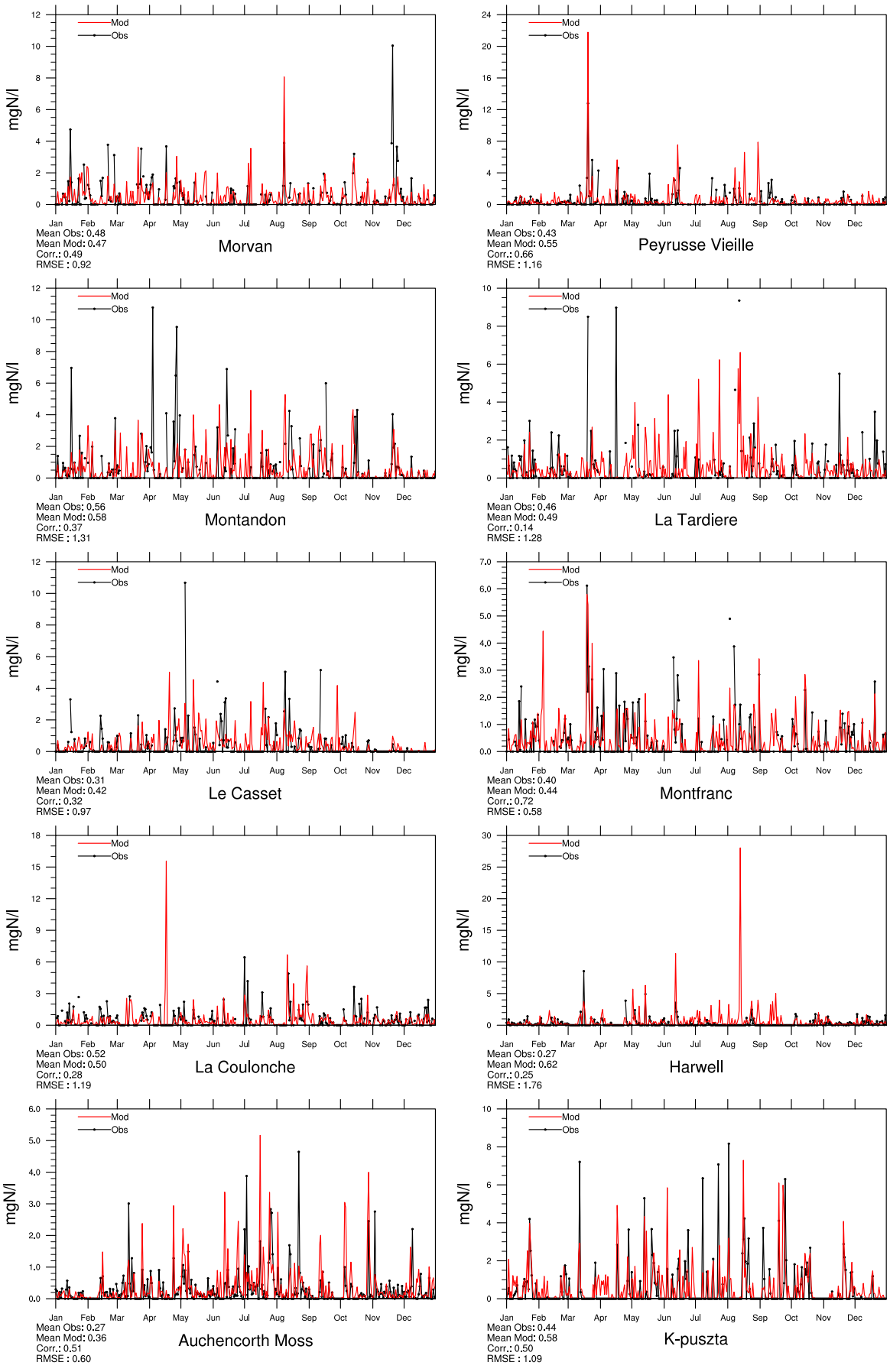

Figure 2.37: Comparison of model results and measurements (daily) for wet deposition of oxidized nitrogen [mg(N)l^{-1}] in 2015.

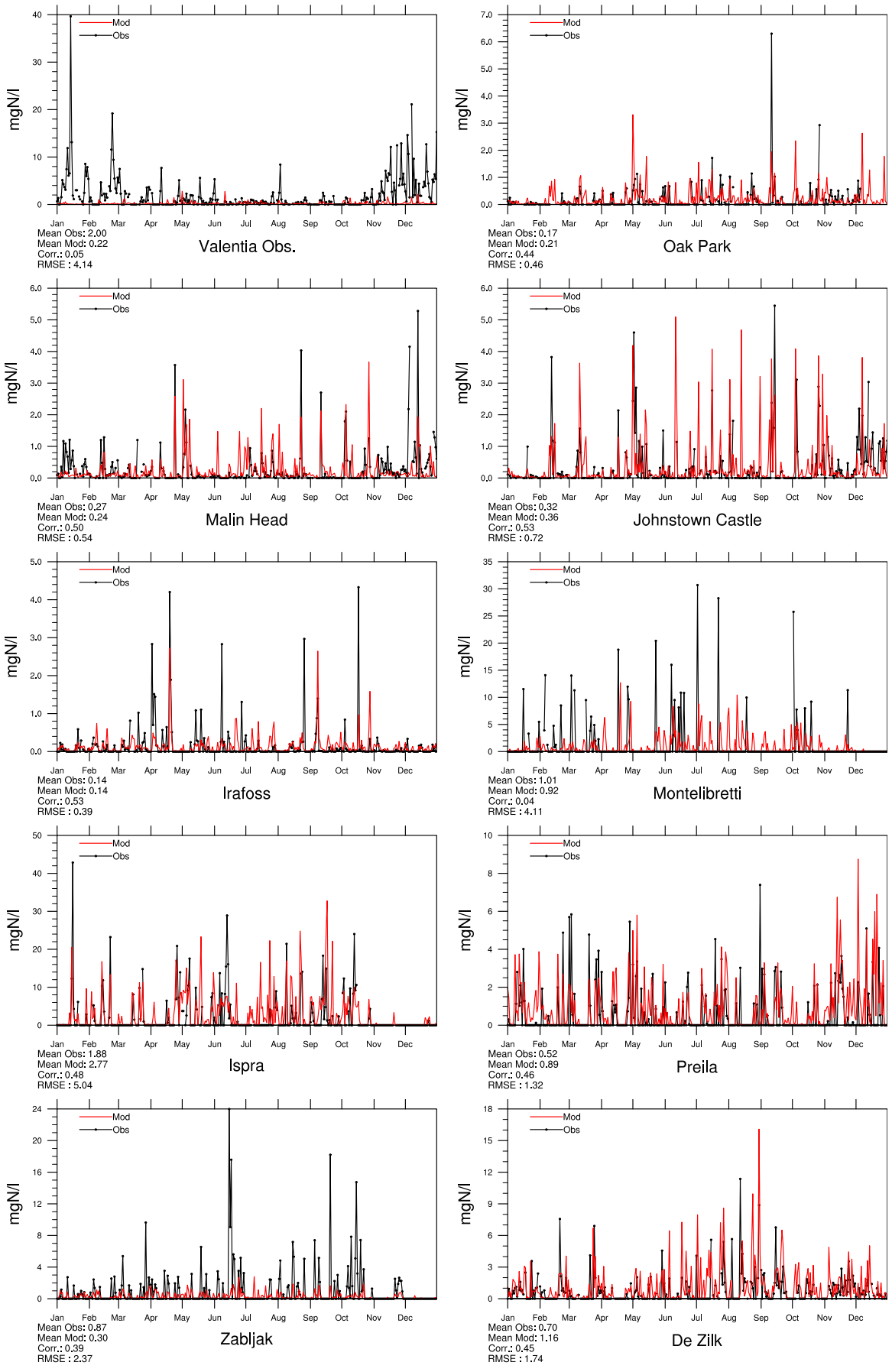

Figure 2.38: Comparison of model results and measurements (daily) for wet deposition of oxidized nitrogen [mg(N)l^{-1}] in 2015.

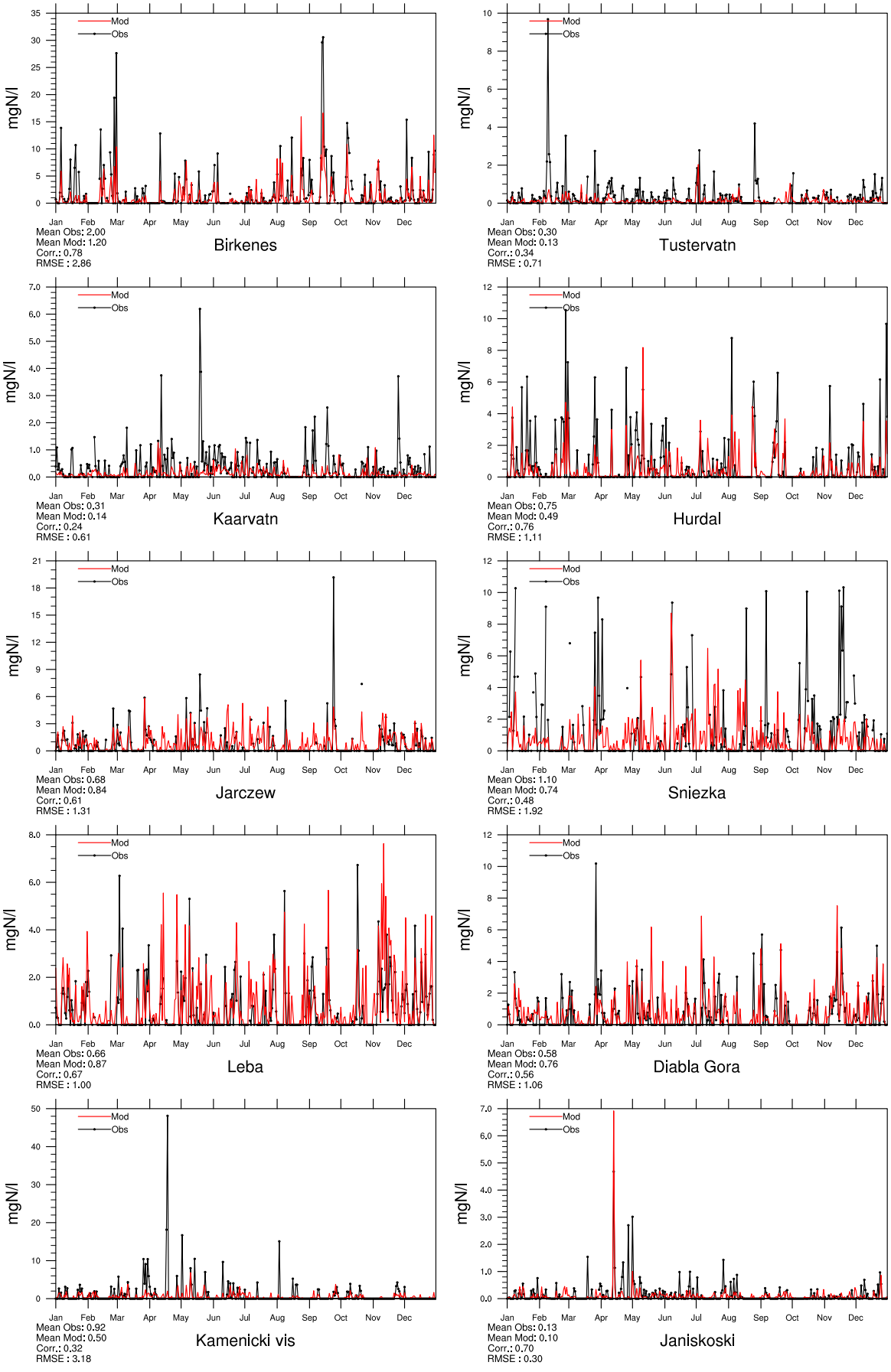

Figure 2.39: Comparison of model results and measurements (daily) for wet deposition of oxidized nitrogen [mg(N)l^{-1}] in 2015.

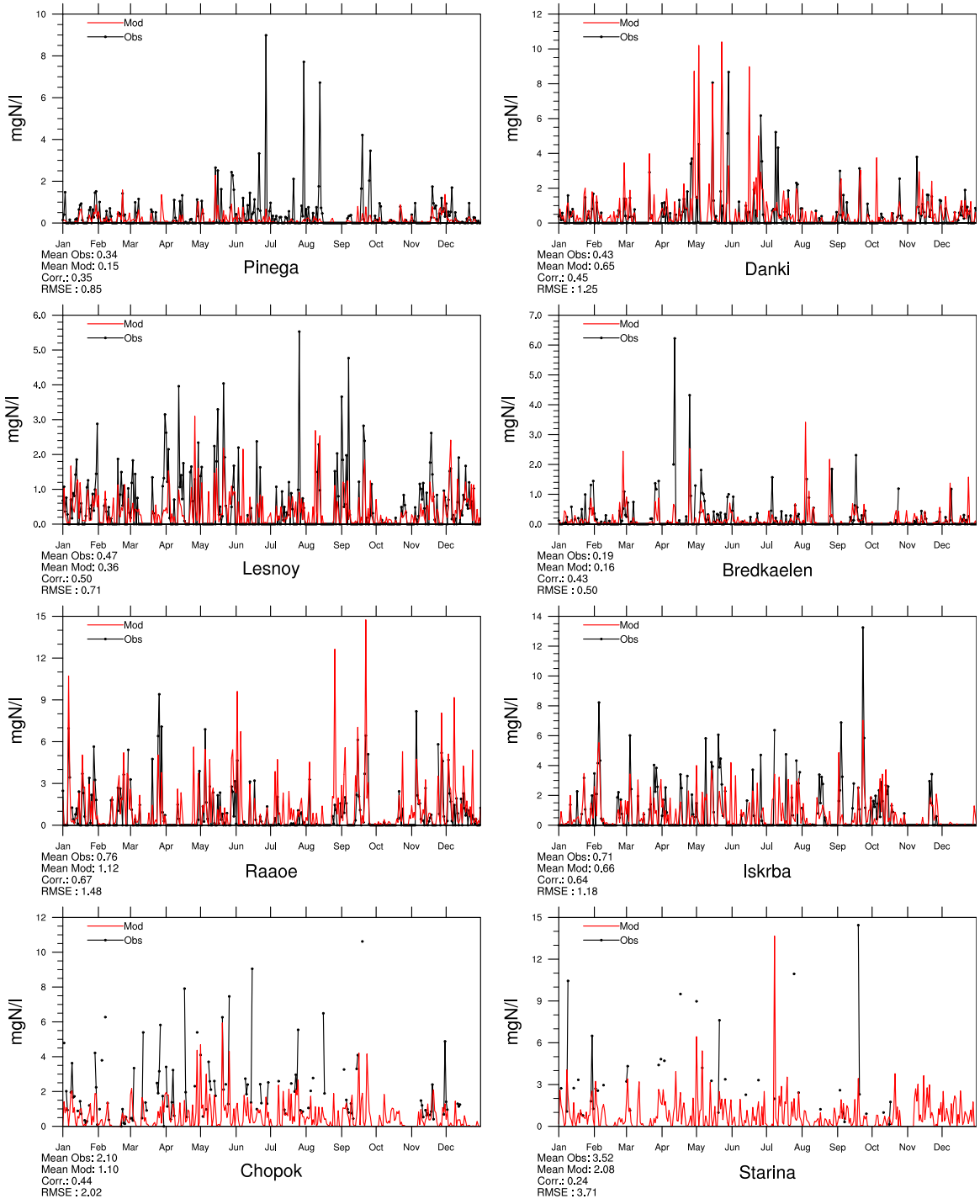

Figure 2.40: Comparison of model results and measurements (daily) for wet deposition of oxidized nitrogen [mg(N)l^{-1}] in 2015.

Reduced nitrogen in precipitation

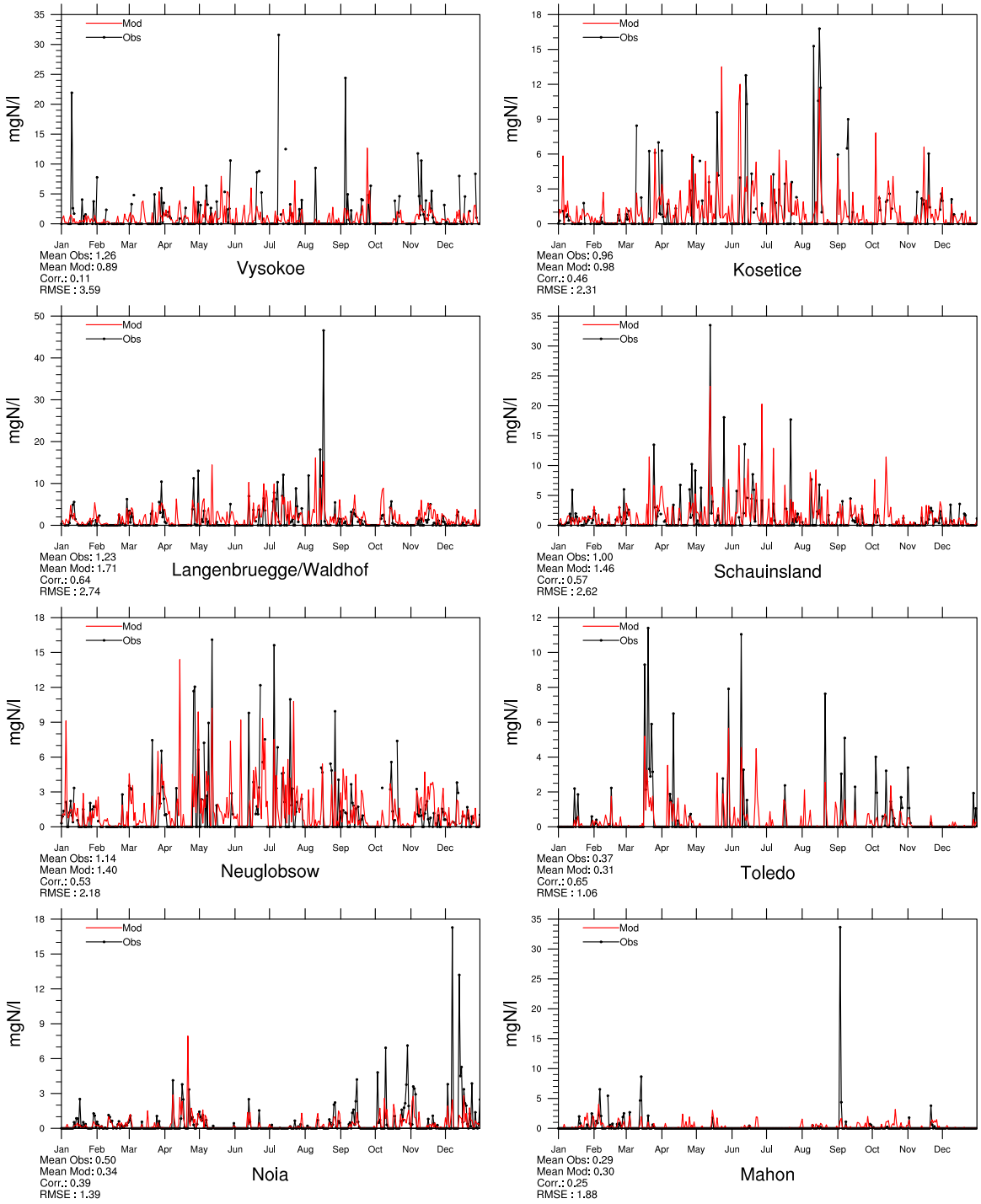

Figure 2.41: Comparison of model results and measurements (daily) for wet deposition of reduced nitrogen [mg(N)l^{-1}] in 2015.

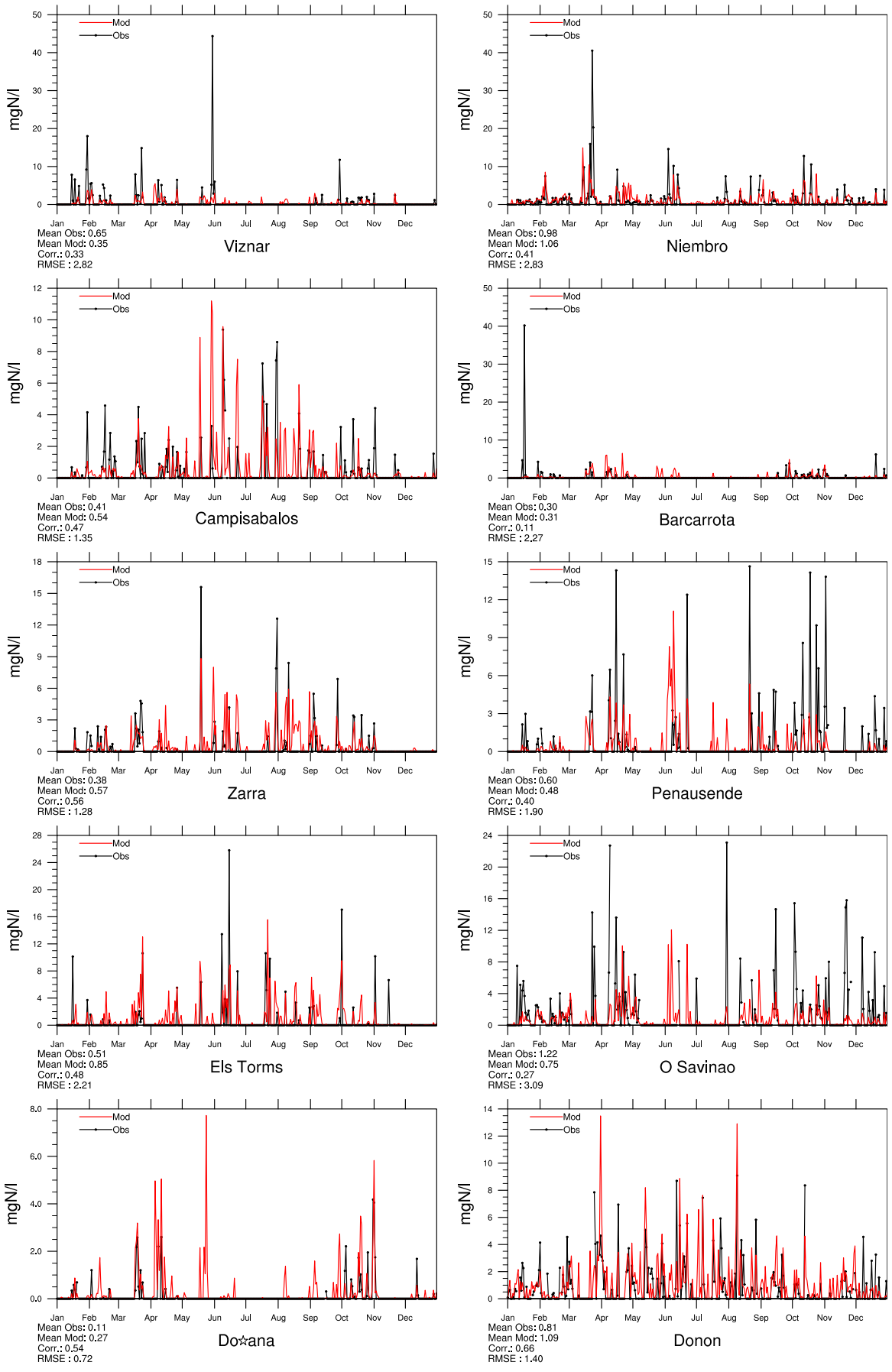

Figure 2.42: Comparison of model results and measurements (daily) for wet deposition of reduced nitrogen [mg(N)l^{-1}] in 2015.

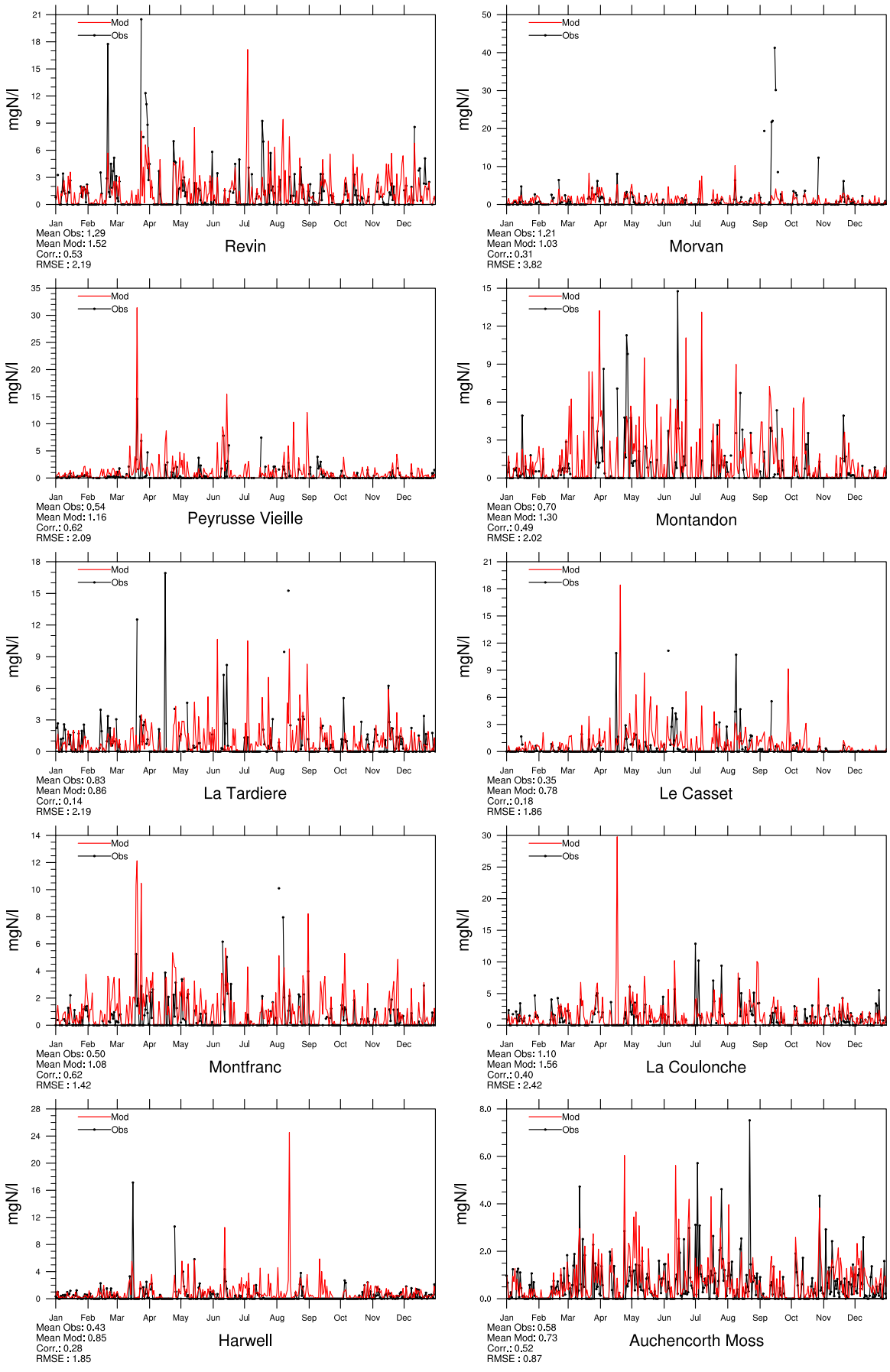

Figure 2.43: Comparison of model results and measurements (daily) for wet deposition of reduced nitrogen [mg(N)l^{-1}] in 2015.

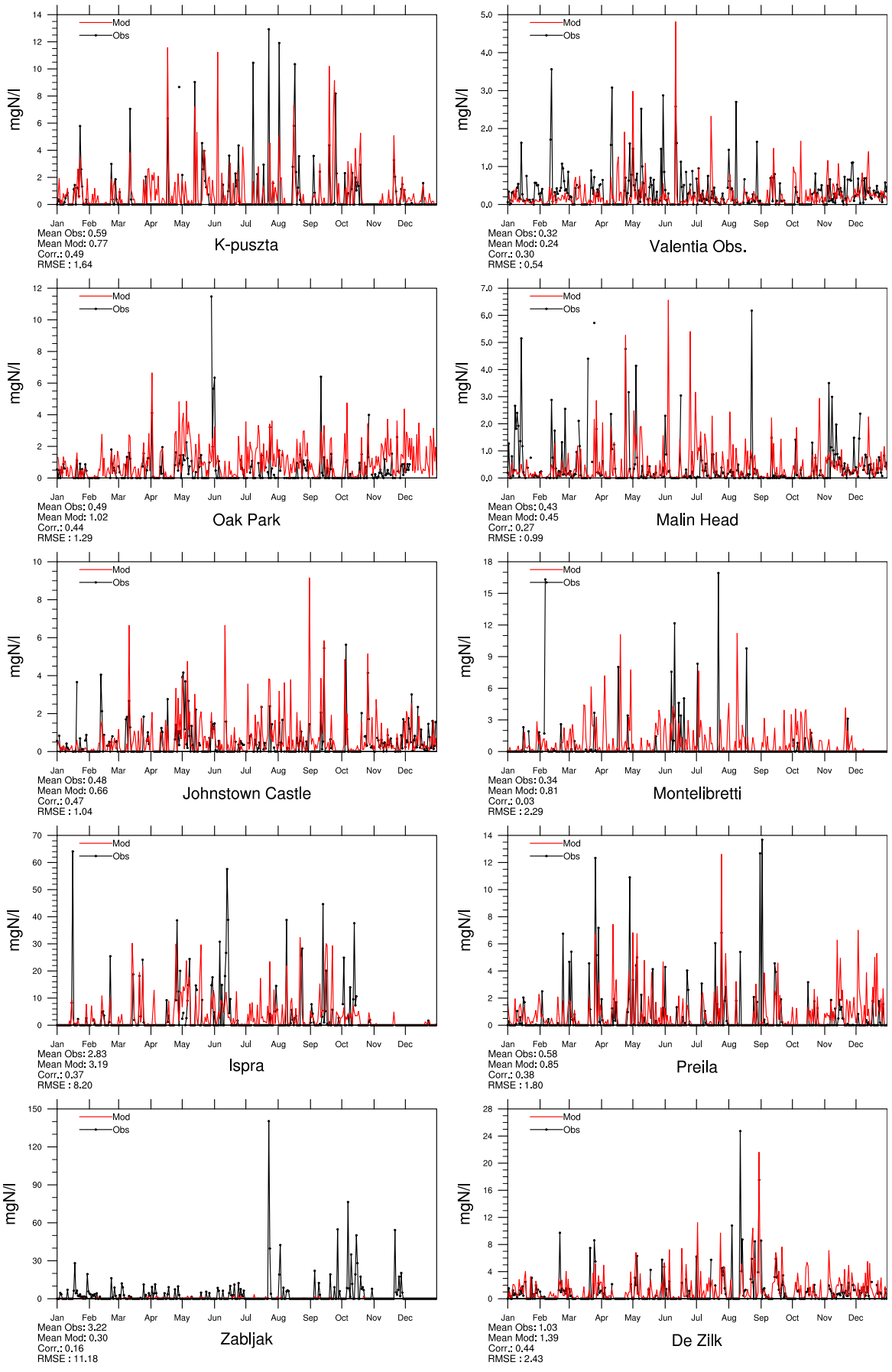

Figure 2.44: Comparison of model results and measurements (daily) for wet deposition of reduced nitrogen [mg(N)l^{-1}] in 2015.

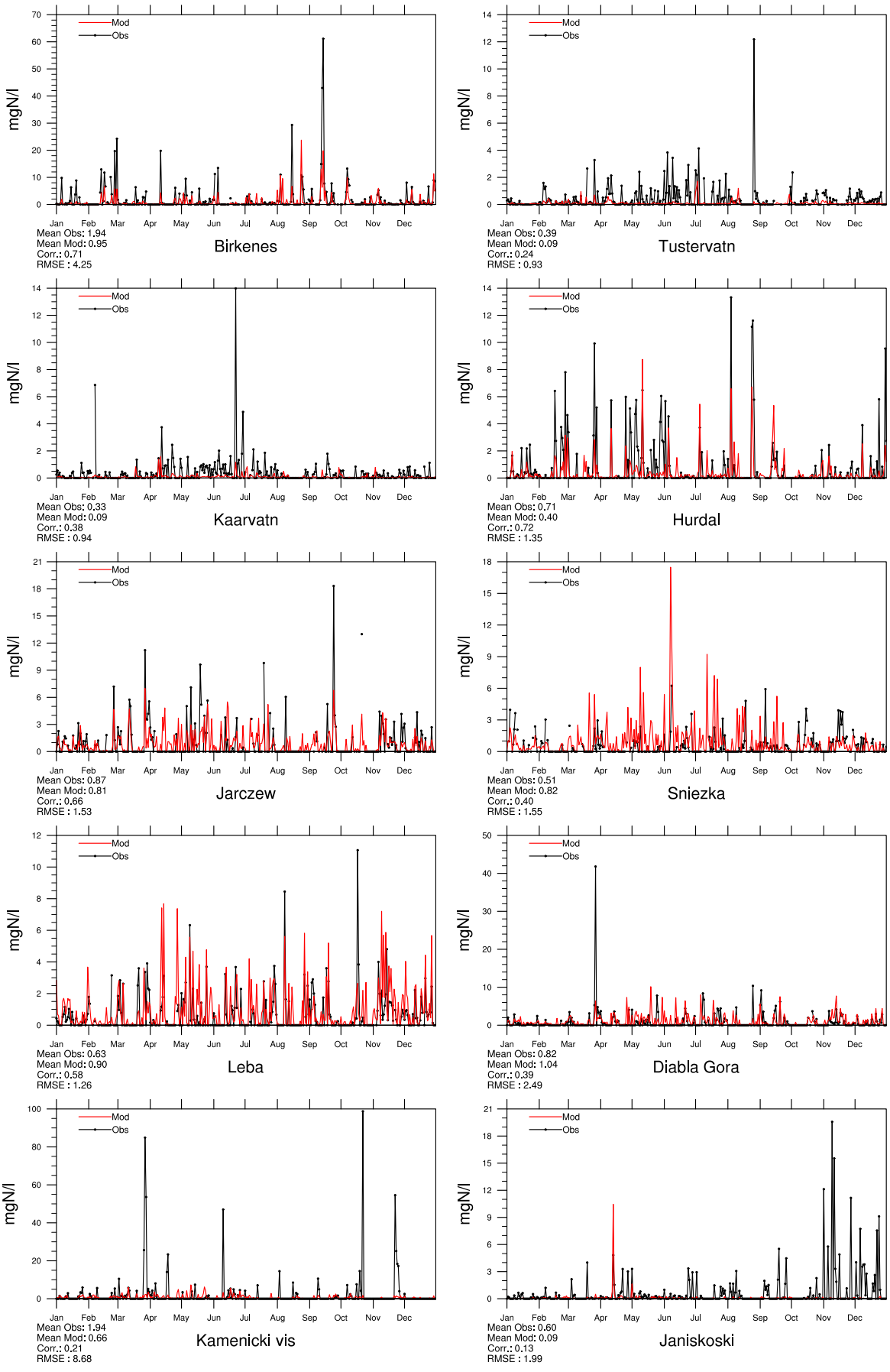

Figure 2.45: Comparison of model results and measurements (daily) for wet deposition of reduced nitrogen [mg(N)l^{-1}] in 2015.

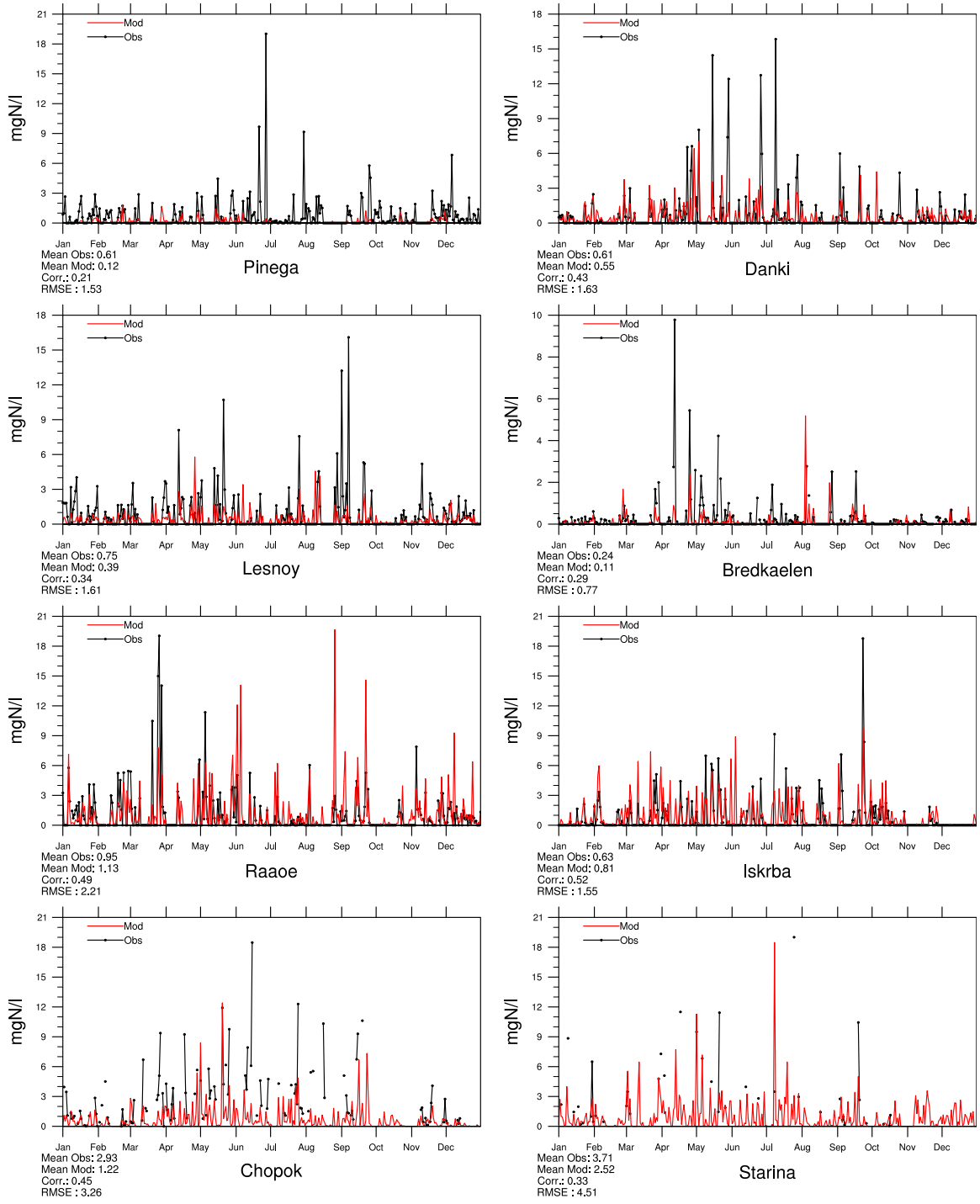

Figure 2.46: Comparison of model results and measurements (daily) for wet deposition of reduced nitrogen [mg(N)l^{-1}] in 2015.

2.3 Combined maps of model results and observations

In this section we present maps (Figures 2.47–2.49) showing both modelled and observed concentrations in air and concentrations in precipitation for selected sulphur and nitrogen species. In general, there is good agreement between model results and observations in 2015.

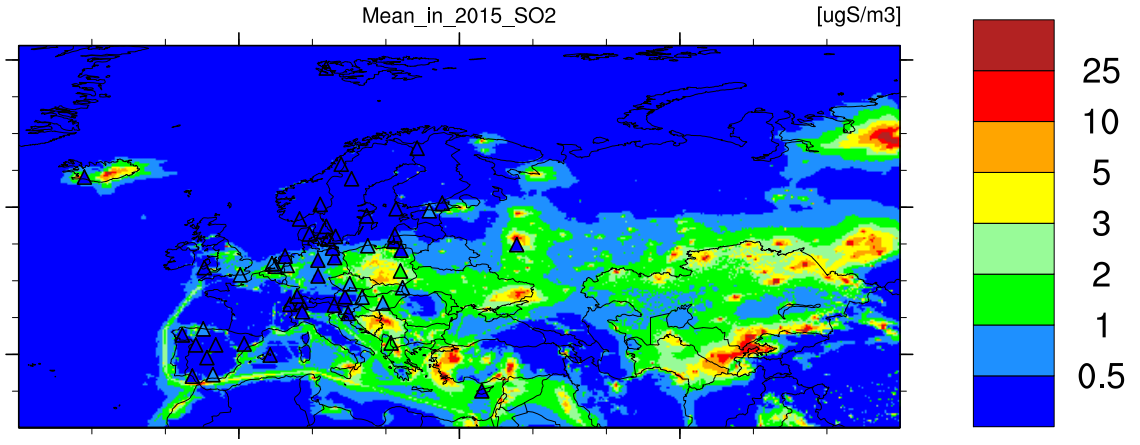

(a) SO_2

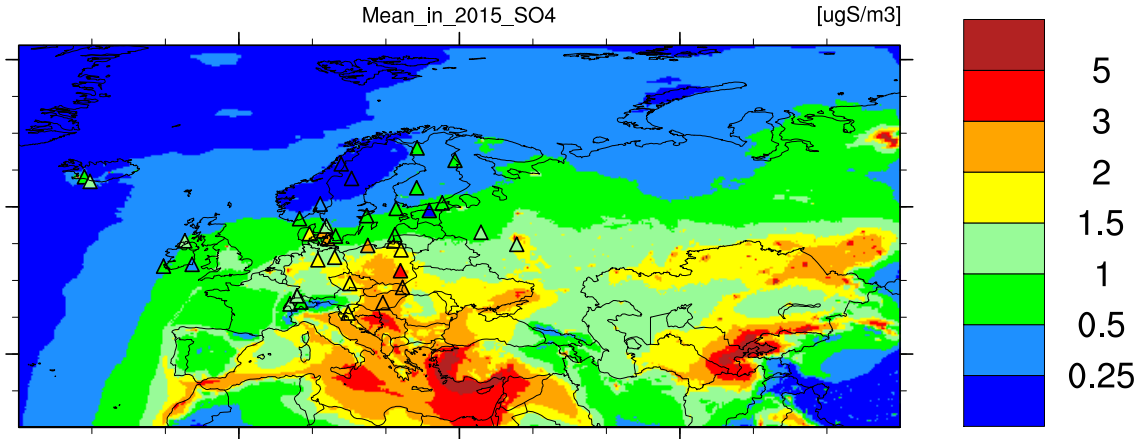

(b) SO_4^{2-}

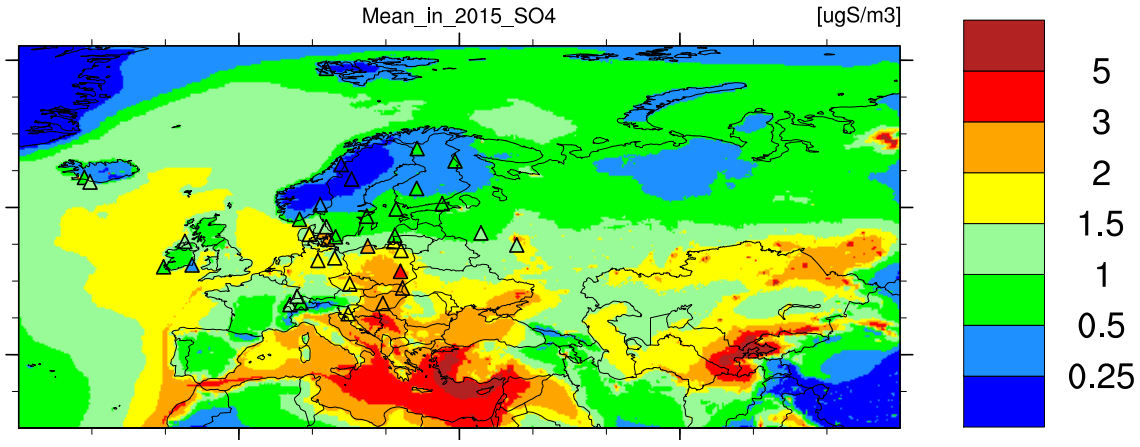

(c) SO_4^{2-}, sea salt corrected

Figure 2.47: Yearly averaged concentrations of SO_2, SO_4^{2-}, and SO_4^{2-} sea salt corrected, in air for 2015 [μg(S) m^{-3}]. The maps show model results, with observations superimposed by triangles.

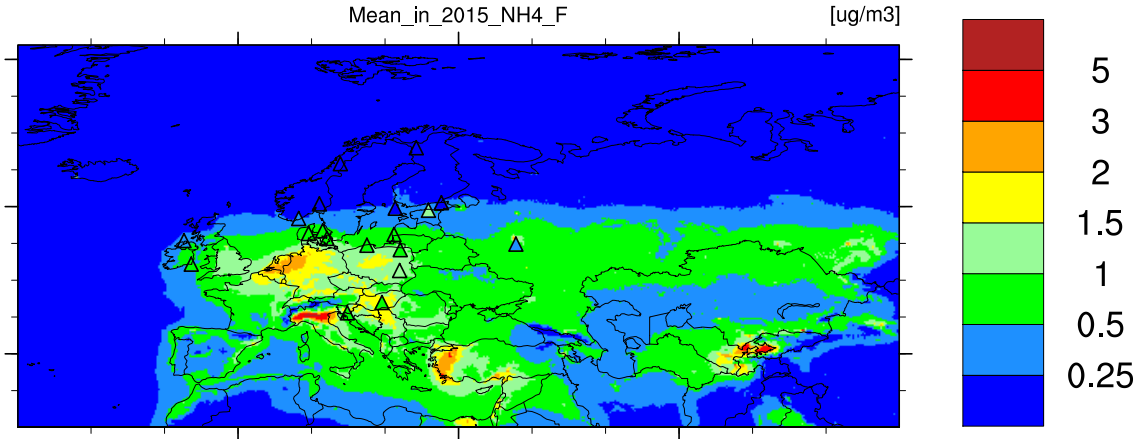

(a) NH4

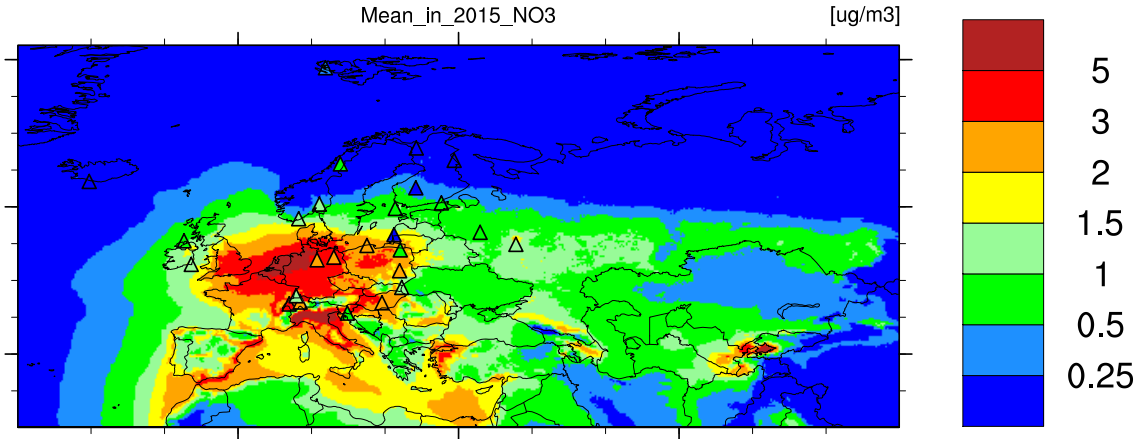

(b) TNO3

Figure 2.48: Yearly averaged concentrations of ammonium (NH_4^+) and total nitrate (TNO_3^-) in air for 2015 [μg(N) m^{-3}]. The maps show model results, with observations superimposed by triangles.

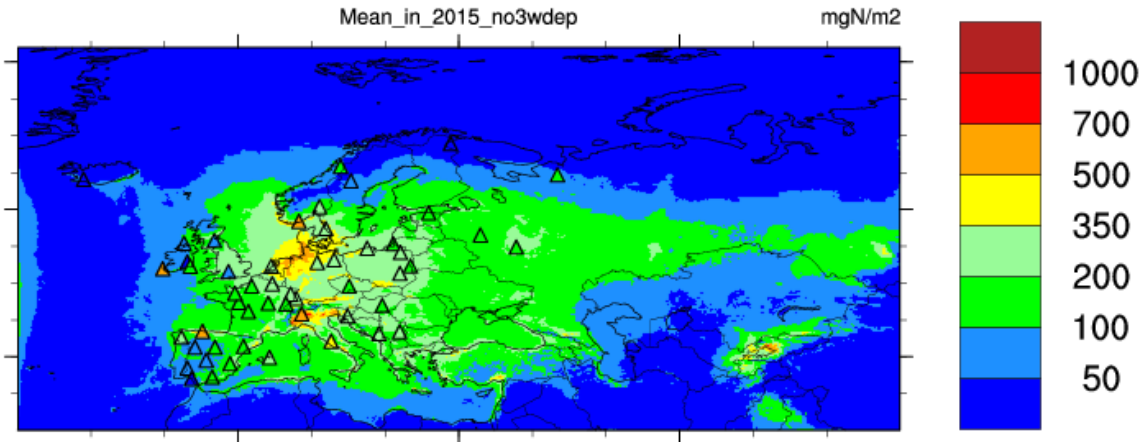

(a) WDEP OXN

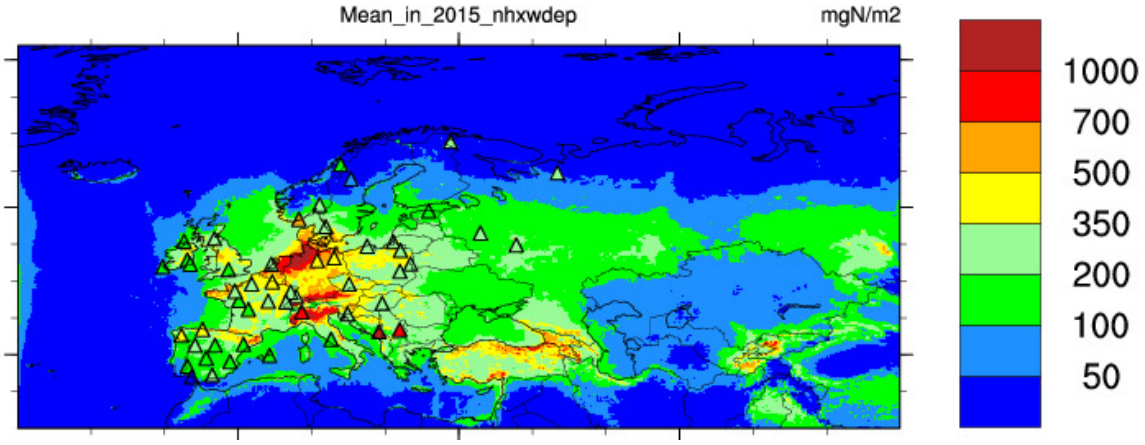

(b) WDEP RDN

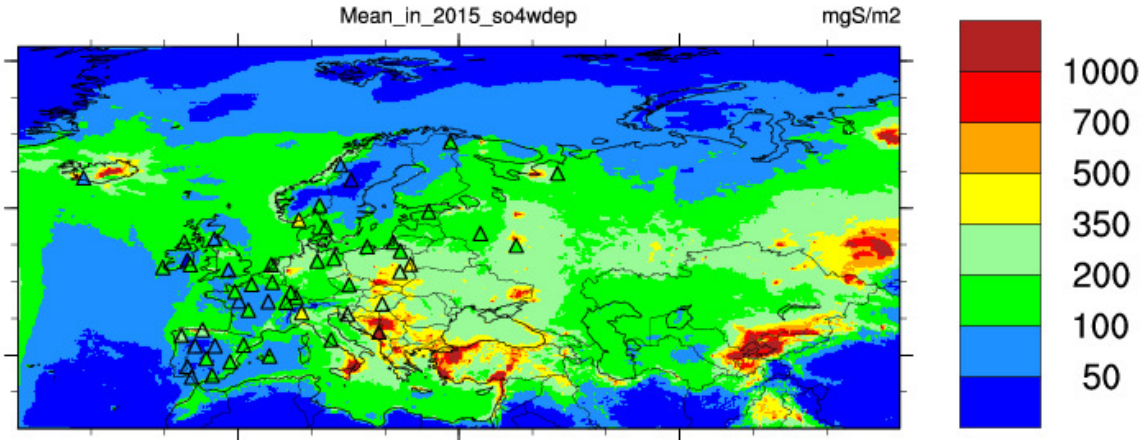

(c) WDEP SOX

Figure 2.49: Yearly wet deposition of oxidized nitrogen (OXN), reduced nitrogen (RDN), oxides of sulphur (SOX), in 2015 [μgN/m2 or μgS/m2]. The maps show model results, with observations superimposed by triangles.

References

H. Fagerli and W. Aas. Using the EMEP intensive measurement data to evaluate the performance of the EMEP model for nitrogen compounds. In *Transboundary Acidification, Eutrophication and Ground Level Ozone in Europe in 2006. EMEP Status Report 1/2008*, pages 109–126. The Norwegian Meteorological Institute, Oslo, Norway, 2008.

H. Fagerli and A.G. Hjellbrekke. Acidification and eutrophication. In *Transboundary Acidification, Eutrophication and Ground Level Ozone in Europe in 2006. EMEP Status Report 1/2008*, pages 41–56. The Norwegian Meteorological Institute, Oslo, Norway, 2008.

H. Fagerli, B. M. Steensen, and A.-G. Hjellbrekke. Acidifying and eutrophying components: validation and combined maps. Supplementary material to EMEP Status Report 1/2012, available online at `www.emep.int`, The Norwegian Meteorological Institute, Oslo, Norway, 2012.

M. Gauss, S. Tsyro, A. C. Benedictow, and A.-G. Hjellbrekke. Acidifying and eutrophying components. Supplementary material to EMEP Status Report 1/2015, available online at `www.emep.int`, The Norwegian Meteorological Institute, Oslo, Norway, 2015.

M. Gauss, S. Tsyro, H. Fagerli, A. C. Benedictow, A.-G. Hjellbrekke, and W. Aas. Acidifying and eutrophying components. Supplementary material to EMEP Status Report 1/2016, available online at `www.emep.int`, The Norwegian Meteorological Institute, Oslo, Norway, 2016.

D. Simpson, A. Benedictow, H. Berge, R. Bergström, L. D. Emberson, H. Fagerli, G. D. Hayman, M. Gauss, J. E. Jonson, M. E. Jenkin, A. Nyíri, C. Richter, V. S. Semeena, S. Tsyro, J.-P. Tuovinen, Á. Valdebenito, and P. Wind. The EMEP MSC-W chemical transport model – technical description. *Atmos. Chem. Physics*, 12(16):7825–7865, 2012. doi:10.5194/acp-12-7825-2012.

D. Simpson, S. Tsyro, P. Wind, and B. M. Steensen. Emep model development. In *Transboundary acidification, eutrophication and ground level ozone in Europe in 2011. EMEP Status Report 1/2013*. The Norwegian Meteorological Institute, Oslo, Norway, 2013.

Cort J. Willmott. On the validation of models. *Physical Geography*, 2:184–194, 1981.

Cort J. Willmott. Some comments on the evaluation of model performance. *Bulletin American Meteorological Society*, 63(11):1309–1313, 1982. doi:10.1175/1520-0477(1982)063<1309:SCOTEO>2.0.CO;2.

CHAPTER 3

Ozone and NO2

In this chapter the EMEP MSC-W model is evaluated with respect to surface ozone concentrations in air. In the following section we present tables of mean values and model performance indicators, and in Sections 3.2 and 3.3 time series are plotted for selected stations to illustrate the performance of the EMEP MSC-W model for the year 2015 with respect to ozone and NO_2. In Section 3.4 we present maps of ozone for 2015, created by combining measurements and model results.

3.1 Tables

Table 3.1 shows for daily maximum ozone and daily mean ozone the number of stations where measurements were available and data coverage criteria were satisfied (N_{stat}), measured yearly average over all stations (Obs), modelled yearly average over all stations (Mod), bias, correlation between observation and model for station yearly averages, root mean square error, and index of agreement (IOA, as defined in Section 2.1).

Model performance for daily maximum ozone is better than for daily mean ozone, mainly due to the difficulty of reproducing night-time ozone correctly. While the bias in daily mean ozone amounts to +9% it is only +4% in the case of daily maximum ozone. The correlation is about the same as last year, and around 0.7.

Modelled daily maximum ozone values have been evaluated against measurements from all stations that supply data to EMEP CCC. Table 3.2 summarises these comparisons, and Figures 3.1 to 3.19 show time series plots for selected stations representing the different regions of Europe. To judge model performance, Table 3.2 shows root mean square error (RMSE) and the *index of agreement* (IOA, defined in Section 2.1).

Similarly to last year (Gauss et al. 2016), the model performance is good for daily maximum ozone. At most of the stations, the index of agreement is between 0.7 and 0.9.

Some more detail is given in the next sections where different regions of the EMEP domain are addressed separately, along with time series plots of model results and observations.

Component	N_{stat}	Obs.	Mod.	Bias (%)	RMSE	Corr.	IOA
Ozone daily max (ppb)	111	41.36	42.81	4	3.57	0.76	0.83
Ozone daily mean (ppb)	111	32.10	35.14	9	5.21	0.68	0.71

Table 3.1: Comparison of model results and observations for 2015. Annual averages over all EMEP sites with measurements. N_{stat}= number of stations, wd=wet deposition, cp= concentration in precipitation, Corr. = spatial correlation coefficient, RMSE = root mean square error, IOA = index of agreement.

Table 3.2: Comparison of modelled versus observed ozone for year 2015. Concentrations are given as means of daily maximum ozone values [ppb]. Correlation coefficients (r), root mean square error (RMSE), and index of agreement (IOA) are included to judge the agreement between model and observations.

Code	Station	Obs. [ppb]	Mod. [ppb]	r	RMSE	IOA
		Nordic countries				
DK05	Keldsnor	37.25	39.11	0.69	6.68	0.81
DK10	Nord, Greenland	33.11	34.90	0.53	7.91	0.67
DK12	Risoe	38.85	38.15	0.77	5.94	0.86
DK31	Ulborg	39.67	40.13	0.77	5.82	0.85
FI09	Utoe	40.01	43.74	0.73	6.18	0.79
FI18	Virolahti III	34.97	37.75	0.71	5.96	0.81
FI22	Oulanka	33.54	34.99	0.73	5.20	0.84
FI37	Aehtaeri II	34.29	37.23	0.71	5.94	0.80
FI96	Pallas	36.99	35.84	0.70	5.07	0.83
NO02	Birkenes II	39.25	39.58	0.72	4.83	0.84
NO15	Tustervatn	38.49	39.38	0.65	4.85	0.80
NO39	Kaarvatn	37.20	41.82	0.63	7.68	0.70
NO42	Spitzbergen, Zeppelin	34.45	38.70	0.52	7.03	0.64
NO43	Prestebakke	37.53	39.72	0.76	5.17	0.84
NO52	Sandve	39.26	44.29	0.70	6.63	0.71
NO56	Hurdal	35.94	39.05	0.78	5.95	0.83
SE05	Bredkaelen	35.85	37.84	0.72	5.19	0.82
SE11	Vavihill	37.16	39.64	0.77	6.03	0.84
SE12	Aspvreten	34.60	41.79	0.73	8.79	0.69
SE13	Esrange	37.43	36.56	0.73	5.33	0.84
SE14	Raaoe	39.21	44.46	0.76	7.39	0.78
SE18	Asa	37.49	39.81	0.78	5.32	0.85
SE19	Oestad	37.82	39.80	0.77	5.27	0.85
SE32	Norra-Kvill	38.42	39.65	0.78	4.75	0.87
SE35	Vindeln	35.18	37.04	0.72	5.22	0.82
SE39	Grimsoe	37.51	38.33	0.74	5.18	0.84
		Eastern European Countries				
CZ01	Svratouch	42.80	44.70	0.82	8.95	0.86
CZ03	Kosetice	43.02	44.97	0.79	9.25	0.84

continued on next page

Code	Station	Obs.	Mod.	r	RMSE	IOA
CZ05	Churanov	46.12	46.97	0.79	8.58	0.83
EE09	Lahemaa	36.61	37.68	0.77	5.18	0.86
EE11	Vilsandy	40.30	43.23	0.77	5.79	0.84
HU02	K-puszta	41.51	45.61	0.82	10.15	0.86
LT15	Preila	38.82	43.79	0.78	8.03	0.81
LV10	Rucava	42.11	41.44	0.79	5.91	0.86
LV16	Zoseni	34.91	38.37	0.75	6.50	0.81
MK07	Lazaropole	58.45	48.26	0.41	15.05	0.54
PL02	Jarczew	37.51	41.64	0.87	8.35	0.89
PL03	Sniezka	49.24	44.57	0.80	8.53	0.83
PL04	Leba	40.09	41.83	0.82	6.09	0.88
PL05	Diabla Gora	38.17	40.71	0.84	7.54	0.88
SK02	Chopok	49.50	47.36	0.67	7.21	0.79
SK04	Stara Lesna	46.66	47.72	0.70	7.36	0.80
SK06	Starina	43.99	45.83	0.71	7.91	0.80
SK07	Topolniky	41.42	47.25	0.82	9.46	0.83
		Central and NW European Countries				
AT02	Illmitz	43.65	46.49	0.85	10.49	0.88
AT05	Vorhegg	42.94	47.36	0.69	9.89	0.74
AT30	Pillersdorf	41.65	44.41	0.84	10.12	0.87
AT32	Sulzberg	49.09	46.44	0.78	9.47	0.84
AT34	Sonnblick	58.51	53.12	0.61	9.48	0.69
AT38	Gerlitzen	53.03	44.45	0.74	11.65	0.73
AT40	Masenberg	47.78	45.31	0.77	8.15	0.85
AT41	Haunsberg	45.16	45.60	0.78	9.85	0.85
AT43	Forsthof	44.50	46.82	0.84	10.04	0.85
AT45	Dunkelsteinerwald	42.22	44.88	0.87	10.66	0.87
AT46	Gaenserndorf	43.19	44.70	0.84	10.47	0.87
AT47	Stixneusiedl	42.02	43.74	0.85	9.53	0.89
AT48	Zoebelboden	42.94	46.43	0.66	9.85	0.78
AT49	Grebenzen	51.28	45.13	0.61	10.25	0.69
AT50	Graz Lustbuehel	40.40	43.80	0.86	9.57	0.91
CH01	Jungfraujoch	41.92	57.08	0.51	17.02	0.47
CH02	Payerne	41.62	46.03	0.78	13.01	0.75
CH03	Taenikon	42.58	46.23	0.81	11.71	0.84
CH04	Chaumont	48.58	47.00	0.73	8.71	0.80
CH05	Rigi	48.66	46.61	0.67	10.72	0.79
DE01	Westerland/Wenningsted	41.03	44.05	0.78	6.78	0.84
DE02	Langenbruegge/Waldhof	38.87	40.29	0.84	7.84	0.89
DE03	Schauinsland	53.65	47.72	0.79	11.83	0.80
DE07	Neuglobsow	38.54	41.34	0.85	8.02	0.89
DE08	Schmuecke	44.51	43.84	0.87	8.13	0.90
DE09	Zingst	38.91	42.30	0.78	7.27	0.84
FR08	Donon	39.16	45.58	0.79	10.27	0.79
FR09	Revin	38.61	42.14	0.82	8.36	0.85
FR10	Morvan	45.89	44.37	0.72	8.58	0.77
FR13	Peyrusse Vieille	43.22	40.99	0.52	8.85	0.67

continued on next page

Code	Station	Obs.	Mod.	r	RMSE	IOA
FR14	Montandon	42.24	45.38	0.63	10.98	0.68
FR15	La Tardiere	40.67	41.40	0.57	8.25	0.74
FR16	Le Casset	51.42	49.56	0.61	7.19	0.75
FR17	Montfranc	45.41	41.71	0.64	7.89	0.72
FR18	La Coulonche	41.35	41.13	0.70	6.37	0.80
FR19	Pic du Midi	49.77	46.69	-0.07	11.15	0.31
FR23	Saint-Nazaire-le-Dser	47.78	47.00	0.79	9.53	0.80
FR25	Verneuil	42.77	41.91	0.72	8.46	0.78
FR30	Puy de Dme	51.24	44.73	0.66	9.68	0.66
GB02	Eskdalemuir	36.60	40.32	0.75	5.79	0.78
GB06	Lough Navar	37.52	39.96	0.74	5.33	0.80
GB13	Yarner Wood	40.68	41.04	0.65	6.14	0.77
GB14	High Muffles	40.04	40.55	0.60	6.90	0.74
GB15	Strath Vaich Dam	41.00	40.06	0.68	4.68	0.81
GB31	Aston Hill	38.56	40.83	0.66	5.60	0.78
GB33	Bush	36.99	39.95	0.74	5.57	0.79
GB35	Great Dun Fell	35.75	40.84	0.39	8.12	0.58
GB36	Harwell	37.68	39.78	0.62	6.62	0.76
GB37	Ladybower	36.70	36.92	0.65	1.92	0.81
GB38	Lullington Heath	36.83	42.79	0.64	8.70	0.67
GB39	Sibton	37.25	39.70	0.73	6.77	0.81
GB43	Narberth	37.96	41.03	0.70	5.63	0.77
GB45	Wicken Fen	39.87	40.00	0.75	6.19	0.84
GB48	Auchencorth Moss	37.02	40.71	0.72	5.54	0.76
GB49	Weybourne	39.61	41.35	0.74	6.37	0.82
GB50	St. Osyth	35.74	42.65	0.70	9.23	0.71
GB52	Lerwick	40.17	38.93	0.76	4.06	0.86
GB53	Charlton Mackrell	40.24	39.39	0.59	6.34	0.74
IE01	Valentia Obs.	38.75	42.19	0.75	5.17	0.78
IE31	Mace Head	42.87	42.94	0.64	4.49	0.79
NL07	Eibergen	33.44	38.92	0.86	9.98	0.84
NL09	Kollumerwaard	36.25	40.20	0.80	7.90	0.83
NL10	Vreedepeel	36.61	39.39	0.88	8.62	0.89
NL44	Cabauw Wielsekade	34.98	35.86	0.83	8.03	0.87
NL91	De Zilk	37.69	38.04	0.83	7.35	0.88
		Mediterranean Countries				
CY02	Ayia Marina	54.49	47.03	0.54	10.19	0.60
ES01	Toledo	52.55	47.50	0.70	10.46	0.70
ES05	Noia	42.75	42.44	0.65	6.77	0.76
ES06	Mahon	45.36	42.34	0.37	9.31	0.57
ES07	Viznar	50.72	48.12	0.72	9.83	0.76
ES08	Niembro	44.12	42.81	0.72	5.59	0.83
ES09	Campisabalos	43.90	46.59	0.71	7.03	0.79
ES10	Cabo de Creus	42.71	48.86	0.72	8.77	0.74
ES11	Barcarrota	39.44	44.96	0.63	10.62	0.67
ES12	Zarra	51.36	45.35	0.65	10.50	0.66
ES13	Penausende	44.78	45.09	0.75	6.27	0.83

continued on next page

Code	Station	Obs.	Mod.	r	RMSE	IOA
ES14	Els Torms	46.79	44.56	0.81	8.60	0.81
ES16	O Savinao	39.47	42.92	0.68	8.63	0.73
ES17	Doana	46.91	48.94	0.73	7.13	0.83
GR01	Aliartos	43.90	45.33	0.68	10.95	0.67
GR02	Finokalia	52.88	51.70	0.59	7.00	0.73
IT01	Montelibretti	42.95	52.89	0.77	14.97	0.81
IT04	Ispra	44.21	55.89	0.83	17.77	0.85
MT01	Giordan lighthouse	51.67	49.75	0.32	8.48	0.60
SI08	Iskrba	44.36	46.08	0.74	9.34	0.77
SI31	Zarodnje	50.80	46.06	0.81	10.24	0.82
SI32	Krvavec	55.09	46.96	0.74	11.26	0.72
SI33	Kovk	55.07	47.95	0.77	13.11	0.74

3.2 Time series for ozone

In this section we present time series plots for a selection of stations that have supplied data on ozone levels to EMEP CCC for 2015. The plots show daily model results and measurements of ozone, where available.

Nordic sites

In addition to the statistics for the Nordic sites listed in Table 3.2, measured and modelled ozone levels are compared for Nordic sites in Figures 3.1–3.4. As seen in the plots the model performs well for ozone, both in terms of levels and seasonality.

At the majority of Nordic sites the IOA is between 0.8 and 0.9. Among the 20 sites, for which data were analyzed both in Gauss et al. (2016) and this year, the model performance has decreased at most sites, but the magnitude of these changes is small.

The biases are positive in most cases (more positive biases than last year). Stations with relatively large ($>$ 3ppb) biases are Utoe (FI09), Kaarvatn (NO39), Spitzbergen (NO42), Hurdal (NO56), Sandve (NO52), Aspvreten (SE12), and Raaoe (SE14). DK10, NO42, and SE12 are the only stations where the Index of Agreement is lower than 0.7.

Eastern European sites

Measured and modelled maximum ozone levels for sites in the Eastern European region are shown in Figures 3.5 to 3.7. These sites are mostly typical continental sites with a clear summer maximum, reflecting local/regional ozone production in summer, and a winter minimum. In general the model performance is rather good, and largely in line with the performance in earlier years (Gauss et al. 2015,?).

Out of the 17 sites, for which data were analized both in (Gauss et al. 2016) and this year, the model performance, in terms of the index of agreement, has increased at 9 sites, decreased at 7 sites and remained unchanged at 1 site. The index of agreement is larger than 0.8 at most stations, and below 0.7 only at one station (MK07).

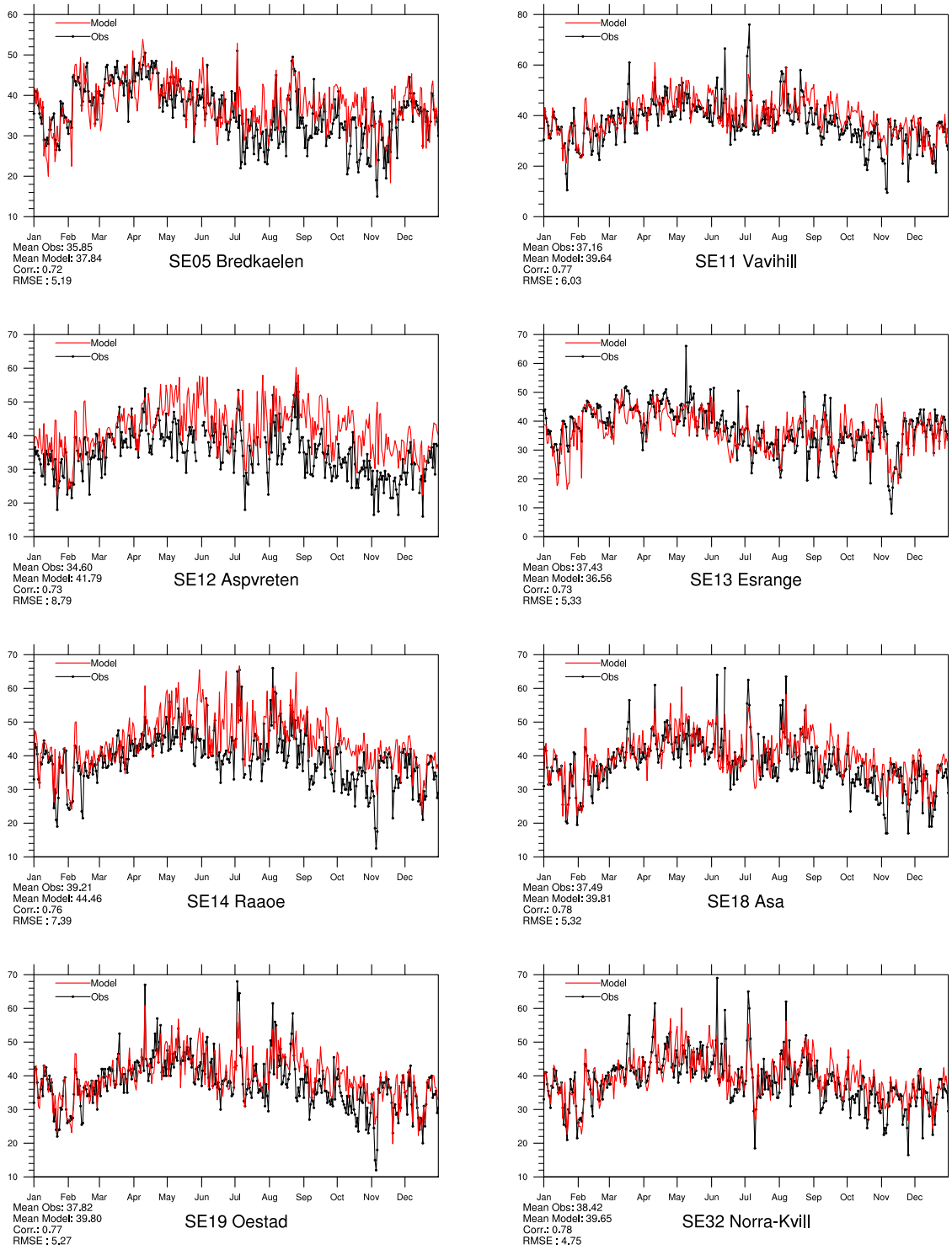

Figure 3.1: Modelled versus Observed Daily Maximum Ozone [ppb] at Swedish sites for 2015. *Note that in some plots the vertical axis does not start at zero.*

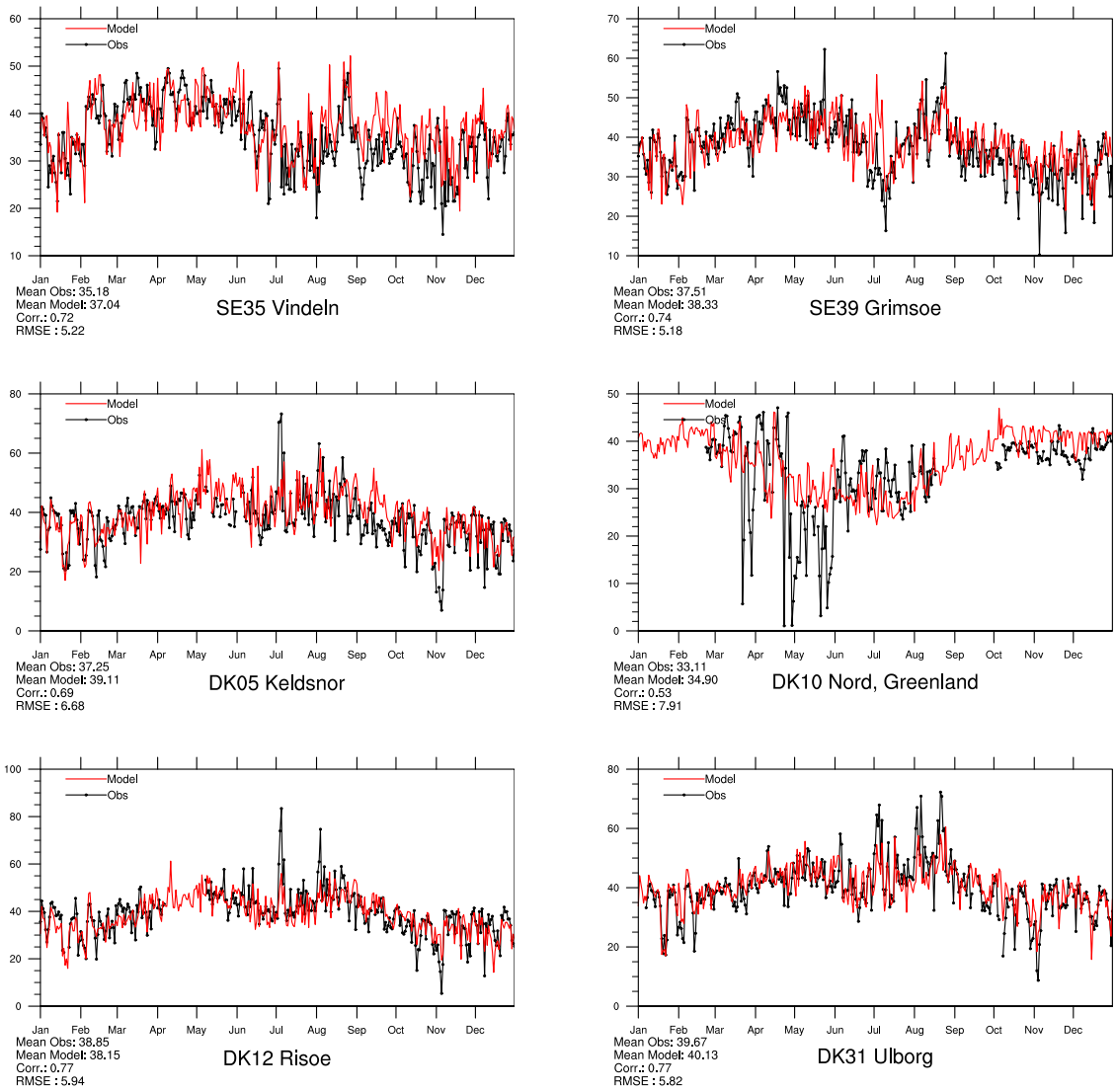

Figure 3.2: Modelled versus Observed Daily Maximum Ozone [ppb] at Swedish and Danish sites for 2015. *Note that in some plots the vertical axis does not start at zero.*

The bias is postive at most sites, but biases >3ppb are seen only at HU02, LT15, LV16, MK07 (large and negative), PL03 (negative), and SK07.

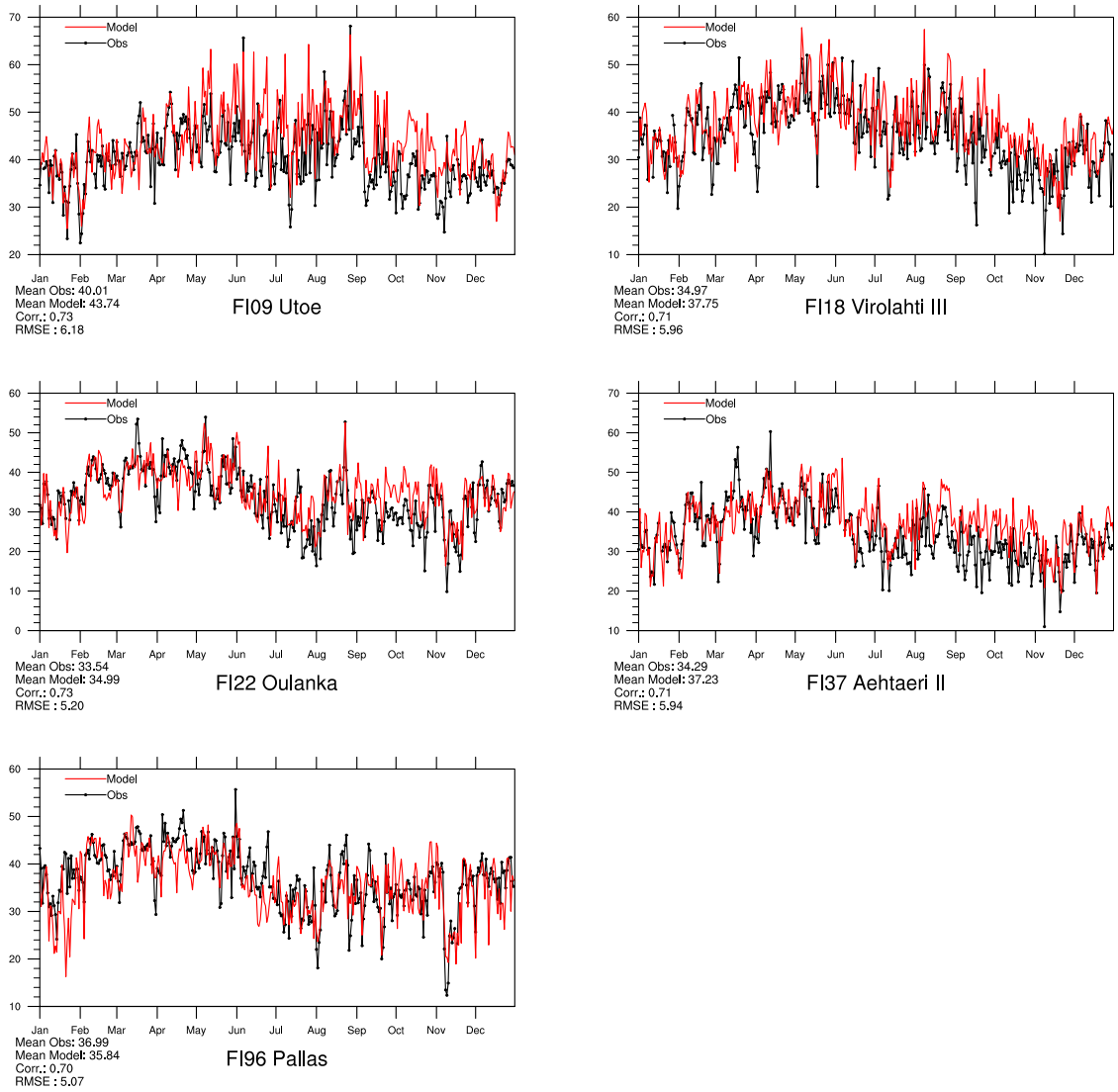

Figure 3.3: Modelled versus Observed Daily Maximum Ozone [ppb] at Finnish sites for 2015. *Note that in some plots the vertical axis does not start at zero.*

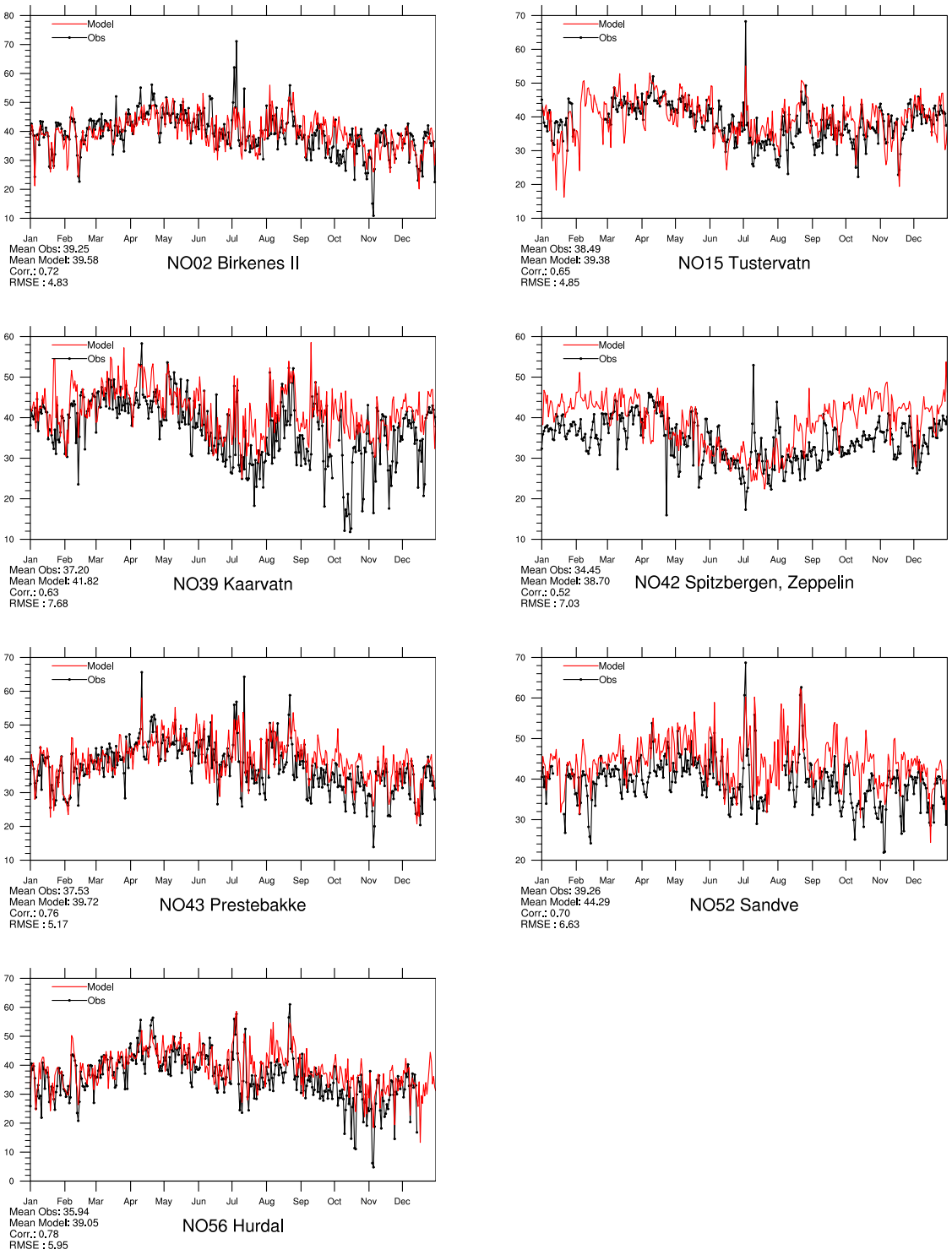

Figure 3.4: Modelled versus Observed Daily Maximum Ozone [ppb] at Norwegian sites for 2015. *Note that in some plots the vertical axis does not start at zero.*

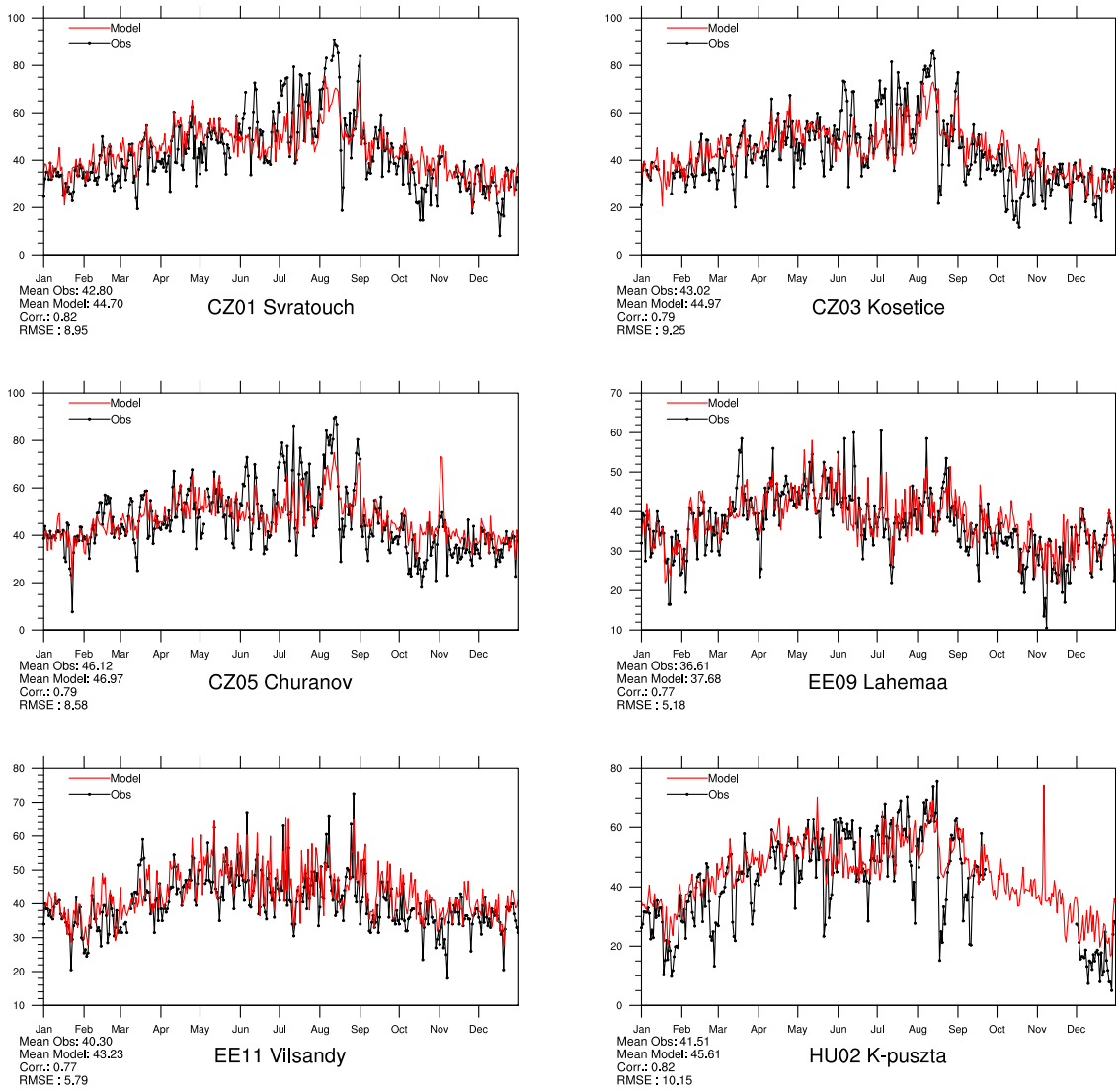

Figure 3.5: Modelled versus Observed Daily Maximum Ozone [ppb] at Eastern European sites for 2015. *Note that in some plots the vertical axis does not start at zero.*

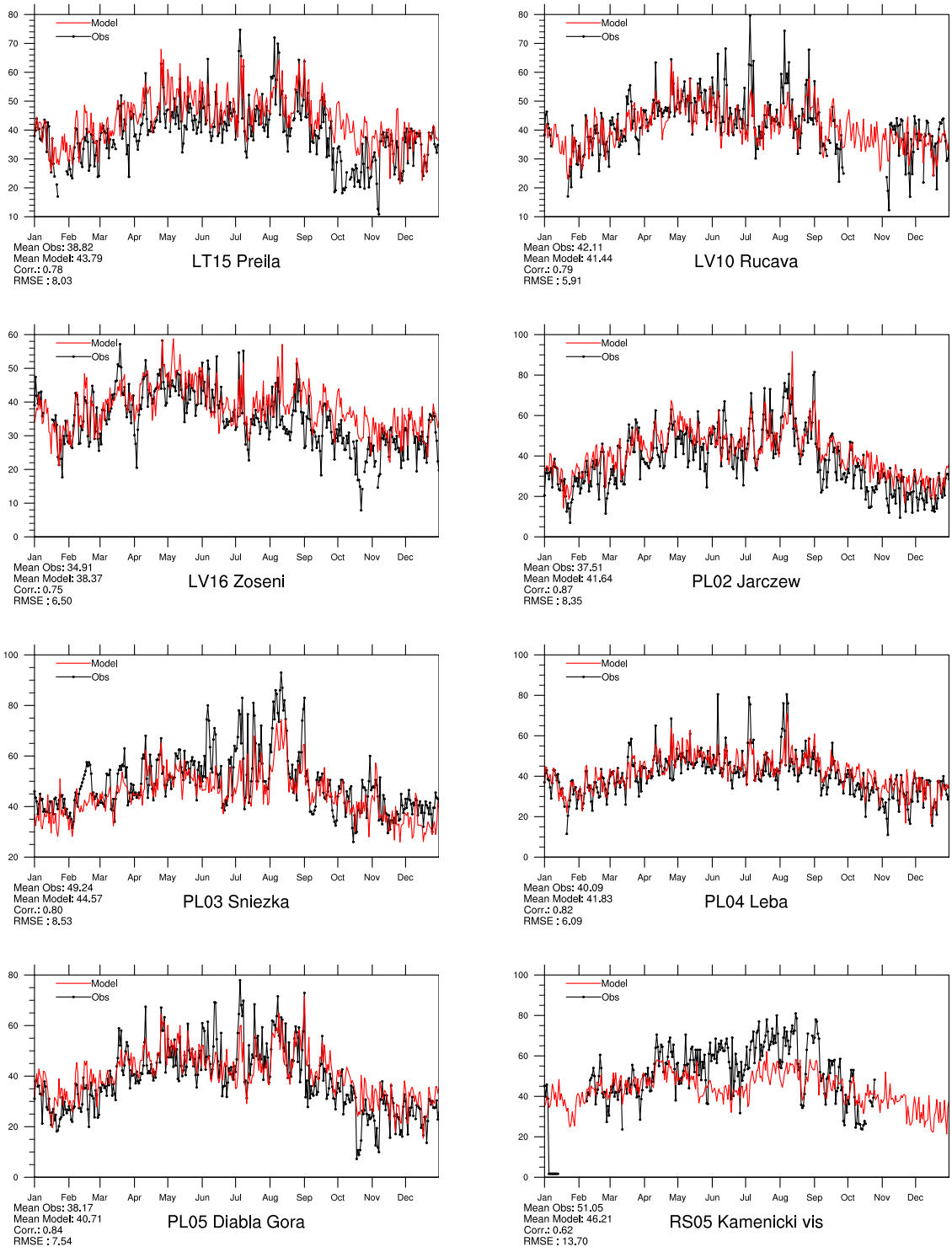

Figure 3.6: Modelled versus Observed Daily Maximum Ozone [ppb] at Eastern European sites for 2015. *Note that in some plots the vertical axis does not start at zero.*

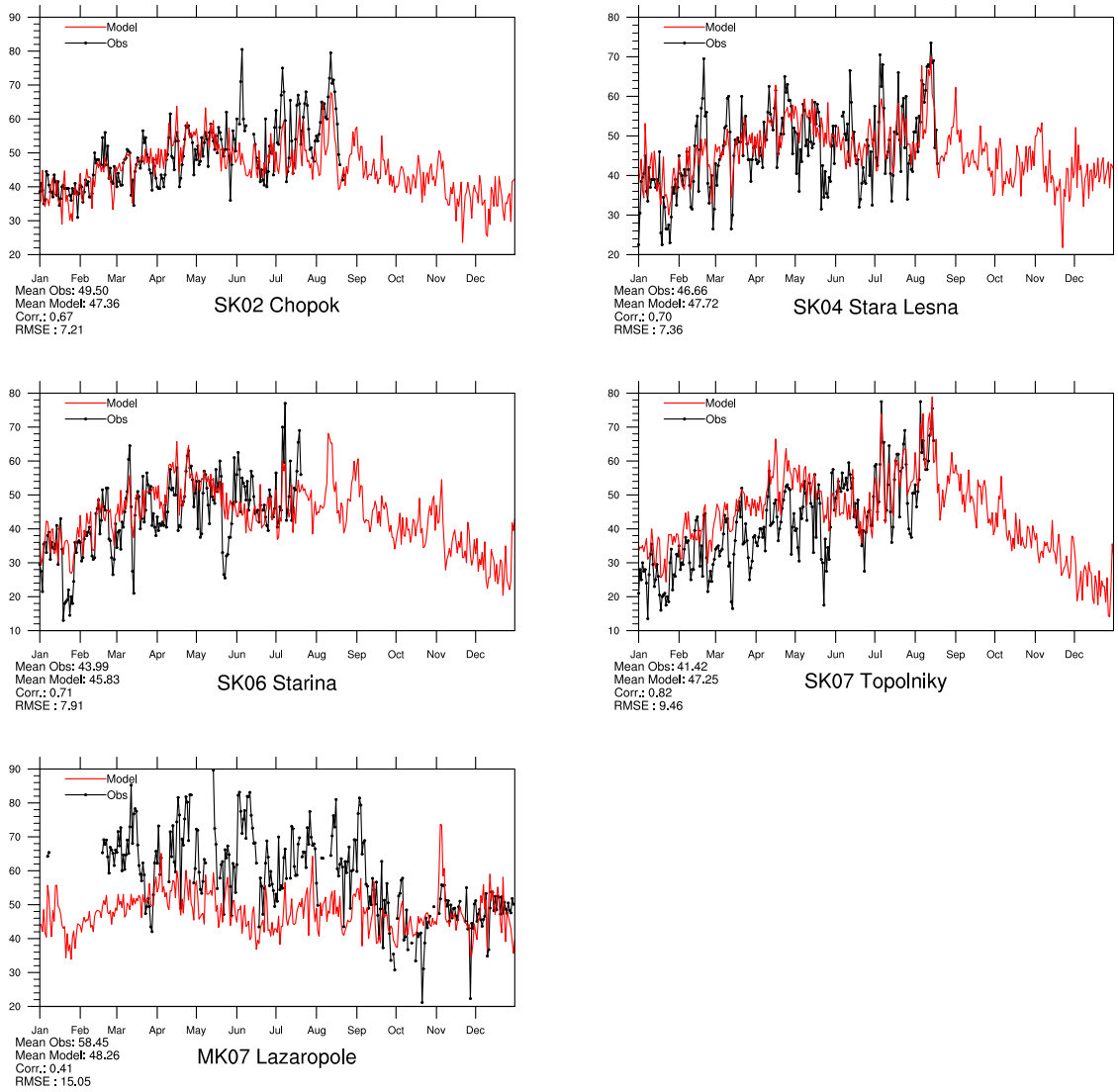

Figure 3.7: Modelled versus Observed Daily Maximum Ozone [ppb] at Eastern European sites for 2015. *Note that in some plots the vertical axis does not start at zero.*

Central and Northwestern European sites

Measured and modelled maximum ozone levels for selected sites in Central and Northwestern Europe are shown in Figures 3.8–3.16. These sites are mainly typical continental sites with a clear summer maximum, reflecting local/regional ozone production in summer, and a winter minimum. Concentrations at the site Mace Head in Ireland (IE31) are partly used to specify background conditions for the EMEP model, so that good performance, at least for the seasonal cycle, is guaranteed.

The overall model performance is good in this area, but the index of agreement has decreased with respect to last year (Gauss et al. 2016) at a majority of stations.

As usual, the comparison between model and observation has problems in mountainous areas, most notably at Jungfraujoch (CH01), Sonnblick (AT34), Le Casset (FR16), Pic du Midi (FR19), and Puy de Dome (FR30). Relatively large biases ($>$ 3ppb) biases are found mainly in the Alps, but also at DE01, DE03, DE09, FR08, FR09, FR14, FR17, FR19, FR30, GB02, GB35, GB38, GB43, GB48, GB50, IE01, NL07, and NL09.

Mediterranean sites

Measured and modelled ozone levels for selected sites in the Mediterranean region are shown in Figures 3.17–3.19. The meteorological situation in and around the Mediterranean basin differs considerably from the rest of Europe. This region also receives more solar radiation resulting in conditions favourable for ozone production. Hence these sites have some of the highest ozone levels in Europe.

In general the model performance is good for most sites in this region, with IOA values between 0.7 and 0.9. Exceptions with IOA below 0.7 are CY02, ES06, ES11, ES12, GR01, and MT01.

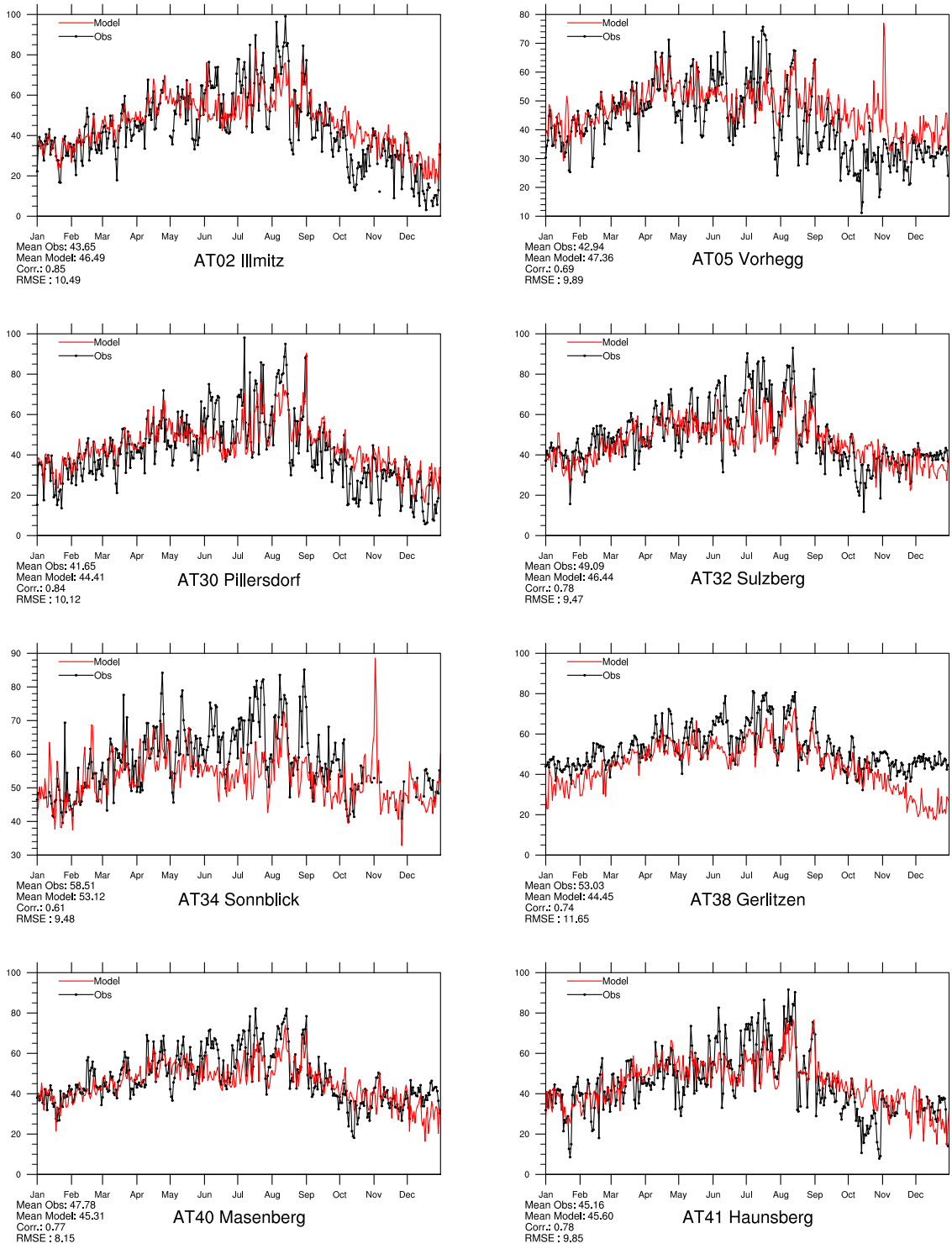

Figure 3.8: Modelled versus Observed Daily Maximum Ozone [ppb] at Austrian sites for 2015. *Note that in some plots the vertical axis does not start at zero.*

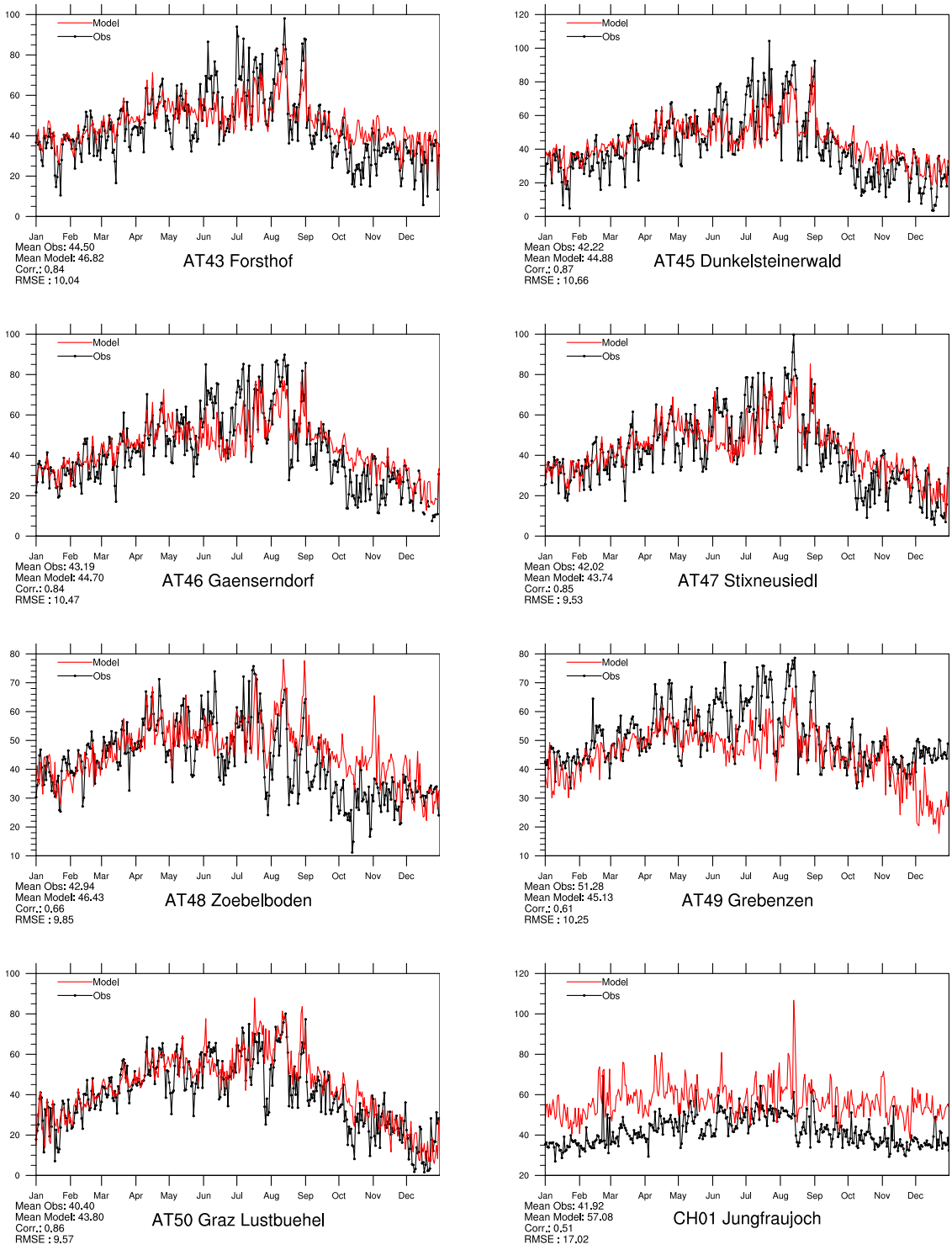

Figure 3.9: Modelled versus Observed Daily Maximum Ozone [ppb] at Austrian sites for 2015.

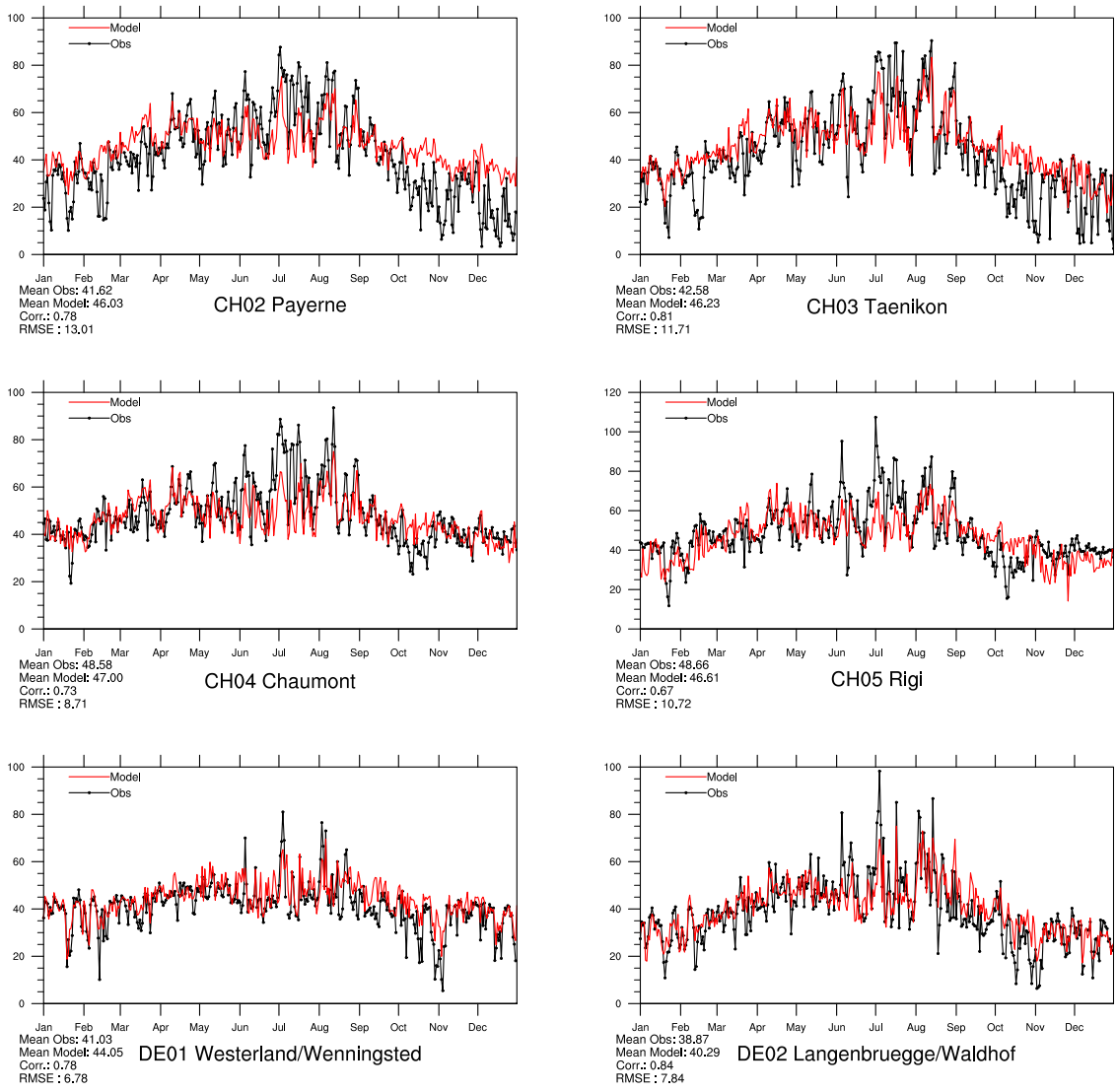

Figure 3.10: Modelled versus Observed Daily Maximum Ozone [ppb] at sites in Belgium and Switzerland for 2015. *Note that in some plots the vertical axis does not start at zero.*

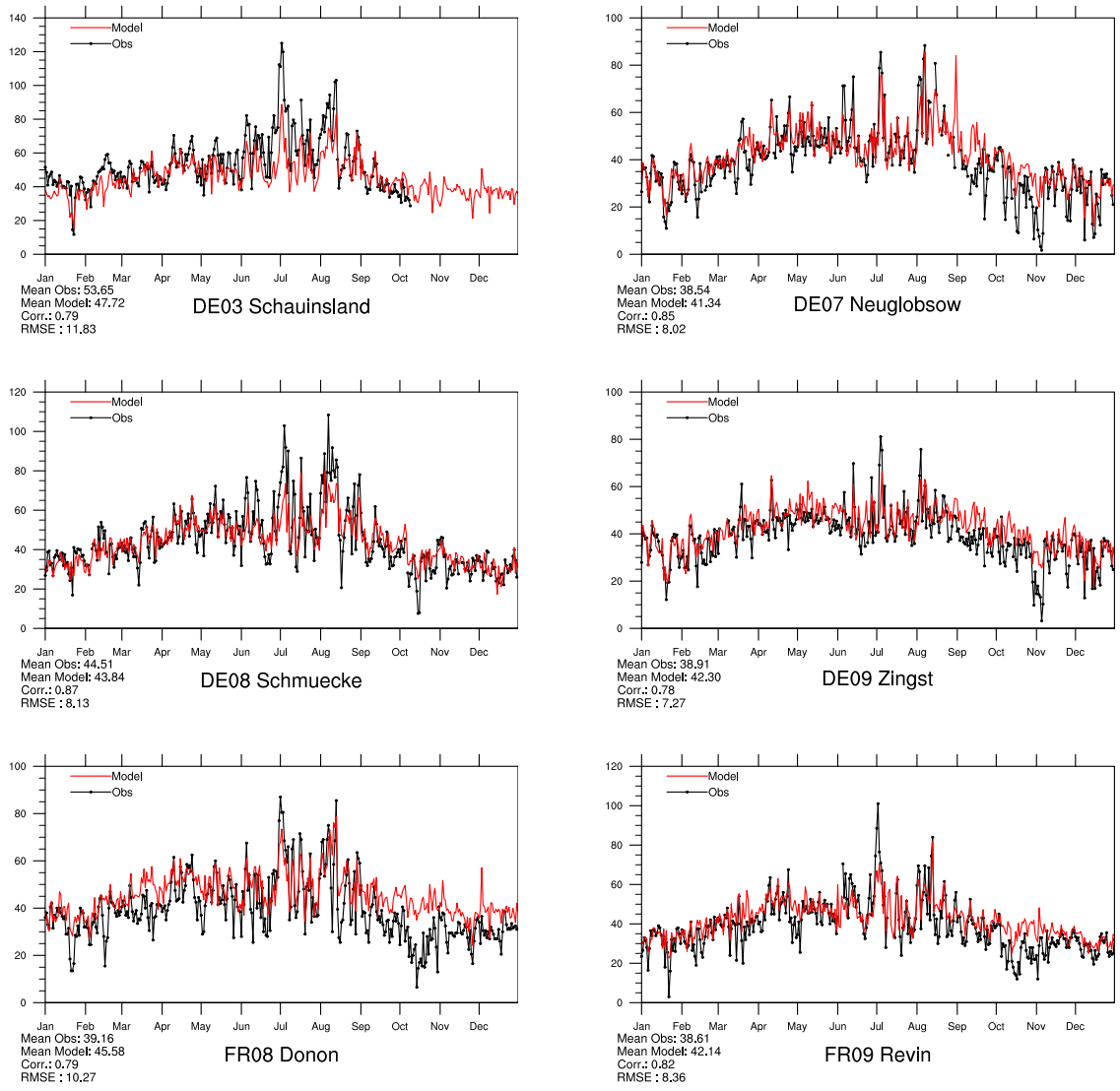

Figure 3.11: Modelled versus Observed Daily Maximum Ozone [ppb] at sites in Germany and France for 2015. *Note that in some plots the vertical axis does not start at zero.*

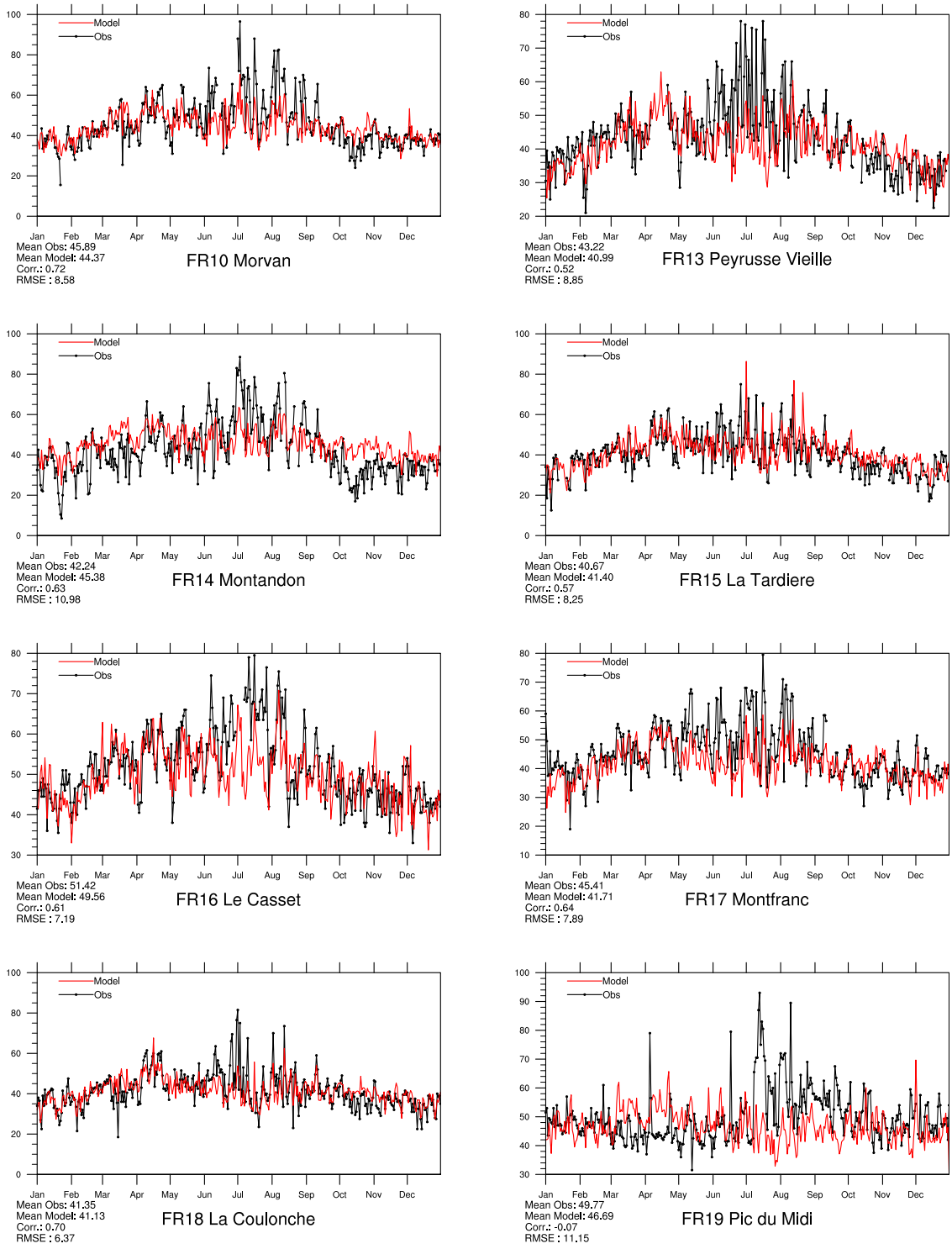

Figure 3.12: Modelled versus Observed Daily Maximum Ozone [ppb] at French sites for 2015. *Note that in some plots the vertical axis does not start at zero.*

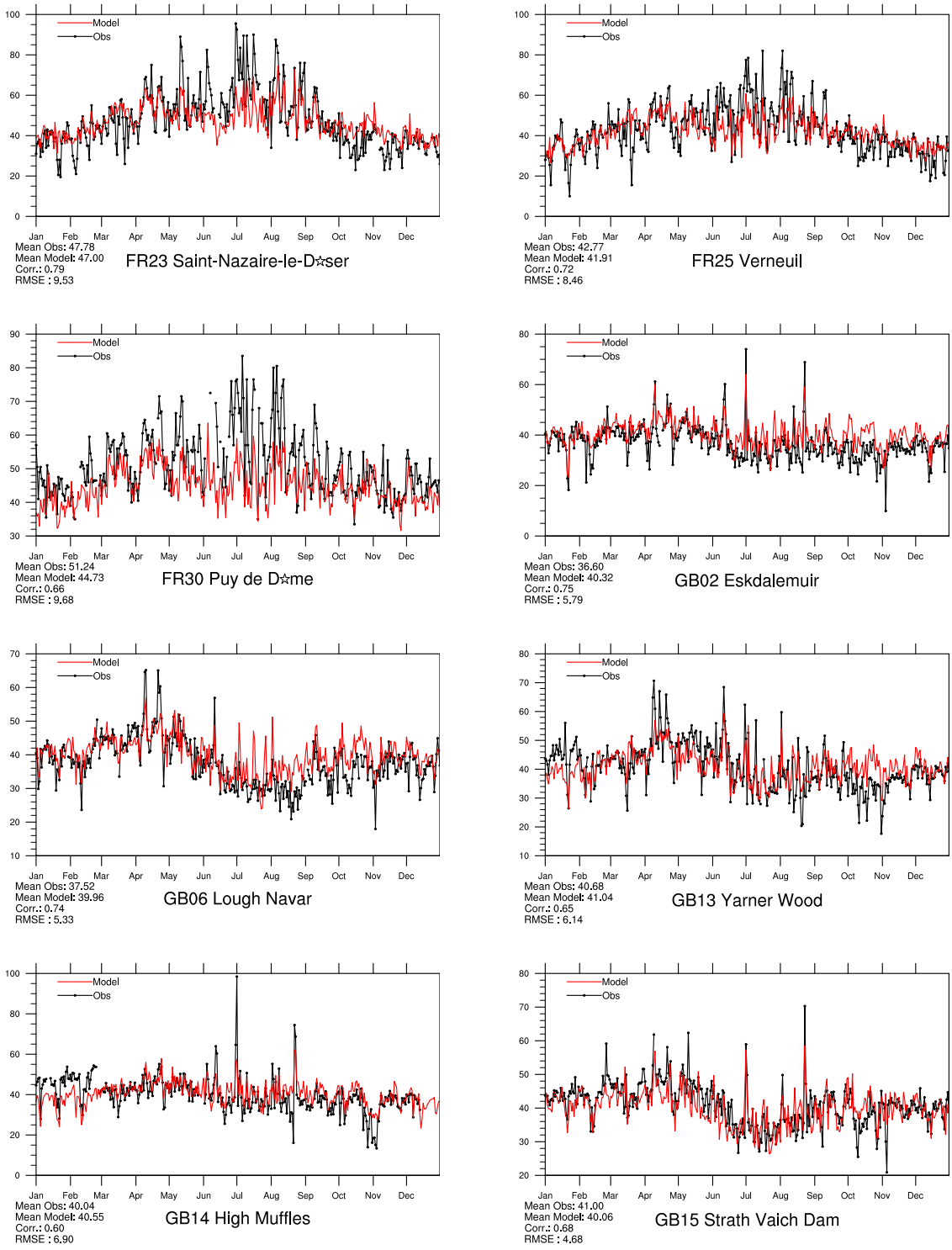

Figure 3.13: Modelled versus Observed Daily Maximum Ozone [ppb] at French and British sites for 2015. *Note that in some plots the vertical axis does not start at zero.*

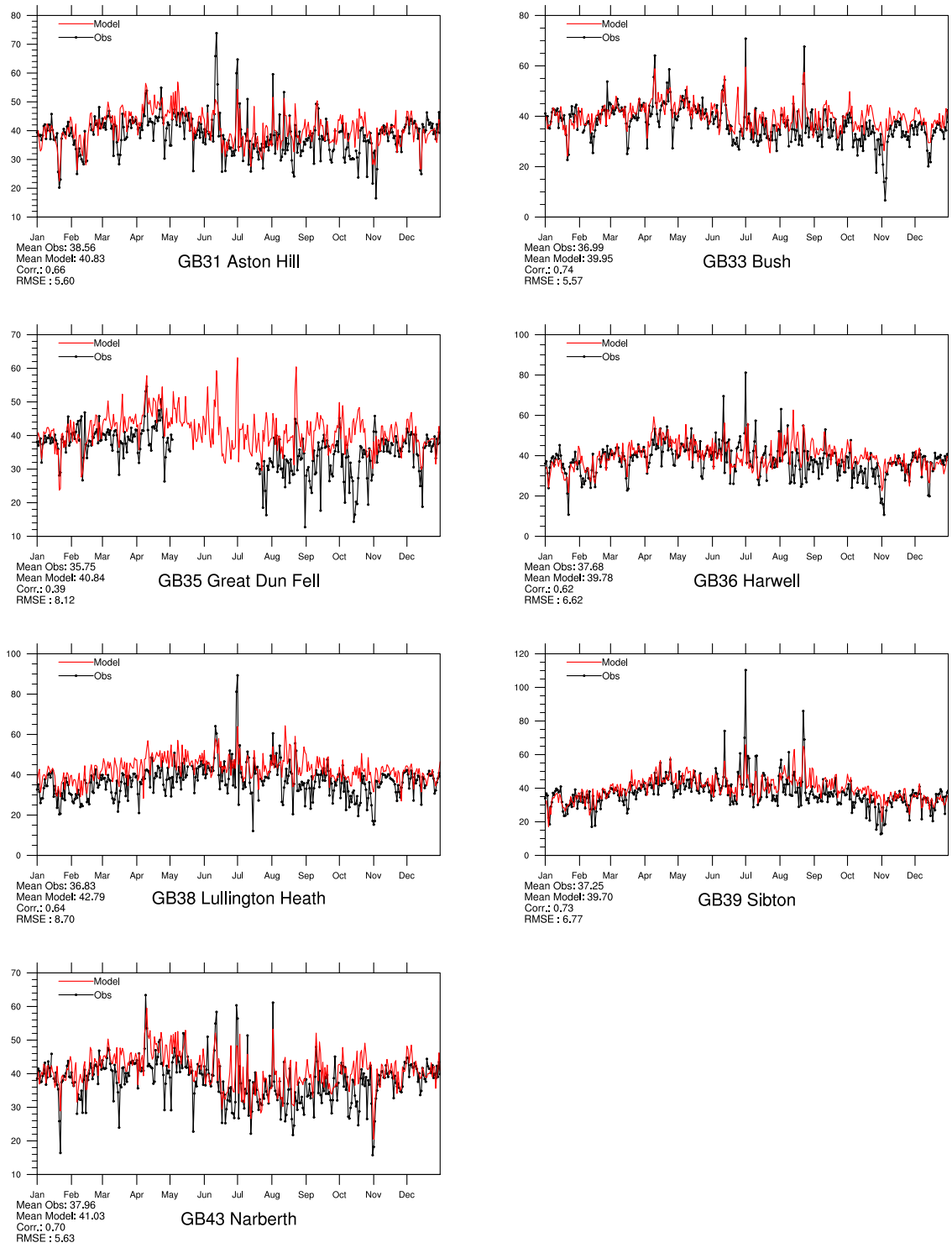

Figure 3.14: Modelled versus Observed Daily Maximum Ozone [ppb] at British sites for 2015. *Note that in some plots the vertical axis does not start at zero.*

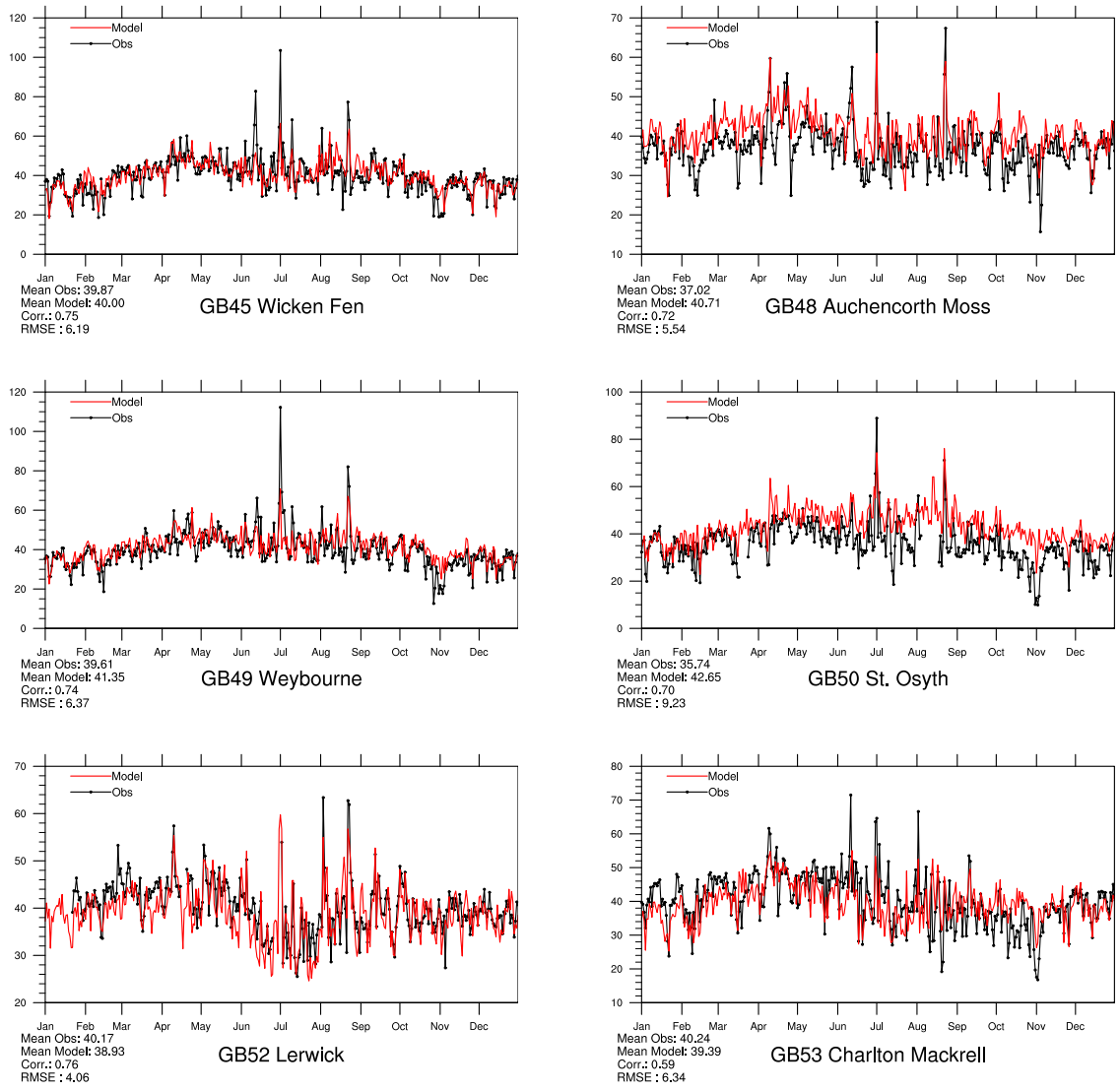

Figure 3.15: Modelled versus Observed Daily Maximum Ozone [ppb] at British sites for 2015. *Note that in some plots the vertical axis does not start at zero.*

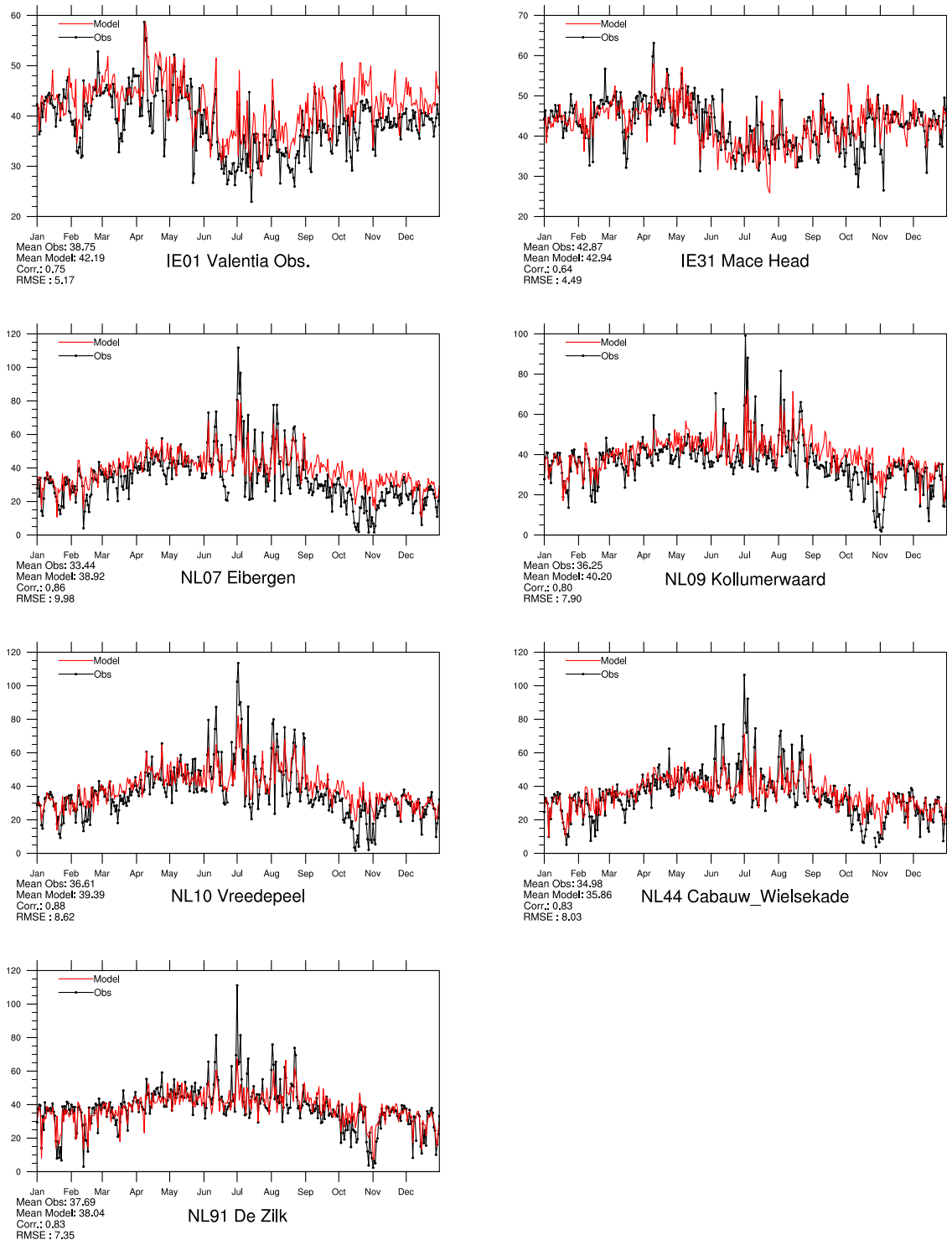

Figure 3.16: Modelled versus Observed Daily Maximum Ozone [ppb] at Irish and Dutch sites for 2015. *Note that in some plots the vertical axis does not start at zero.*

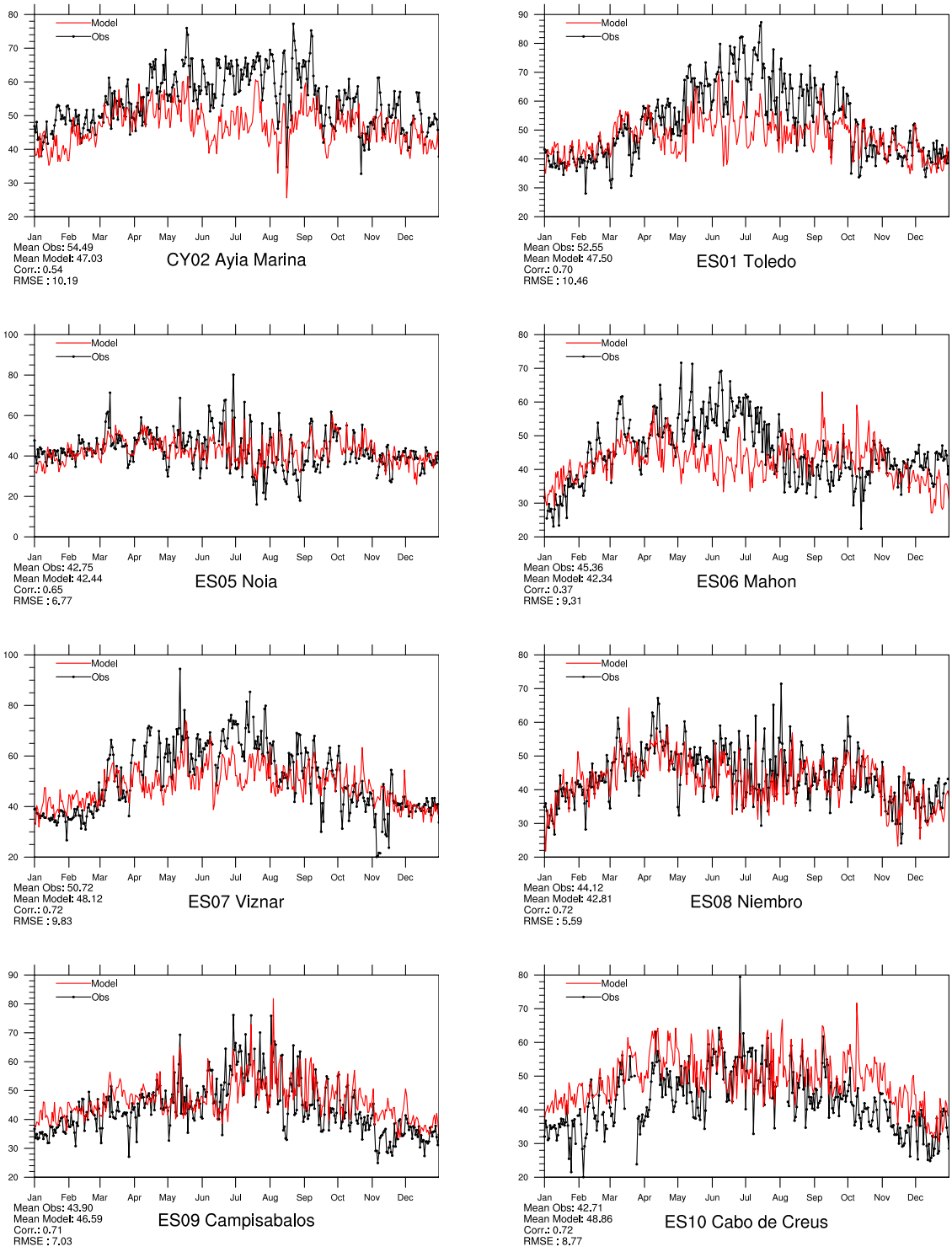

Figure 3.17: Modelled versus Observed Daily Maximum Ozone [ppb] at Mediterranean sites (Cyprus and Spain) for 2015. *Note that in some plots the vertical axis does not start at zero.*

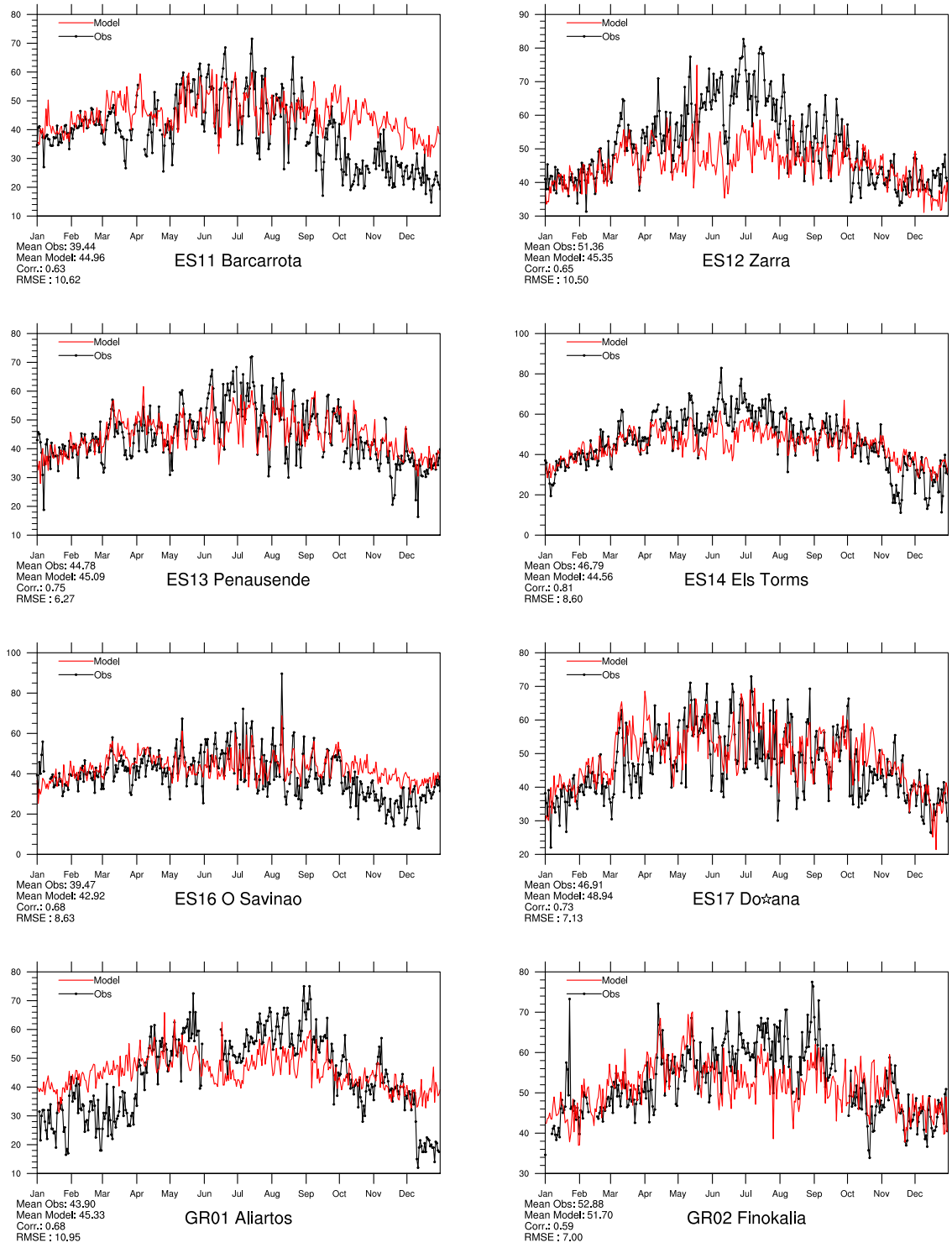

Figure 3.18: Modelled versus Observed Daily Maximum Ozone [ppb] at Mediterranean Sites (Spain and Greece) for 2015. *Note that in some plots the vertical axis does not start at zero.*

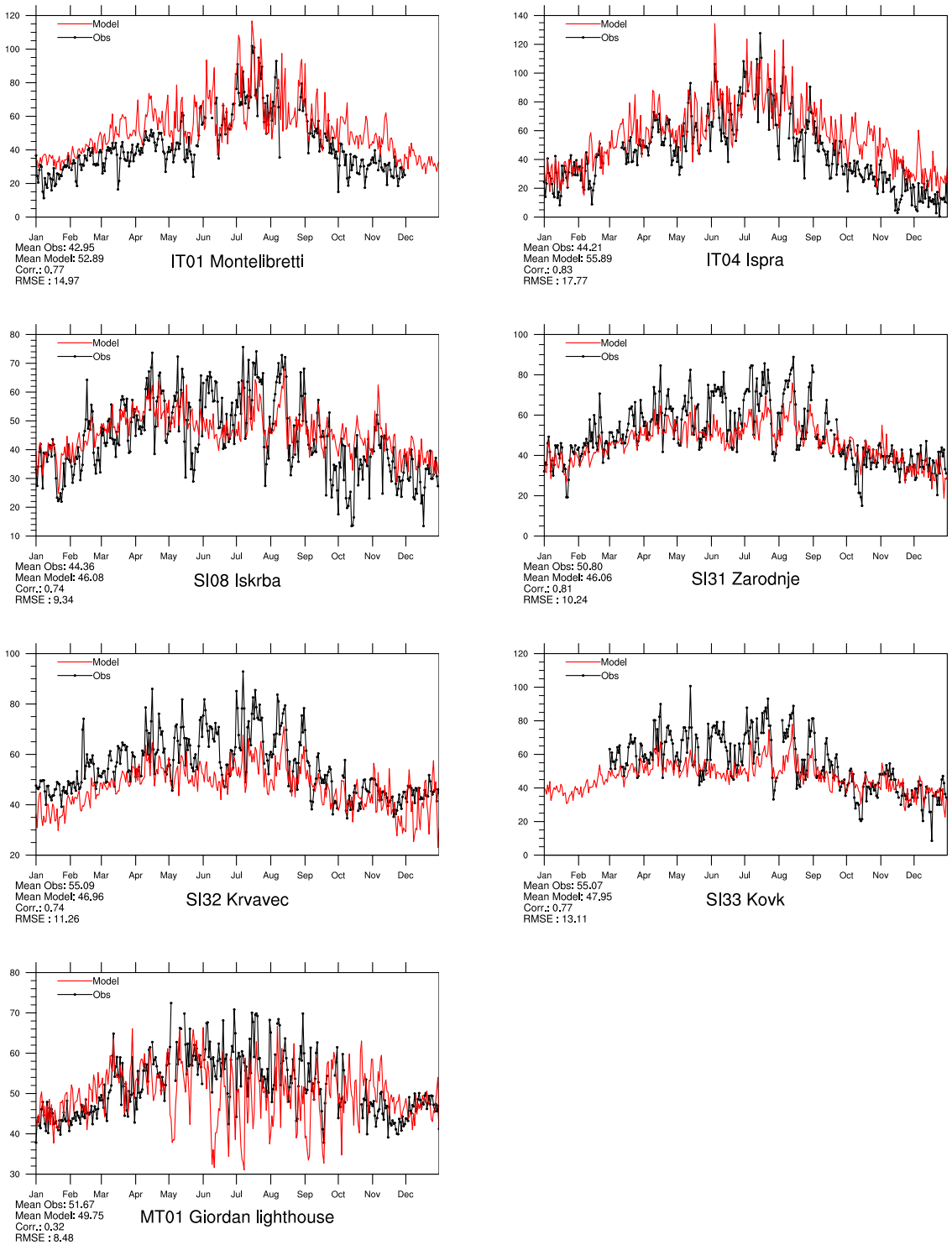

Figure 3.19: Modelled versus Observed Daily Maximum Ozone [ppb] at Mediterranean Sites for 2015.

3.3 Time series for nitrogen dioxide

In this section we present time series plots for a selection of stations that have supplied data on NO_2 levels to EMEP CCC for 2015. The plots show daily model results and measurements of NO_2, where available. The plots are arranged in alphabetical order by country code.

After communication with the providers of measurements (via CCC), specific comments about selected stations are added here for reference:

- AM01 (Amberd/Armenia): Very low NO_2 concentrations were measured compared to the model, but this is consistent with earlier years and the temporal variability is in better agreement;
- IE01 (Valentina Observatory/Ireland): The high measured NO_2 values have been discussed with MET Ireland. Parallel measurements confirm the high concentrations. The sources for these are, however, unclear;
- NO39 (Kårvatn/Norway): A high NO_2 peak was measured on 11 August. Higher levels have been observed at this site earlier due to episodes. There is no indication for contamination or similar issues.

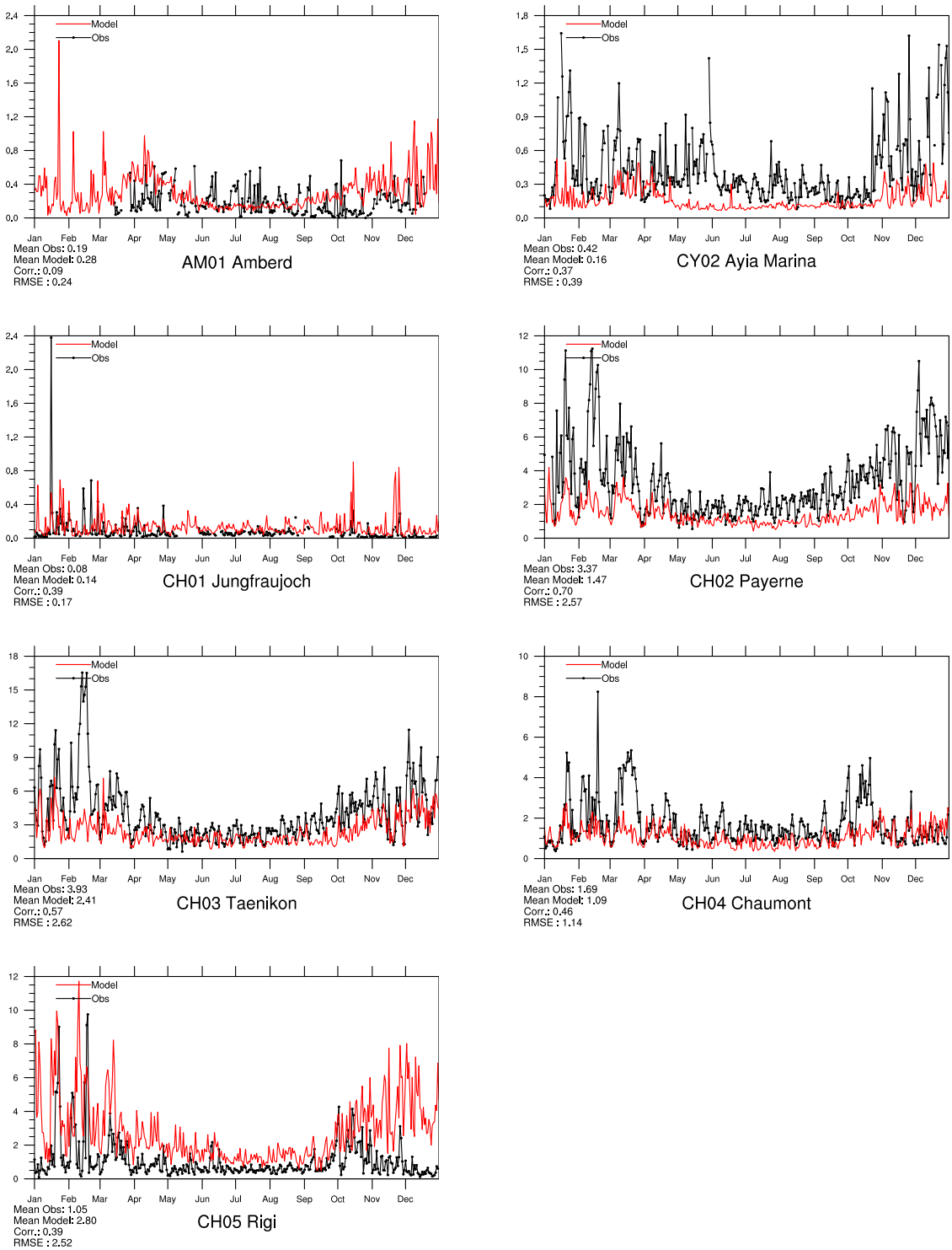

Figure 3.20: Modelled versus Observed Daily Mean NO_2 (μg(N) m^{-3}) for 2015.

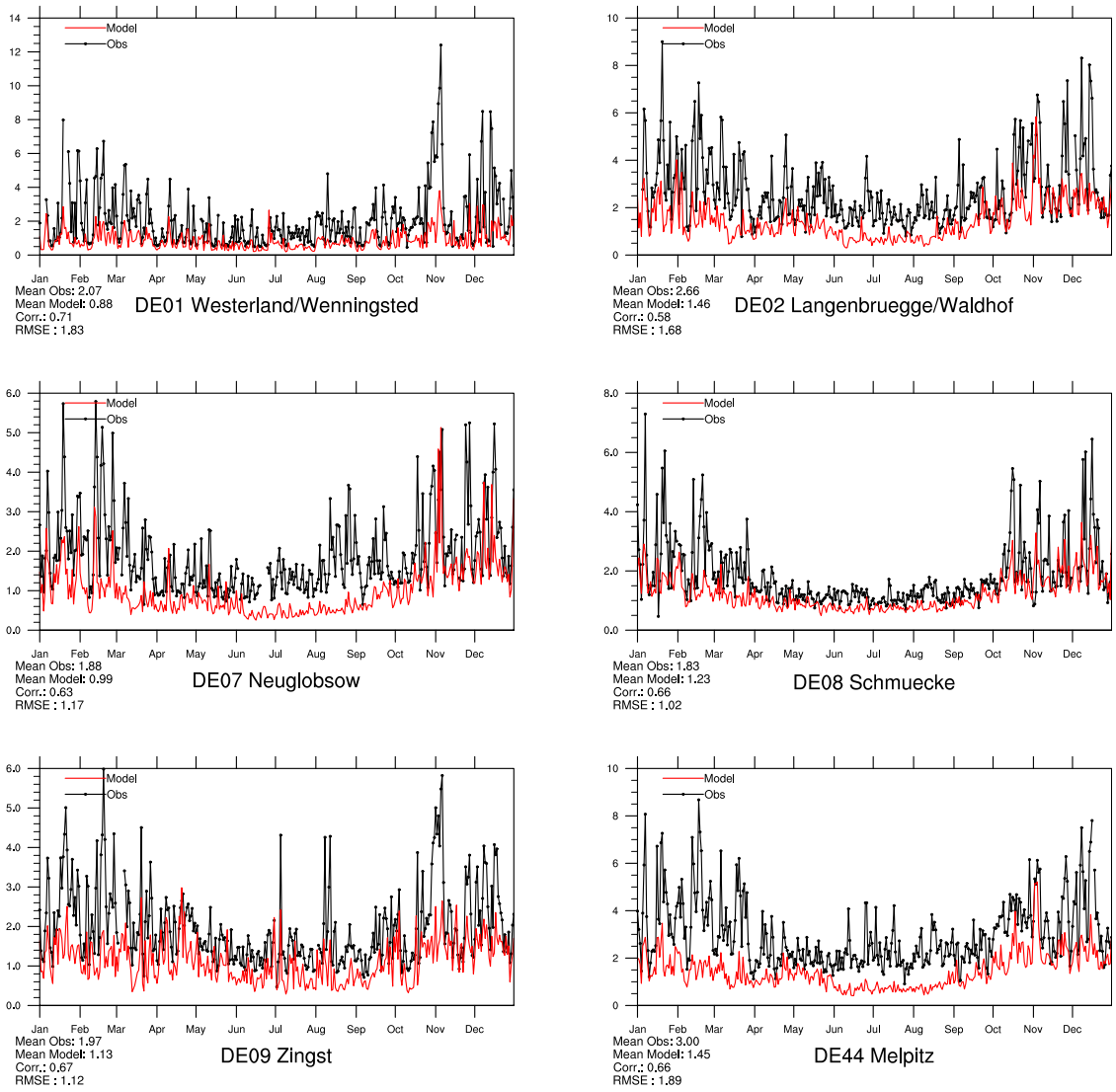

Figure 3.21: Modelled versus Observed Daily Mean NO_2 (μg(N) m^{-3}) for 2015.

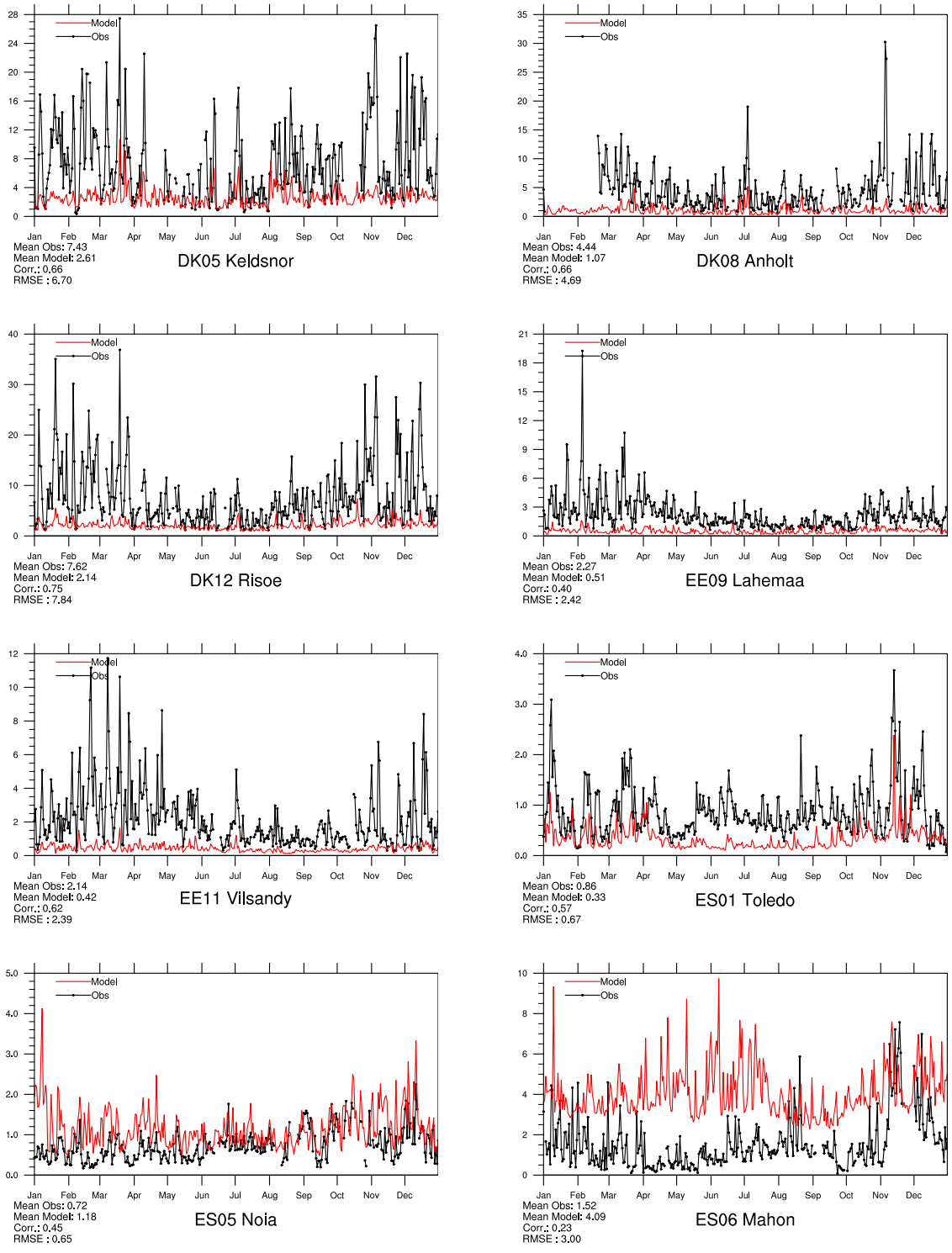

Figure 3.22: Modelled versus Observed Daily Mean NO_2 (μg(N) m^{-3}) for 2015.

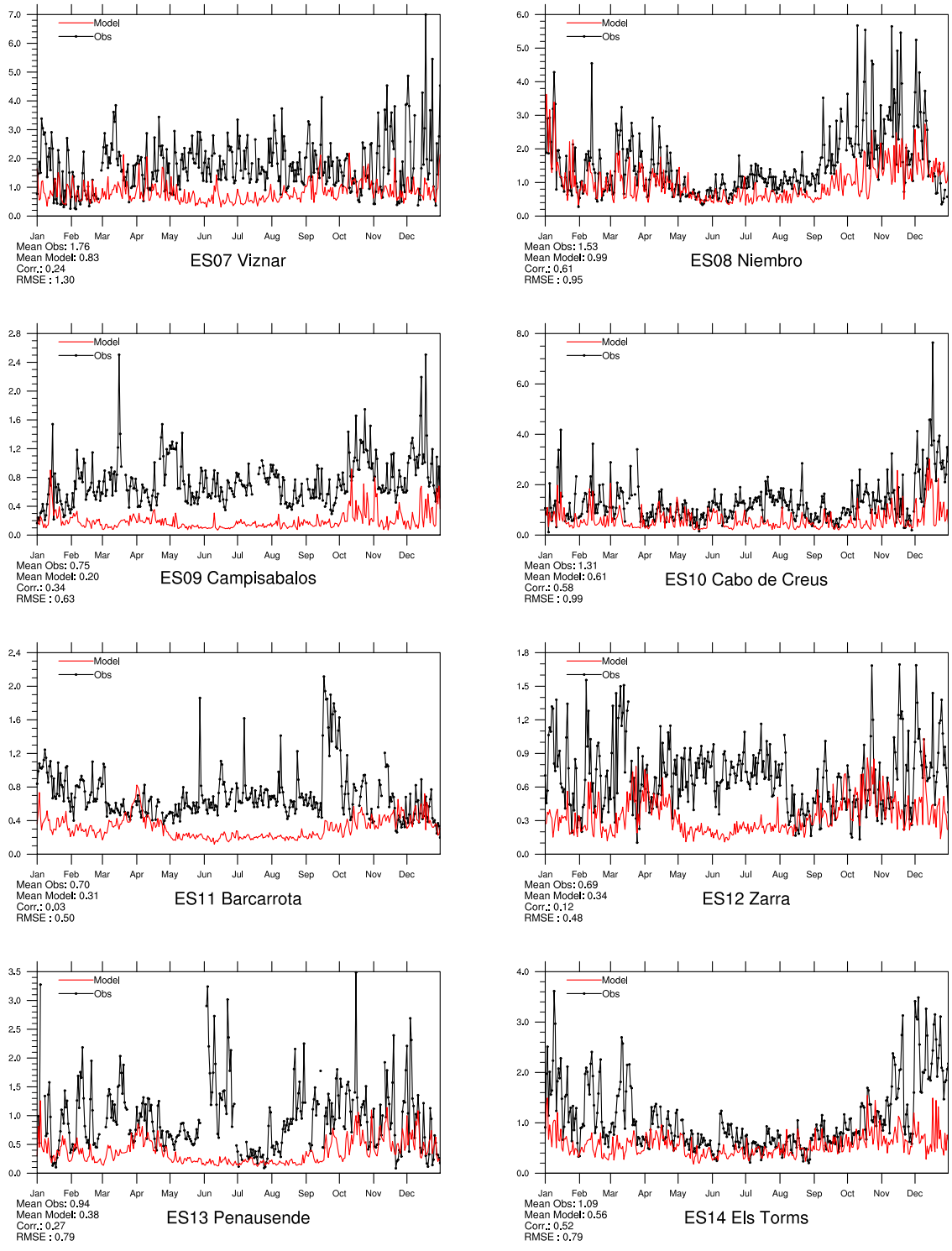

Figure 3.23: Modelled versus Observed Daily Mean NO_2 (μg(N) m^{-3}) for 2015.

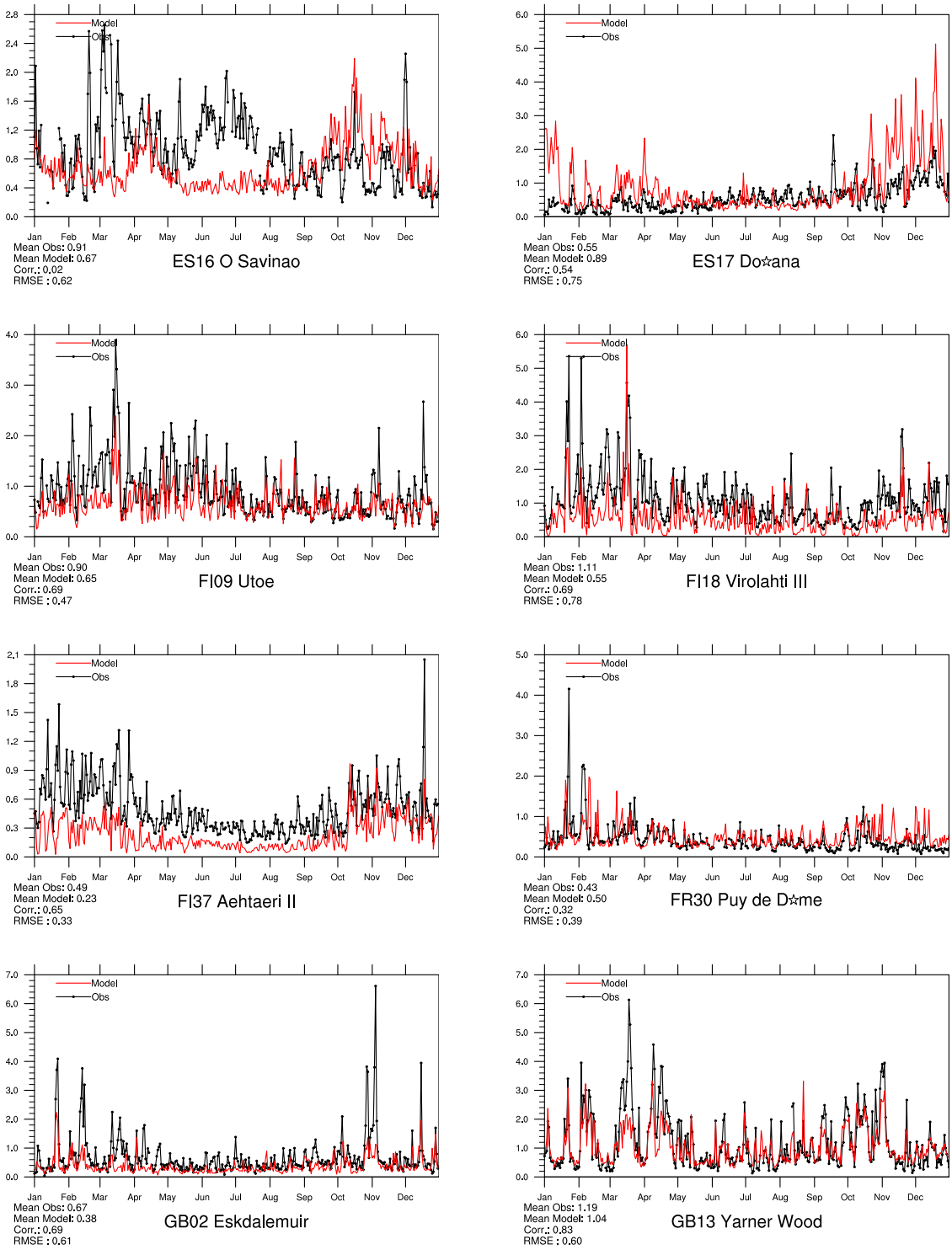

Figure 3.24: Modelled versus Observed Daily Mean NO_2 (μg(N) m^{-3}) for 2015.

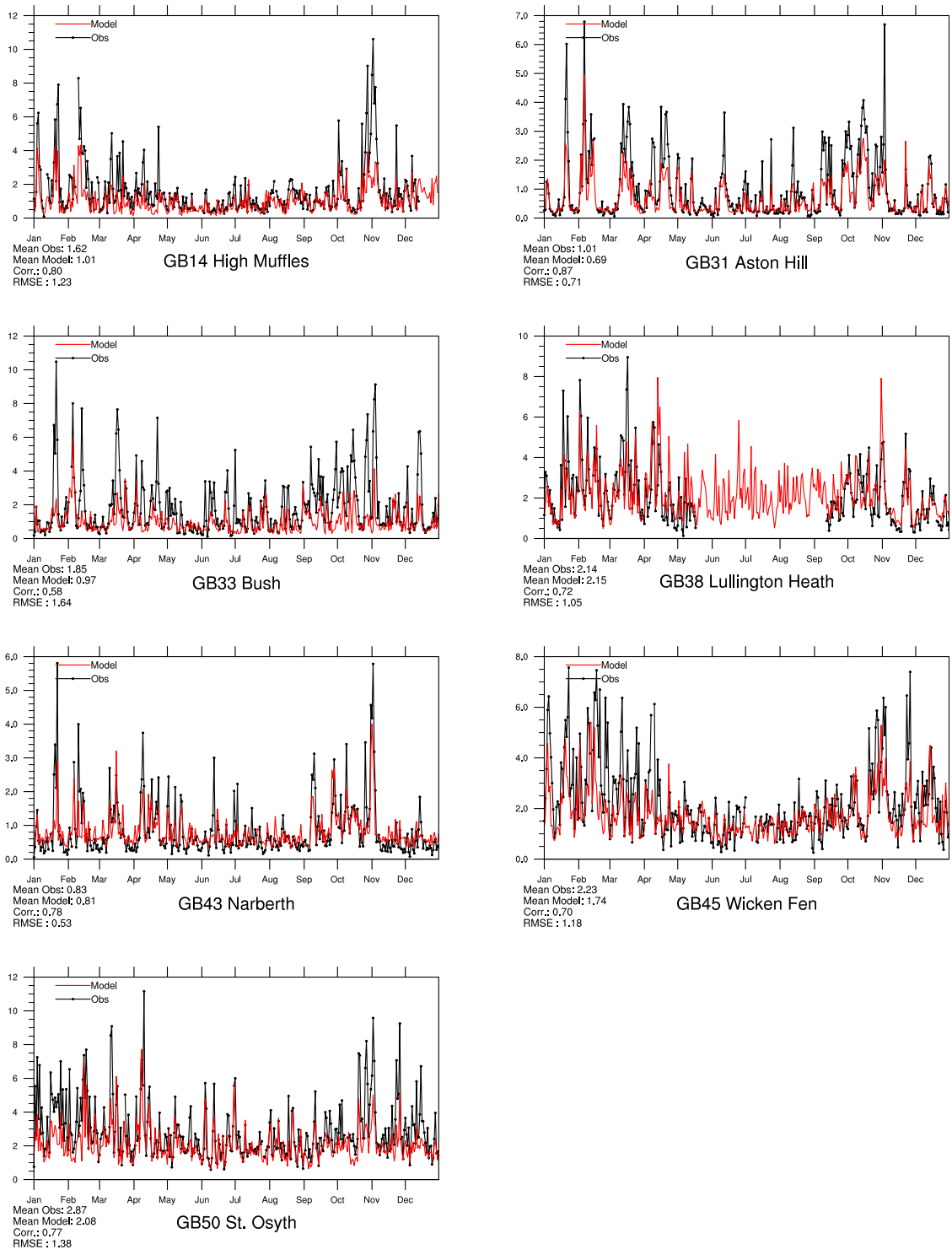

Figure 3.25: Modelled versus Observed Daily Mean NO_2 (μg(N) m^{-3}) for 2015.

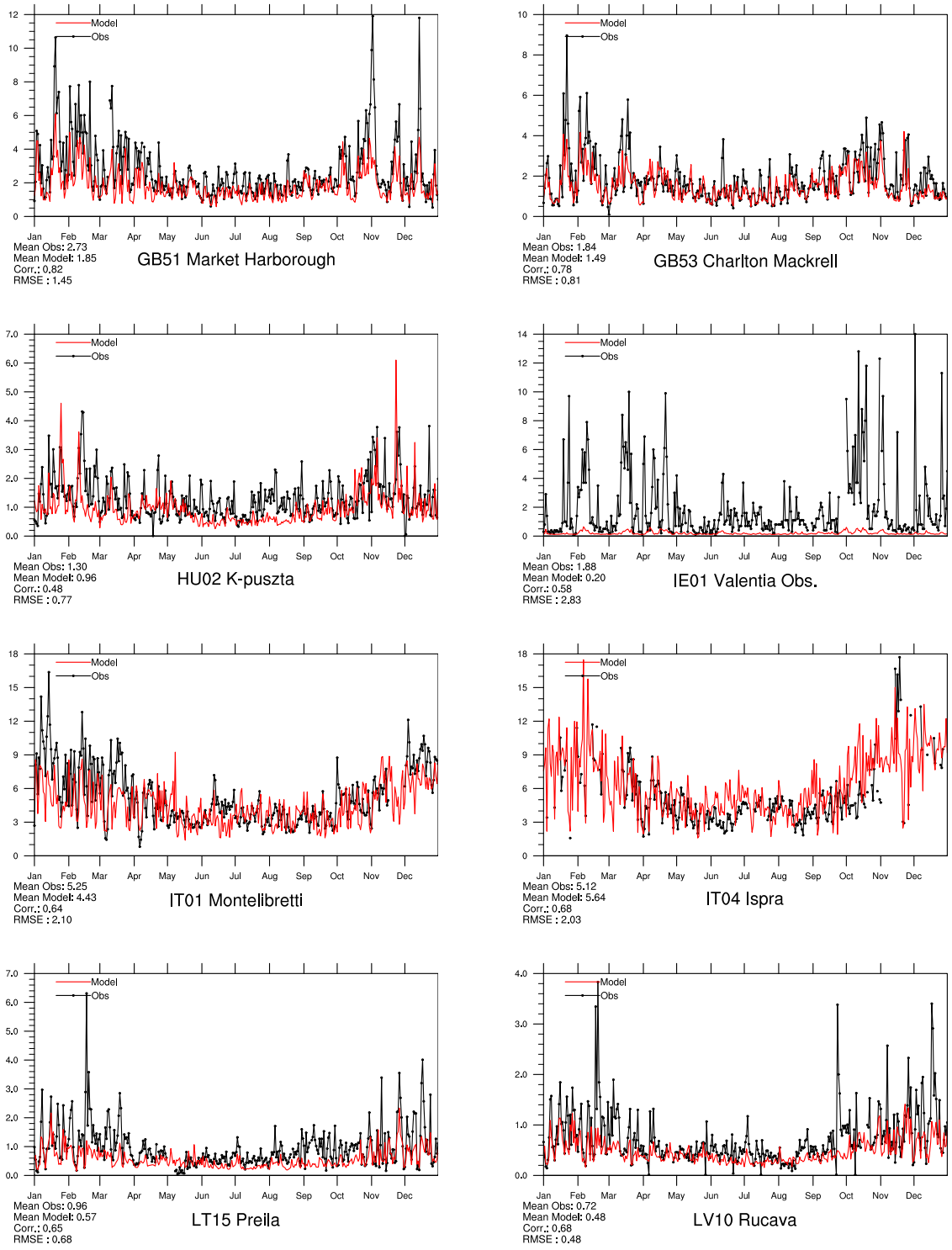

Figure 3.26: Modelled versus Observed Daily Mean NO_2 (μg(N) m^{-3}) for 2015.

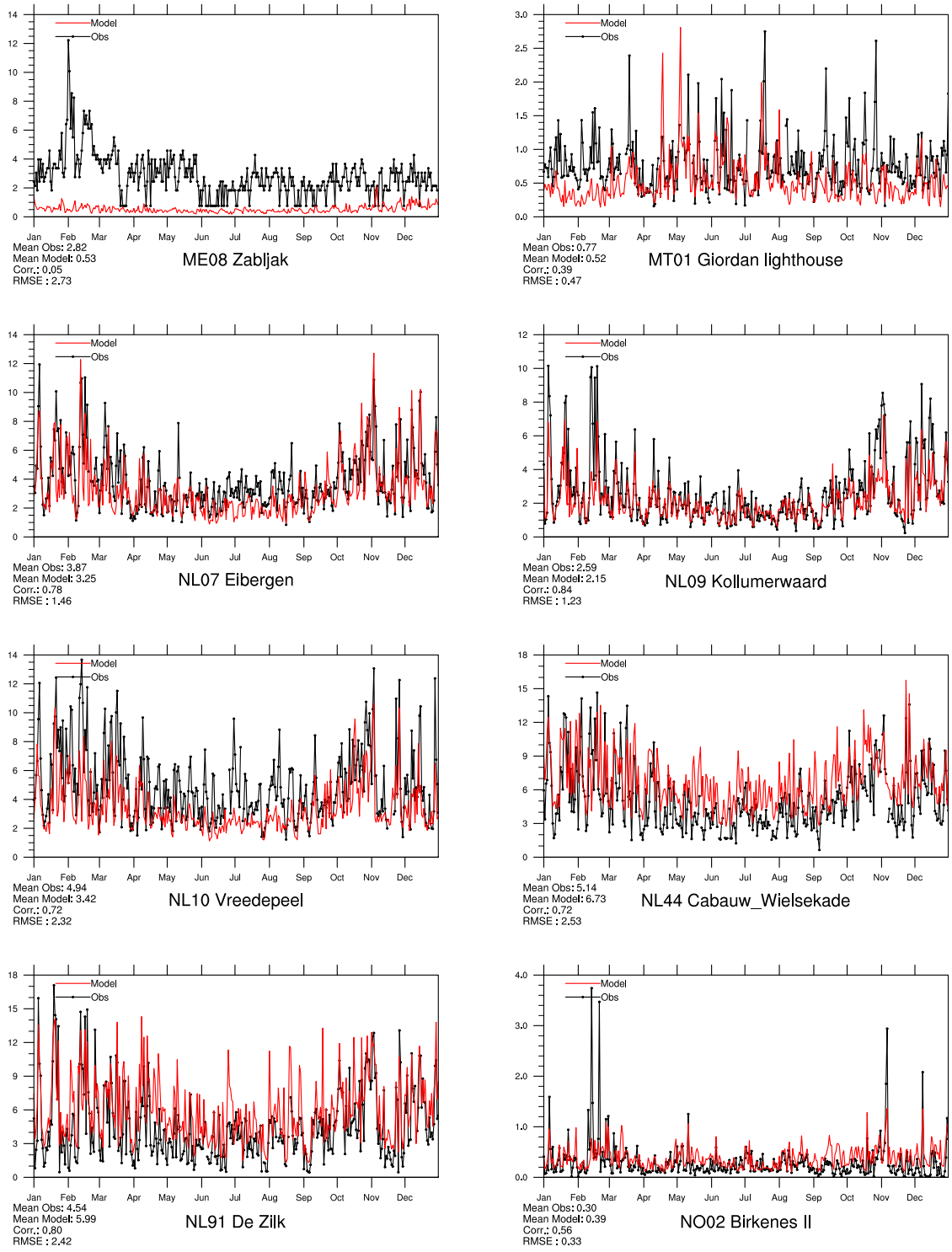

Figure 3.27: Modelled versus Observed Daily Mean NO_2 (μg(N) m^{-3}) for 2015.

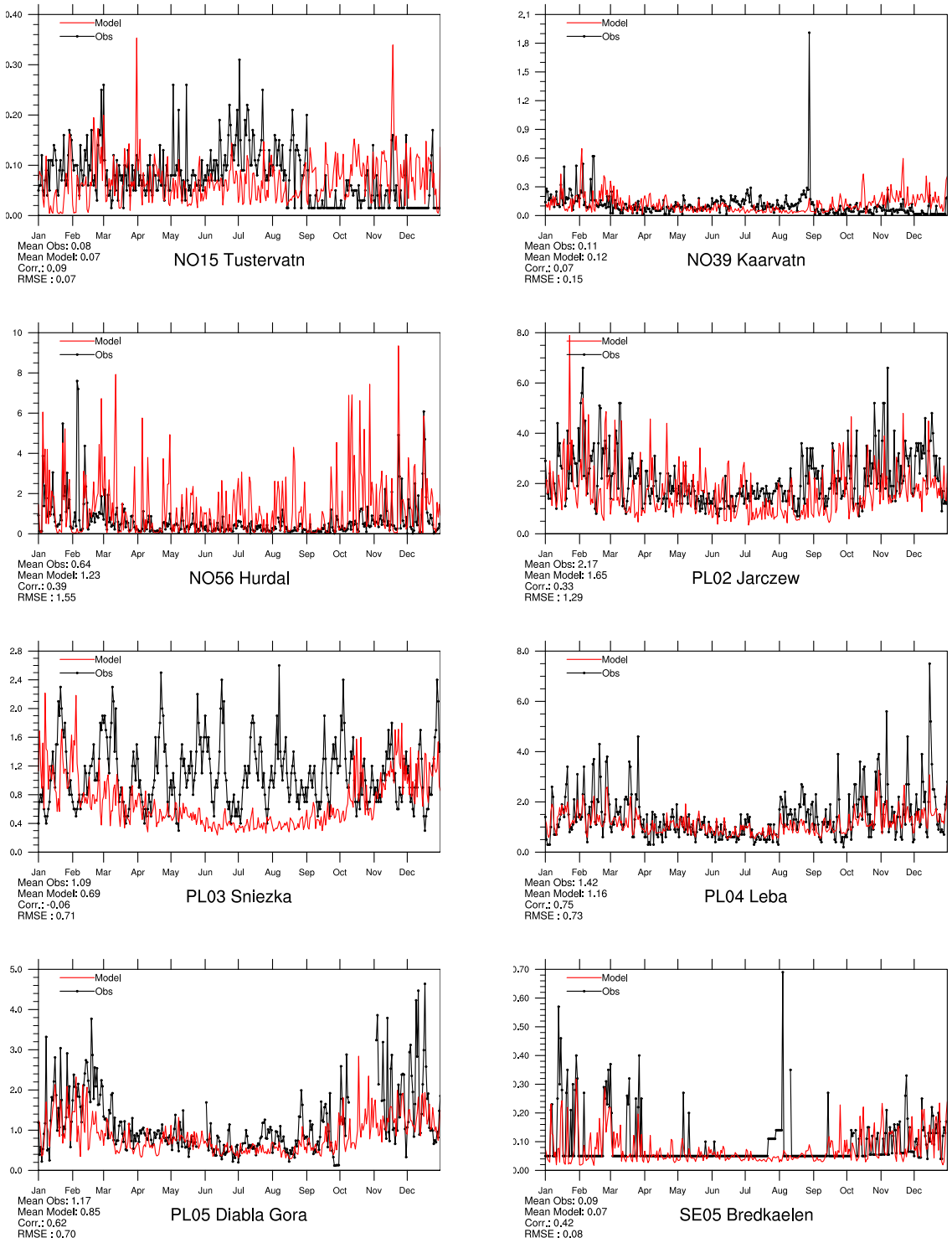

Figure 3.28: Modelled versus Observed Daily Mean NO_2 (μg(N) m^{-3}) for 2015.

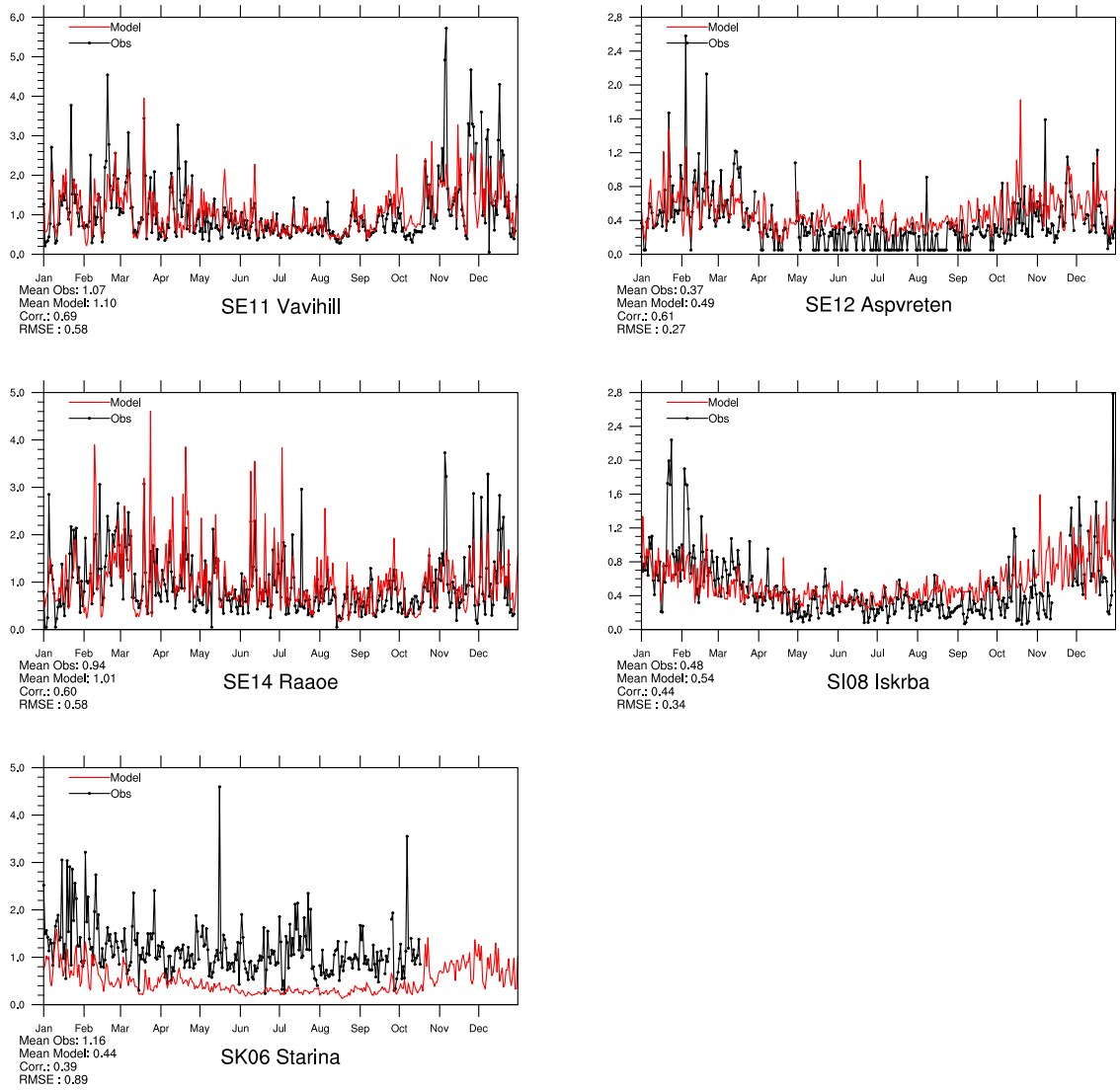

Figure 3.29: Modelled versus Observed Daily Mean NO_2 (μg(N) m^{-3}) for 2015.

3.4 Combined maps of model results and observations

In Figure 3.30, maps of modeled SOMO35 and maximum daily ozone are shown. Observations, taken from the EMEP network for 2015, are super-imposed with triangles. By and large, the plots show good agreement between model and observations also for this year.

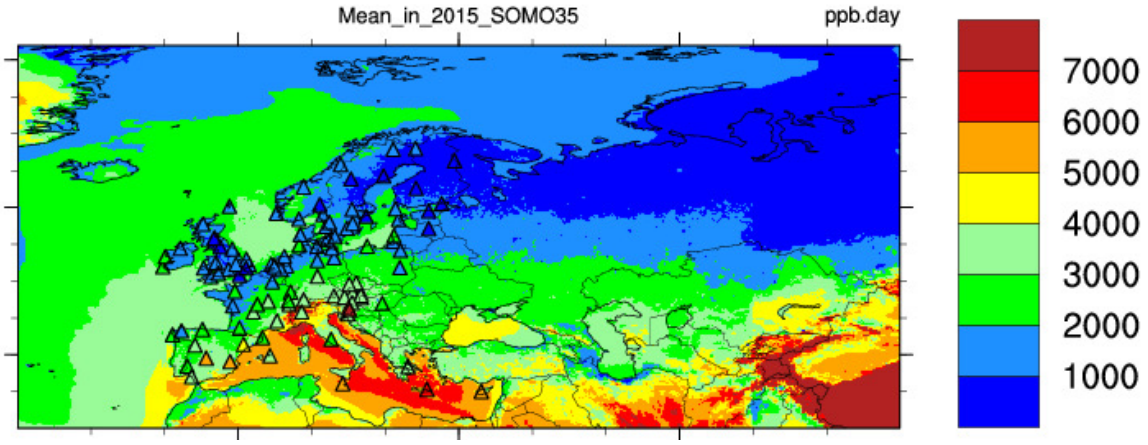

(a) SOMO35

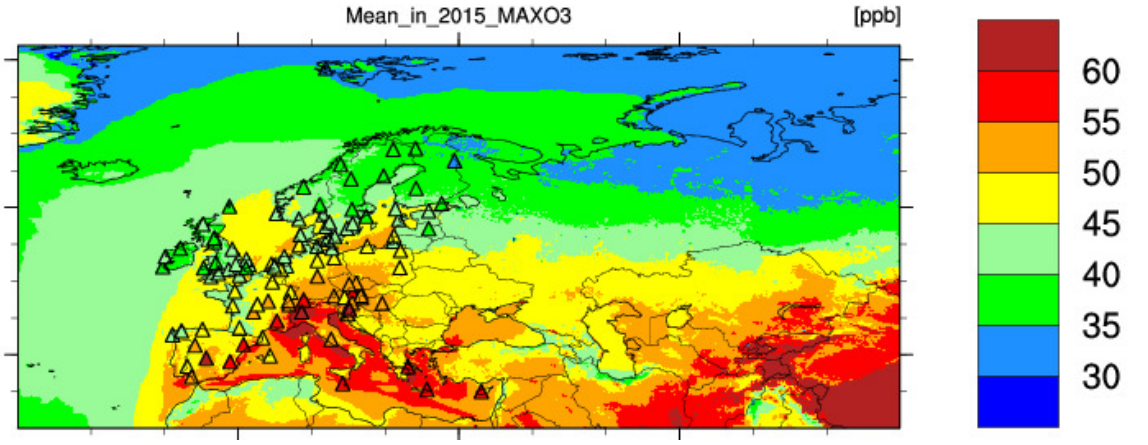

(b) Max ozone

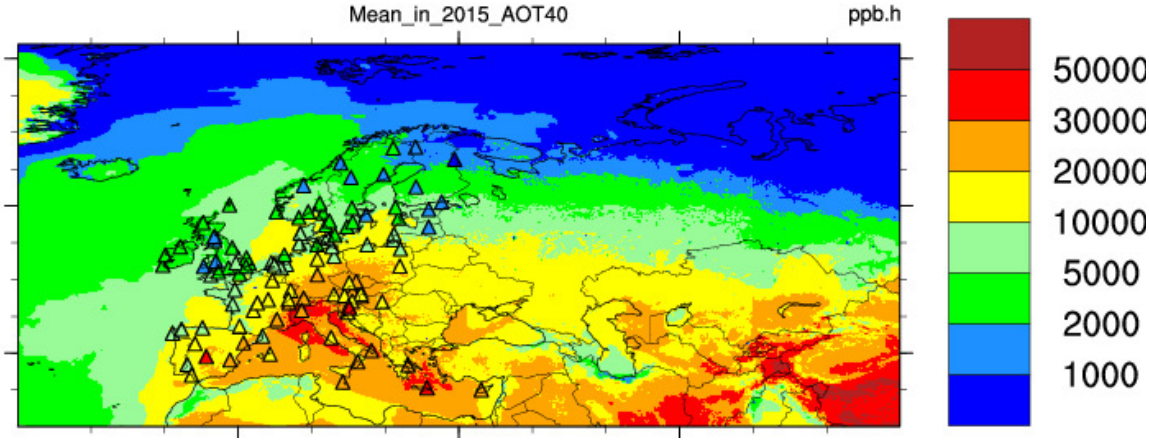

(c) SOMO35

Figure 3.30: SOMO35 (ppb.days), yearly averaged daily maximum ozone (ppb), and AOT40 (ppb.hours). The maps show model results, with observations superimposed by triangles.

References

M. Gauss, A.-G. Hjellbrekke, and S. Solberg. Ozone. Supplementary material to EMEP Status Report 1/2015, available online at www.emep.int, The Norwegian Meteorological Institute, Oslo, Norway, 2015.

M. Gauss, A.-G. Hjellbrekke, and S. Solberg. Ozone. Supplementary material to EMEP Status Report 1/2016, available online at www.emep.int, The Norwegian Meteorological Institute, Oslo, Norway, 2016.

CHAPTER 4

PM_{10}, $PM_{2.5}$ and individual aerosol components

This chapter presents an evaluation of the EMEP MSC-W model performance in terms of particulate matter. Tables of model skill are presented for the entire EMEP domain and timeseries plots are shown for individual EMEP measurement stations with daily PM measurements.

4.1 Tables

Table 4.1 shows for PM and individual components the number of stations where daily measurements were available and data coverage criteria were satisfied (N_{stat}), measured yearly average over all stations (Obs), modelled yearly average over all stations (Mod), bias, correlation between observation and model for station yearly averages, root mean square error, and index of agreement (IOA, as defined in Section 2.1).

On average, the model underestimates annual mean measured PM_{10} by 10% and $PM_{2.5}$ by 1% for 2015, which is a clear improvement since last year. The annual spatial correlations between model results and measurements are 0.74 for PM_{10} and 0.84 for $PM_{2.5}$. The slightly worse model performance in terms of bias and IOA for PM_{10} than for $PM_{2.5}$ is likely due to existing uncertainties in modelling natural PM components, e.g. windblown mineral dust, causing also inaccuracy in coarse NO_3^-. Also, PPM emissions in the coarse fraction are probably more uncertain (fugitive dust, production processes, etc.). Furthermore, there are yet unaccounted components to PM_{10} (biogenic organic aerosol, agricultural dust).

On an annual basis, the model shows quite variable performance for the individual aerosol components. Calculated SO_4 is underestimated by 16% compared to observations. The model overestimates total NO_3^- by 26% and NO_3^- in $PM_{2.5}$ by 42%.

NH_4^+ is quite reasonably reproduced by the model, being biased by -3% against total ammonium data (e.g. sampling without size cut-off).

Modelled elemental carbon (EC) in $PM_{2.5}$ is overestimated by 18% on the annual basis, while organic carbon (OC) is underestimated by 48%. However, it has to be noted that these scores are based on only 3 stations.

Component	N_{stat}	Obs.	Mod.	Bias (%)	RMSE	Corr.	IOA
PM_{10} ($\mu g\ m^{-3}$)	41	14.61	13.12	-10	3.49	0.74	0.84
$PM_{2.5}$ ($\mu g\ m^{-3}$)	30	8.62	8.49	-1	2.37	0.84	0.91
SO_4^{2-}, including sea salt ($\mu g\ m^{-3}$)	33	1.32	1.10	-16	0.49	0.83	0.87
SO_4^{2-}, sea salt corrected ($\mu g\ m^{-3}$)	26	1.10	0.78	-29	0.56	0.86	0.83
SO_4^{2-} in PM_{10} ($\mu g\ m^{-3}$)	14	1.76	1.26	-28	0.58	0.92	0.86
SO_4^{2-} in $PM_{2.5}$ ($\mu g\ m^{-3}$)	2	1.89	1.40	-26	0.50	1.00	0.37
NO_3^- ($\mu g\ m^{-3}$)	20	1.23	1.55	26	0.84	0.79	0.81
NO_3^- in PM_{10} ($\mu g\ m^{-3}$)	14	1.35	1.91	42	0.72	0.83	0.80
NH_4^+ ($\mu g\ m^{-3}$)	19	0.65	0.63	-3	0.22	0.88	0.93
EC in $PM_{2.5}$ ($\mu g(C)\ m^{-3}$)	3	0.68	0.80	18	0.30	1.00	0.91
OC in $PM_{2.5}$ ($\mu g(C)\ m^{-3}$)	3	3.96	2.07	-48	1.94	0.98	0.66
Na+ ($\mu g\ m^{-3}$)	21	0.90	1.06	18	0.33	0.97	0.97
Na+ in PM_{10} ($\mu g\ m^{-3}$)	7	0.45	0.29	-36	0.41	0.84	0.64

Table 4.1: Comparison of model results and observations for 2015. Annual averages over all EMEP sites with measurements. N_{stat}= number of stations, wd=wet deposition, cp= concentration in precipitation, Corr. = spatial correlation coefficient, RMSE = root mean square error, IOA = index of agreement.

Tables 4.2 and 4.3 show model performance for PM_{10} and $PM_{2.5}$ at individual stations, revealing large variability in the model ability to reproduce the observed concentrations in different locations. For most of the sites, the bias varies between -30 and +30%. The temporal correlation is mostly between 0.5 and 0.8.

4.2 Time series

In this section we present time series plots for a selection of stations that have supplied data on particulate matter to EMEP CCC for 2015.

A comprehensive discussion of model performance at individual stations is not given here, but for reference, the following time series plots are shown:

- Figures 4.1–4.4: $PM_{2.5}$ daily measurements
- Figures 4.6–4.11: PM_{10} daily measurements

Table 4.2: Statistical analysis of model calculated PM_{10} against daily observations in 2015. Obs: measured mean, Mod: calculated mean, Bias: calculated as (Mod-Obs)/Obs x100%, R: temporal correlation coefficient, and RMSE: Root mean Square Error.

Site	Name	Obs	Mod	Bias	R	RMSE	IOA
AT02	Illmitz	19.63	13.75	-30.0	0.60	11.68	0.71
AT05	Vorhegg	6.60	7.57	15.0	0.33	7.59	0.54
AT48	Zoebelboden	7.71	7.85	2.0	0.50	5.95	0.70
CH01	Jungfraujoch	2.35	3.52	50.0	0.70	3.64	0.80
CH02	Payerne	13.25	12.09	-9.0	0.68	7.15	0.81
CH03	Taenikon	13.19	13.65	3.0	0.68	7.29	0.81
CH04	Chaumont	7.71	10.40	35.0	0.43	8.11	0.62
CH05	Rigi	7.59	13.96	84.0	0.38	13.42	0.47
CY02	Ayia Marina	22.51	22.14	-2.0	0.26	30.00	0.39
CZ05	Churanov	9.02	7.86	-13.0	0.46	6.03	0.65
DE01	Westerland/Wenningsted	19.34	19.16	-1.0	0.66	9.72	0.80
DE02	Langenbruegge/Waldhof	16.35	14.41	-12.0	0.50	10.58	0.70
DE03	Schauinsland	10.14	10.65	5.0	0.40	8.34	0.64
DE07	Neuglobsow	14.79	11.22	-24.0	0.54	9.19	0.70
DE08	Schmuecke	11.29	10.48	-7.0	0.34	8.54	0.58
DE09	Zingst	14.90	14.40	-3.0	0.63	8.23	0.79
DE44	Melpitz	19.36	13.72	-29.0	0.53	10.69	0.67
ES01	Toledo	13.50	10.51	-22.0	0.67	10.33	0.77
ES05	Noia	6.40	10.85	70.0	0.44	7.83	0.59
ES06	Mahon	17.99	13.16	-27.0	0.55	8.43	0.68
ES07	Viznar	17.69	17.83	1.0	0.59	15.99	0.73
ES08	Niembro	16.35	18.70	14.0	0.33	21.44	0.40
ES09	Campisabalos	9.10	8.06	-11.0	0.79	7.41	0.84
ES10	Cabo de Creus	17.40	15.50	-11.0	0.59	7.36	0.74
ES11	Barcarrota	15.27	10.31	-32.0	0.67	9.14	0.76
ES12	Zarra	11.77	10.46	-11.0	0.65	8.18	0.79
ES13	Penausende	9.23	8.13	-12.0	0.72	6.77	0.82
ES14	Els Torms	14.28	11.29	-21.0	0.65	7.17	0.77
ES16	O Savinao	10.01	9.85	-2.0	0.70	5.43	0.82
ES17	Doana	16.95	15.23	-10.0	0.58	9.76	0.73
GB36	Harwell	11.63	13.24	14.0	0.71	6.82	0.81
GB48	Auchencorth Moss	6.06	7.52	24.0	0.51	5.41	0.68
IT01	Montelibretti	27.05	18.33	-32.0	0.56	14.68	0.67
LV10	Rucava	15.53	7.73	-50.0	0.39	12.82	0.53
NL07	Eibergen	17.66	19.25	9.0	0.60	10.38	0.75
NL09	Kollumerwaard	15.35	17.71	15.0	0.54	11.28	0.68
NL10	Vreedepeel	19.46	17.86	-8.0	0.67	9.01	0.81
NL44	Cabauw Wielsekade	16.93	19.39	15.0	0.64	10.24	0.76
NL91	De Zilk	16.72	18.76	12.0	0.54	10.70	0.69
PL05	Diabla Gora	17.32	10.48	-39.0	0.54	12.44	0.62
PL09	Zielonka	17.52	10.66	-39.0	0.59	11.77	0.67
RS05	Kamenicki vis	17.87	13.77	-23.0	0.53	9.76	0.70
SE05	Bredkaelen	3.46	2.02	-42.0	0.63	2.43	0.68
SE14	Raaoe	15.15	14.19	-6.0	0.81	5.79	0.89
SI08	Iskrba	12.52	10.13	-19.0	0.64	6.37	0.77

Table 4.3: Statistical analysis of model calculated $PM_{2.5}$ against daily observations in 2015. Obs: measured mean, Mod: calculated mean, Bias: calculated as (Mod-Obs)/Obs x100%, R: temporal correlation coefficient, and RMSE: Root mean Square Error.

Site	Name	Obs	Mod	Bias	R	RMSE	IOA
AT02	Illmitz	14.70	12.15	-17.0	0.63	8.81	0.77
CH02	Payerne	9.75	10.42	7.0	0.68	6.87	0.81
CH05	Rigi	5.77	11.64	102.0	0.64	9.63	0.62
CY02	Ayia Marina	9.88	13.74	39.0	0.46	9.09	0.60
DE02	Langenbruegge/Waldhof	12.05	11.17	-7.0	0.54	9.34	0.73
DE03	Schauinsland	7.98	8.90	12.0	0.44	7.05	0.66
DE07	Neuglobsow	10.27	8.65	-16.0	0.58	7.66	0.74
DE08	Schmuecke	8.11	8.57	6.0	0.38	6.76	0.62
DE44	Melpitz	14.73	10.97	-26.0	0.59	8.40	0.73
EE09	Lahemaa	5.21	3.49	-33.0	0.62	3.81	0.71
EE11	Vilsandy	4.20	3.88	-8.0	0.58	3.93	0.73
ES01	Toledo	6.61	6.20	-6.0	0.67	4.92	0.72
ES06	Mahon	7.04	7.70	9.0	0.36	4.91	0.56
ES07	Viznar	10.34	11.05	7.0	0.60	7.77	0.71
ES08	Niembro	7.05	11.47	63.0	0.52	11.18	0.48
ES09	Campisabalos	4.82	4.91	2.0	0.73	3.92	0.78
ES10	Cabo de Creus	8.49	7.45	-12.0	0.50	5.63	0.69
ES11	Barcarrota	8.46	6.23	-26.0	0.57	5.28	0.71
ES12	Zarra	5.96	7.05	18.0	0.77	4.01	0.77
ES13	Penausende	5.80	5.44	-6.0	0.62	3.99	0.76
ES14	Els Torms	8.34	8.09	-3.0	0.66	4.57	0.78
ES16	O Savinao	8.30	6.86	-17.0	0.70	4.21	0.82
GB36	Harwell	6.91	8.56	24.0	0.77	6.04	0.84
GB48	Auchencorth Moss	3.40	4.16	22.0	0.59	4.17	0.72
HU02	K-puszta	17.36	14.06	-19.0	0.62	10.31	0.76
IT04	Ispra	17.52	24.69	41.0	0.74	15.14	0.80
LV10	Rucava	10.47	5.92	-43.0	0.66	7.53	0.69
NL09	Kollumerwaard	10.84	11.52	6.0	0.78	7.68	0.88
NL10	Vreedepeel	12.28	14.33	17.0	0.78	7.28	0.87
NL44	Cabauw Wielsekade	11.32	16.56	46.0	0.72	11.57	0.77
NL91	De Zilk	9.51	12.27	29.0	0.68	9.75	0.77
PL05	Diabla Gora	12.49	8.77	-30.0	0.57	9.34	0.68
SE05	Bredkaelen	2.26	1.37	-39.0	0.63	1.56	0.71
SE11	Vavihill	5.40	7.39	37.0	0.59	6.54	0.73
SE12	Aspvreten	5.69	3.23	-43.0	0.63	4.27	0.68
SE14	Raaoe	5.02	4.67	-7.0	0.51	4.06	0.66
SI08	Iskrba	10.02	8.88	-11.0	0.65	5.14	0.78

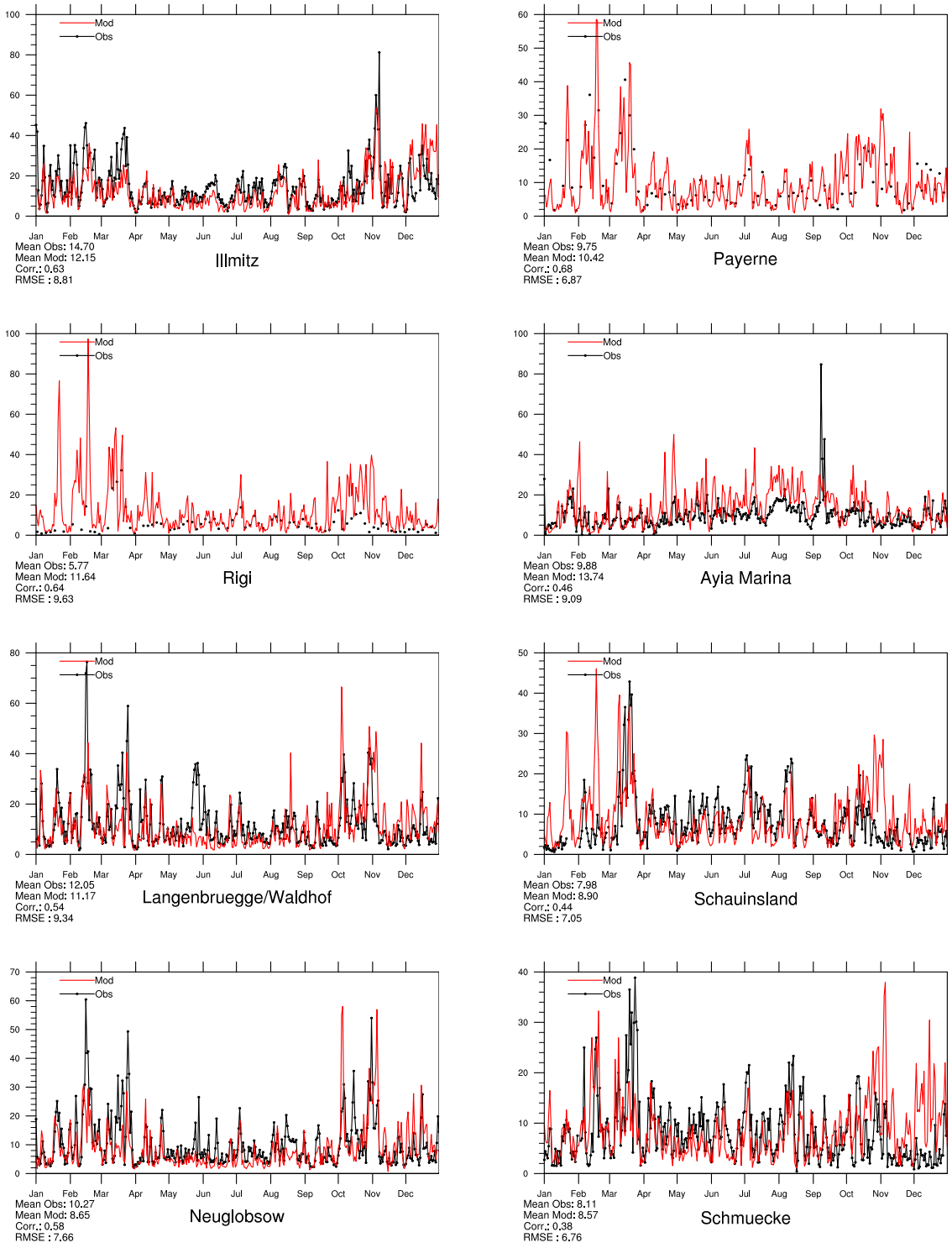

Figure 4.1: Modelled versus Observed Daily $PM_{2.5}$ [μg m^{-3}] in 2015.

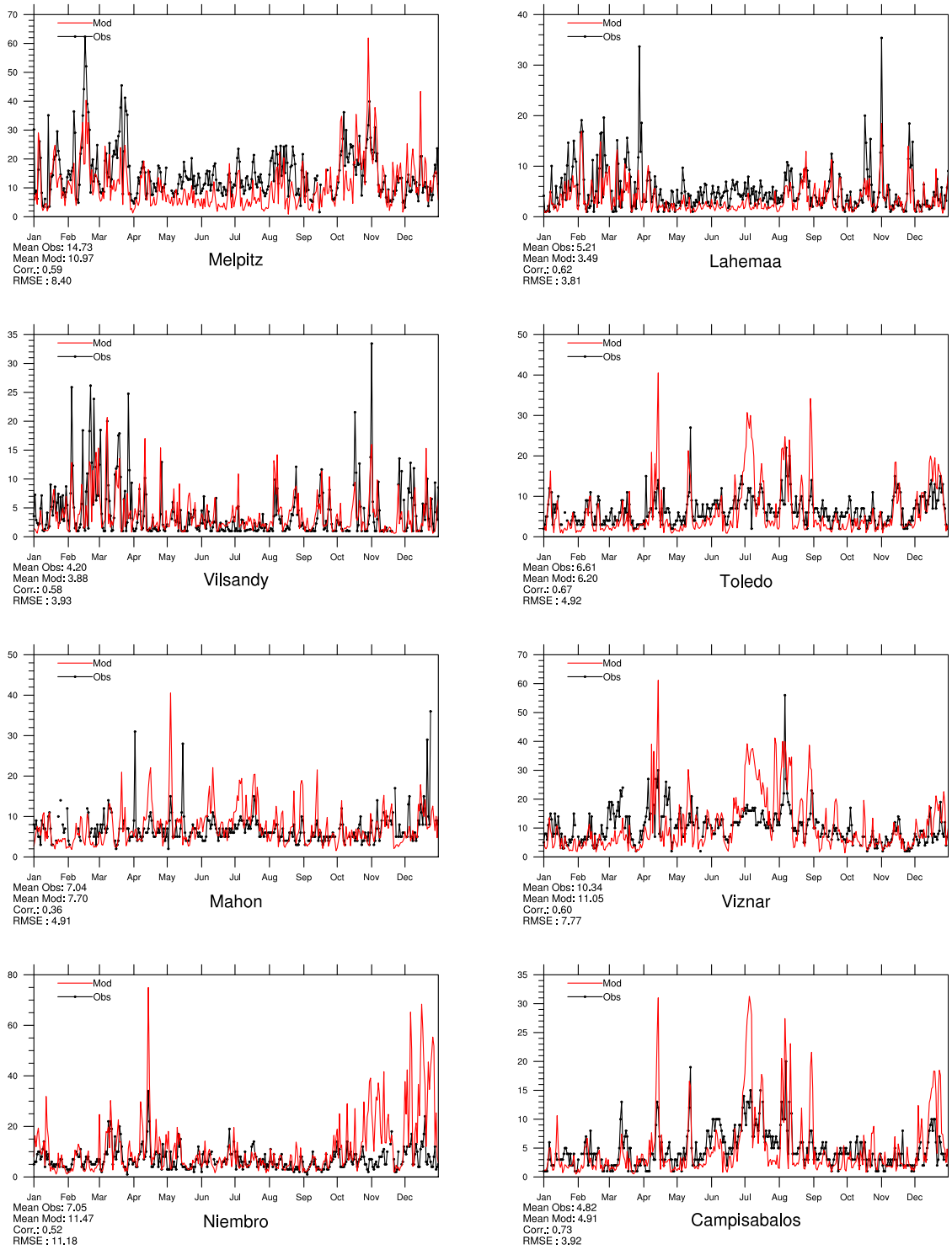

Figure 4.2: Modelled versus Observed Daily $PM_{2.5}$ [μg m^{-3}] in 2015.

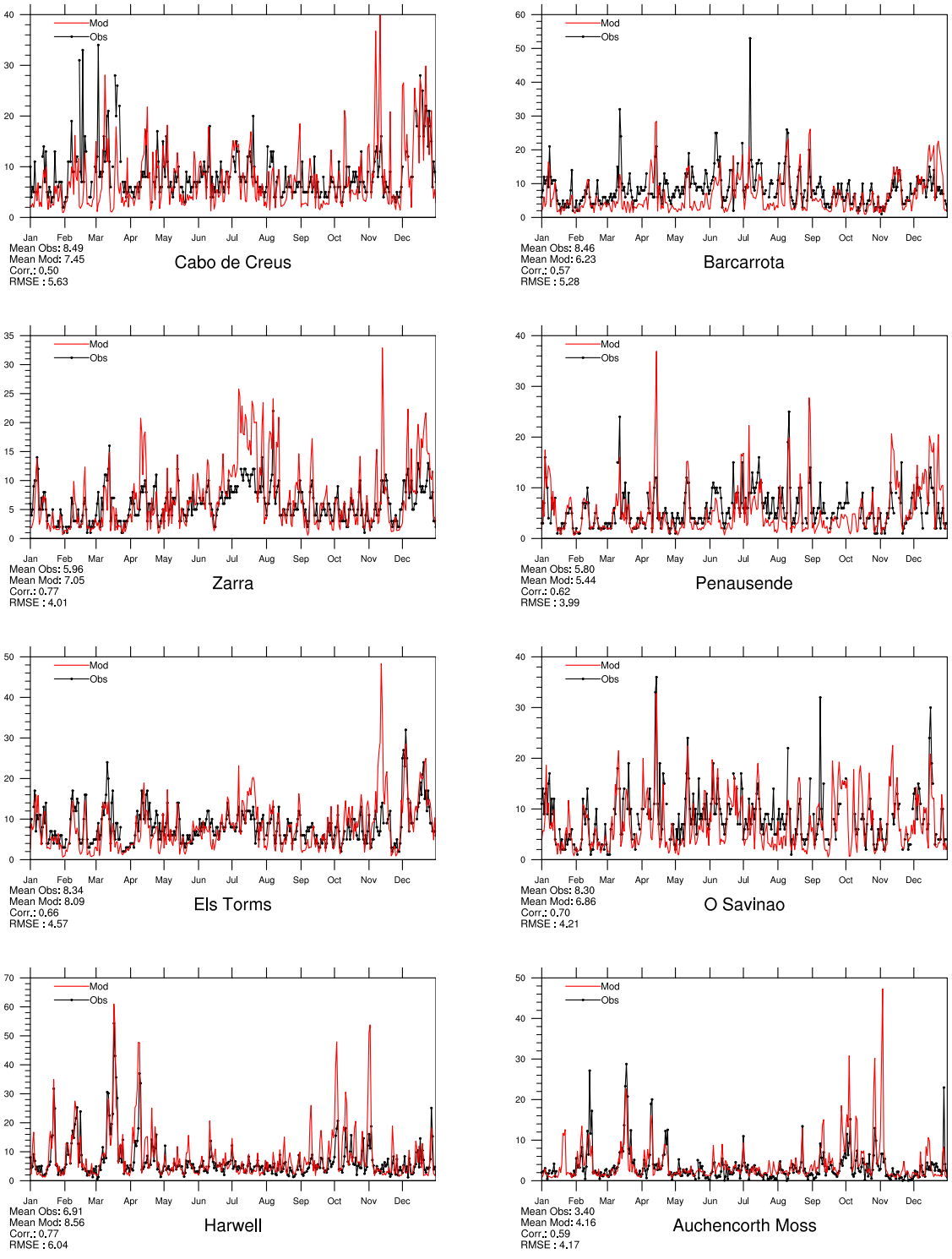

Figure 4.3: Modelled versus Observed Daily $PM_{2.5}$ [μg m^{-3}] in 2015.

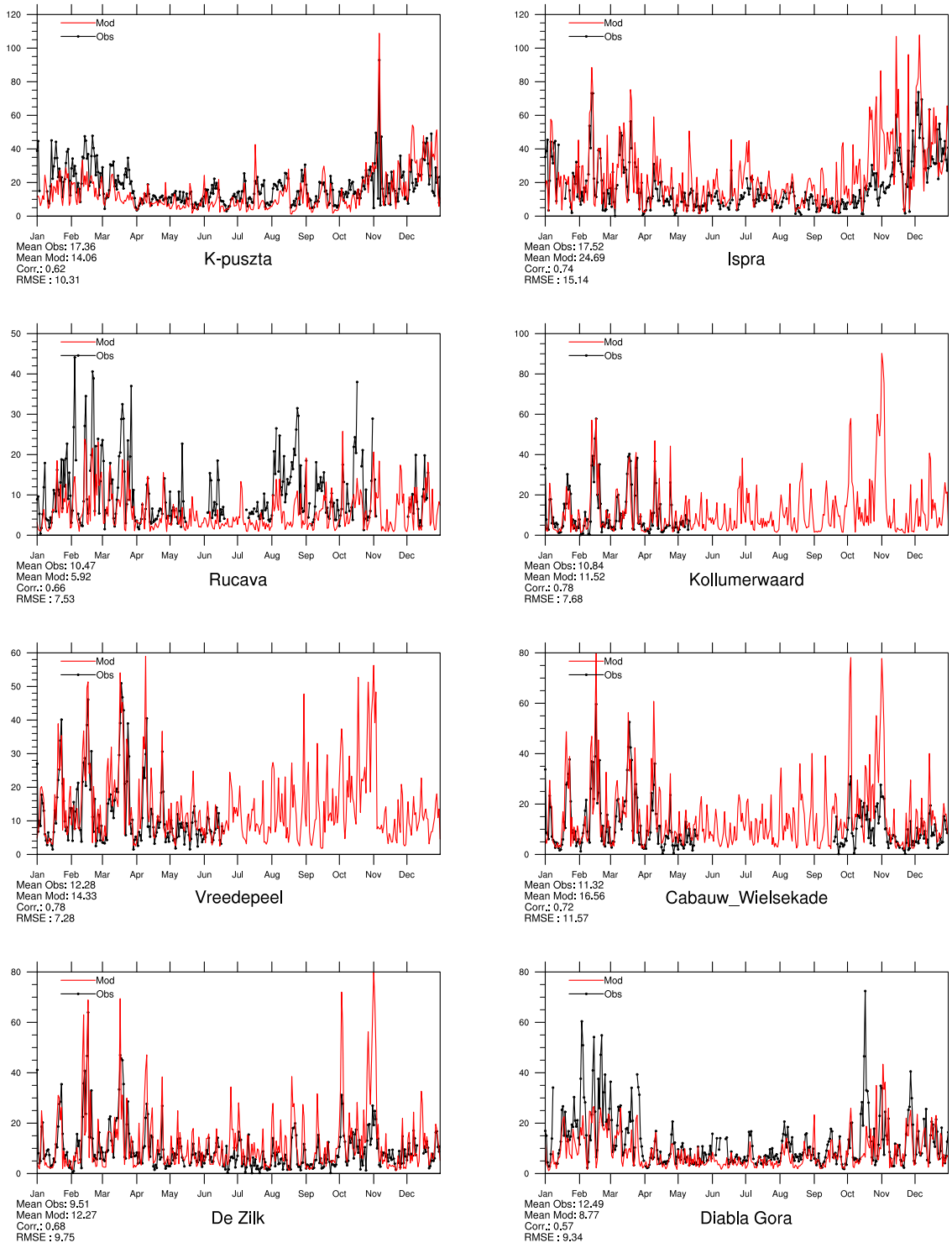

Figure 4.4: Modelled versus Observed Daily $PM_{2.5}$ [μg m^{-3}] in 2015.

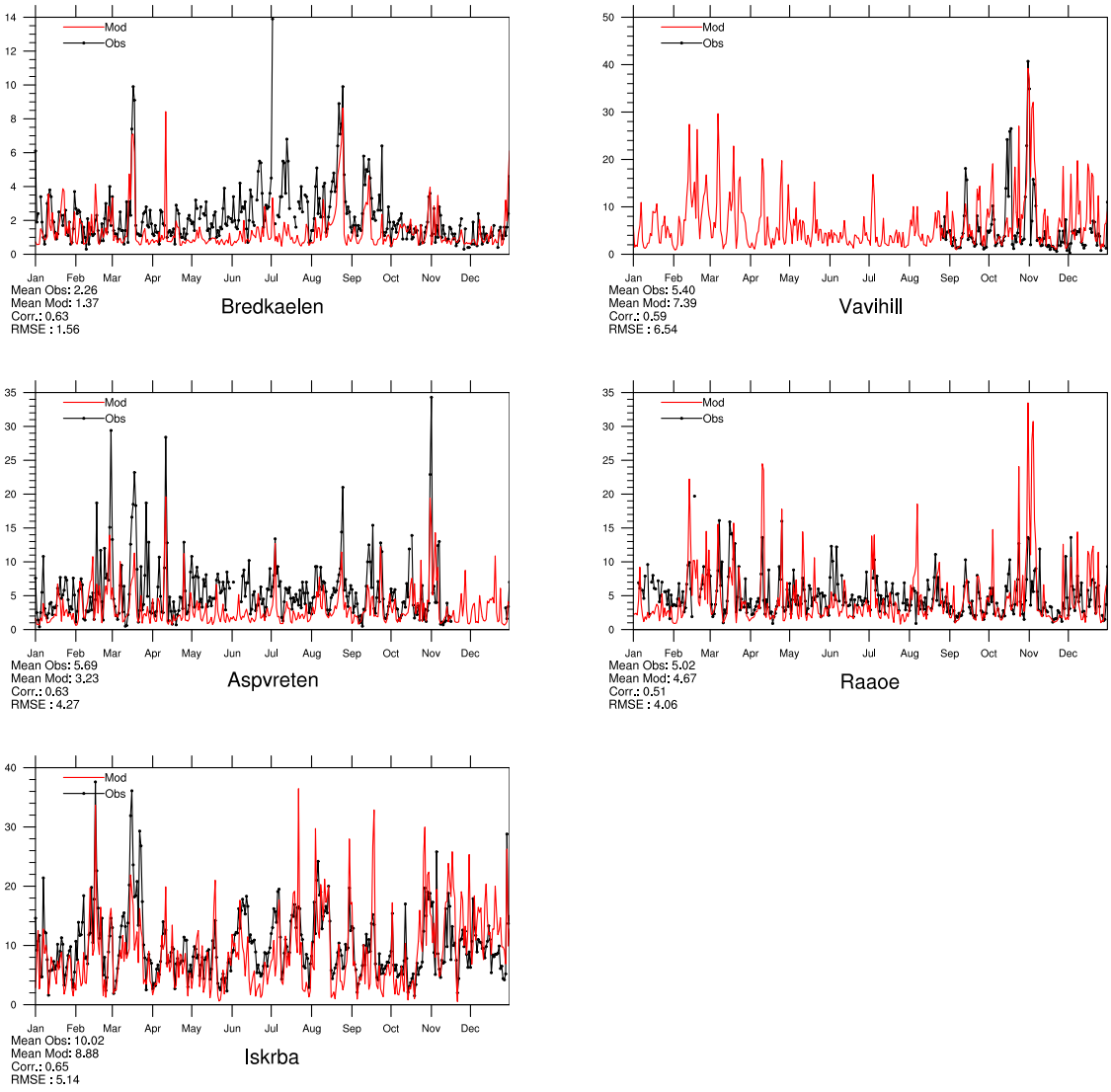

Figure 4.5: Modelled versus Observed Daily $PM_{2.5}$ [μg m^{-3}] in 2015.

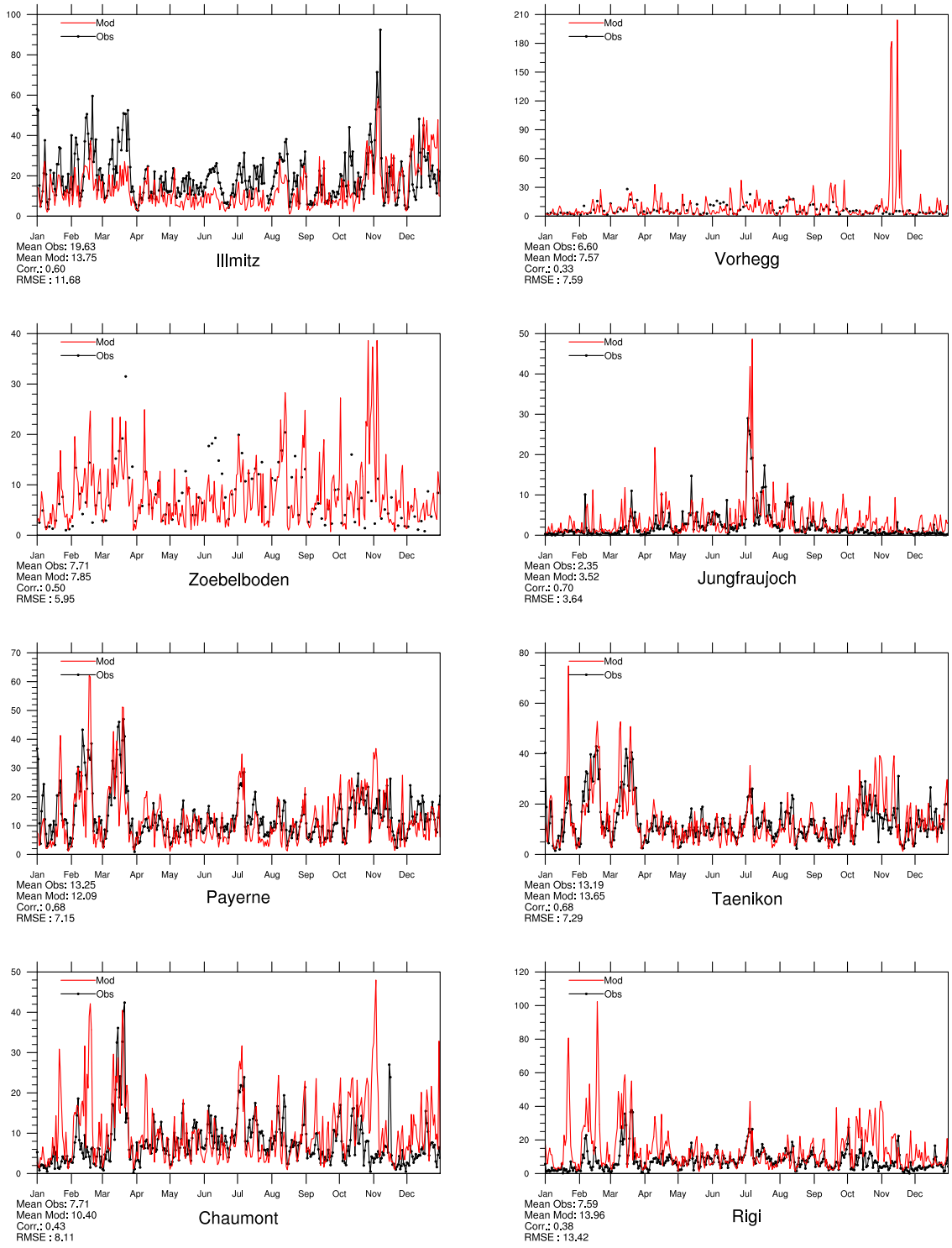

Figure 4.6: Modelled versus Observed Daily PM_{10} [μg m^{-3}] in 2015.

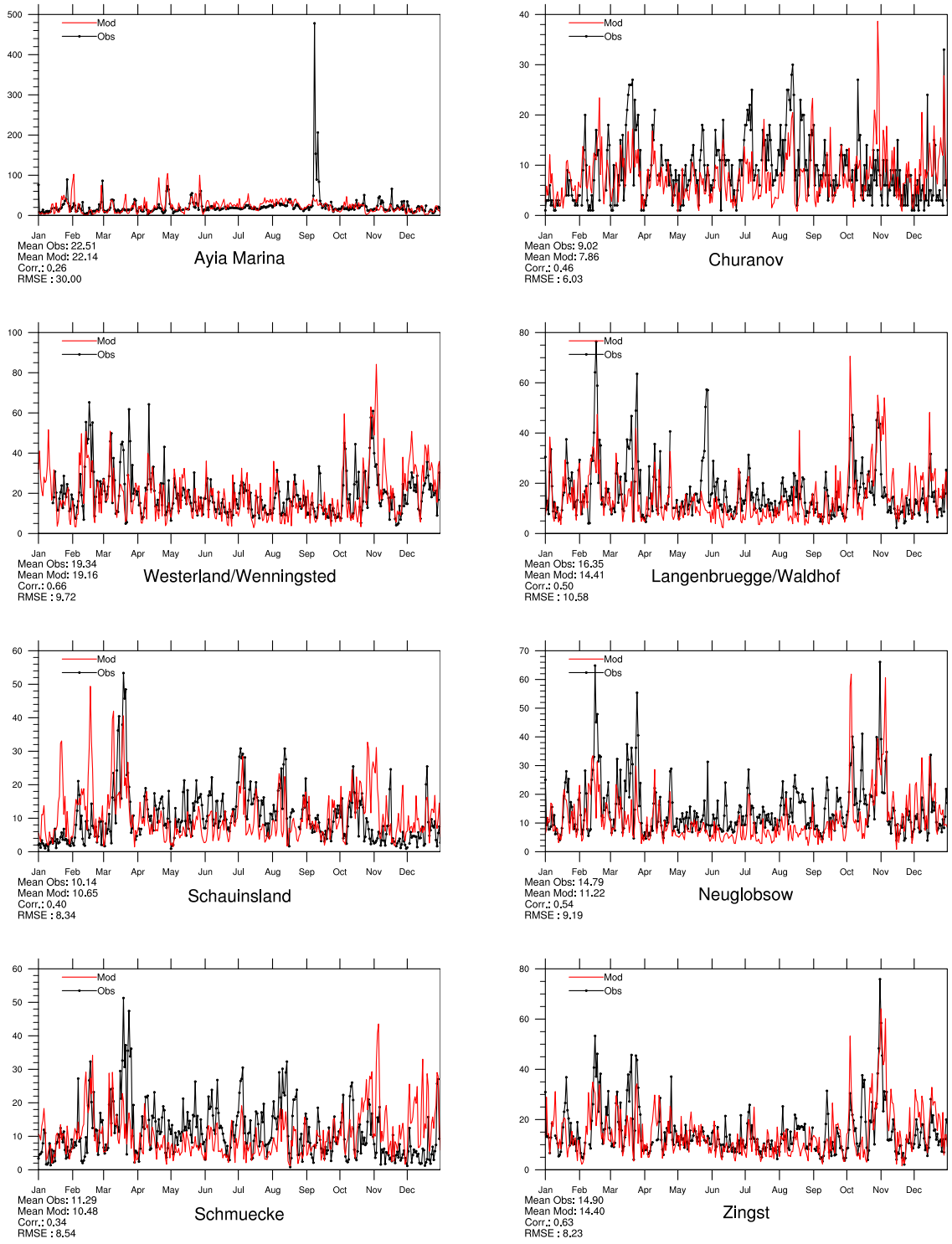

Figure 4.7: Modelled versus Observed Daily PM_{10} [μg m^{-3}] in 2015.

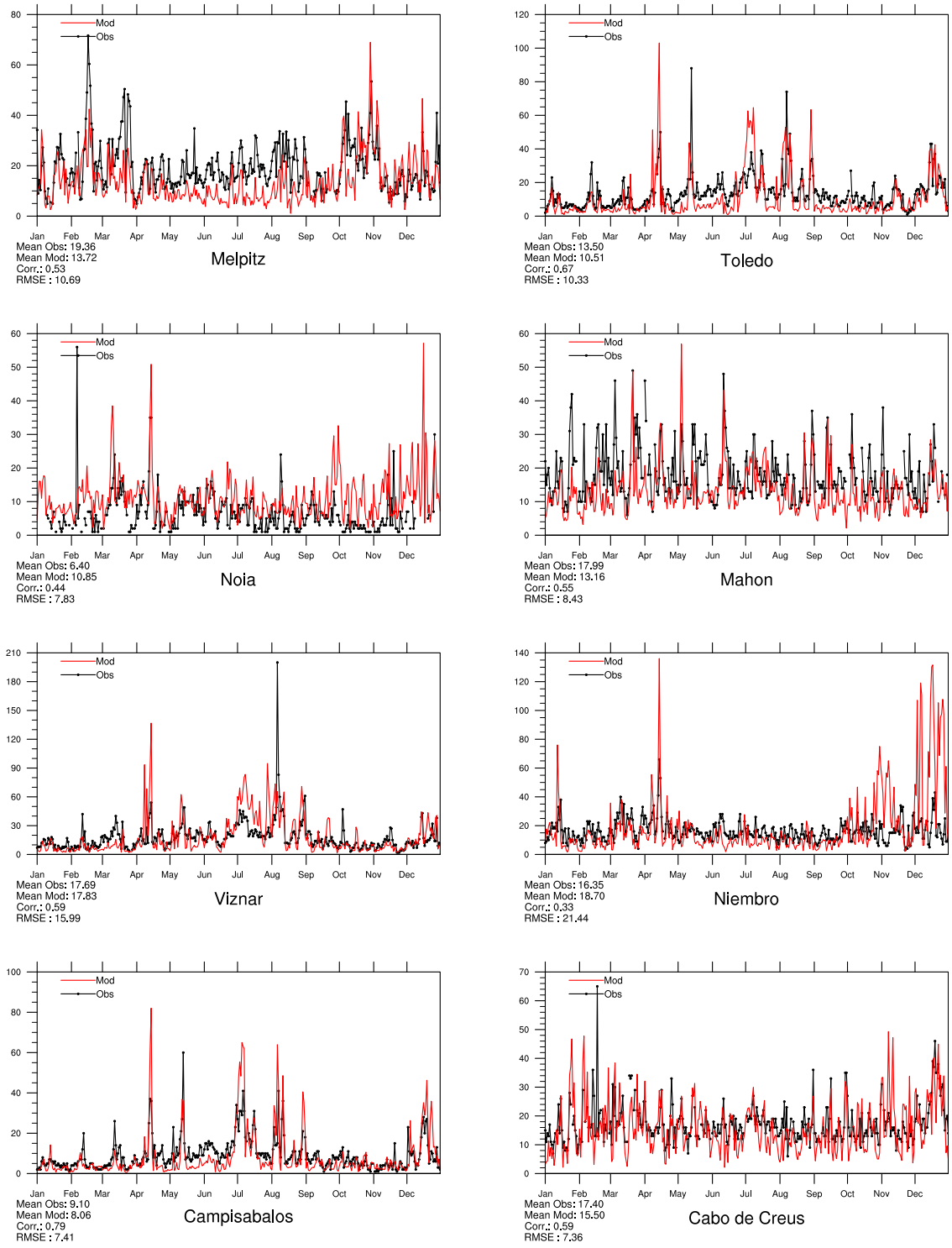

Figure 4.8: Modelled versus Observed Daily PM_{10} [$\mu g\ m^{-3}$] in 2015.

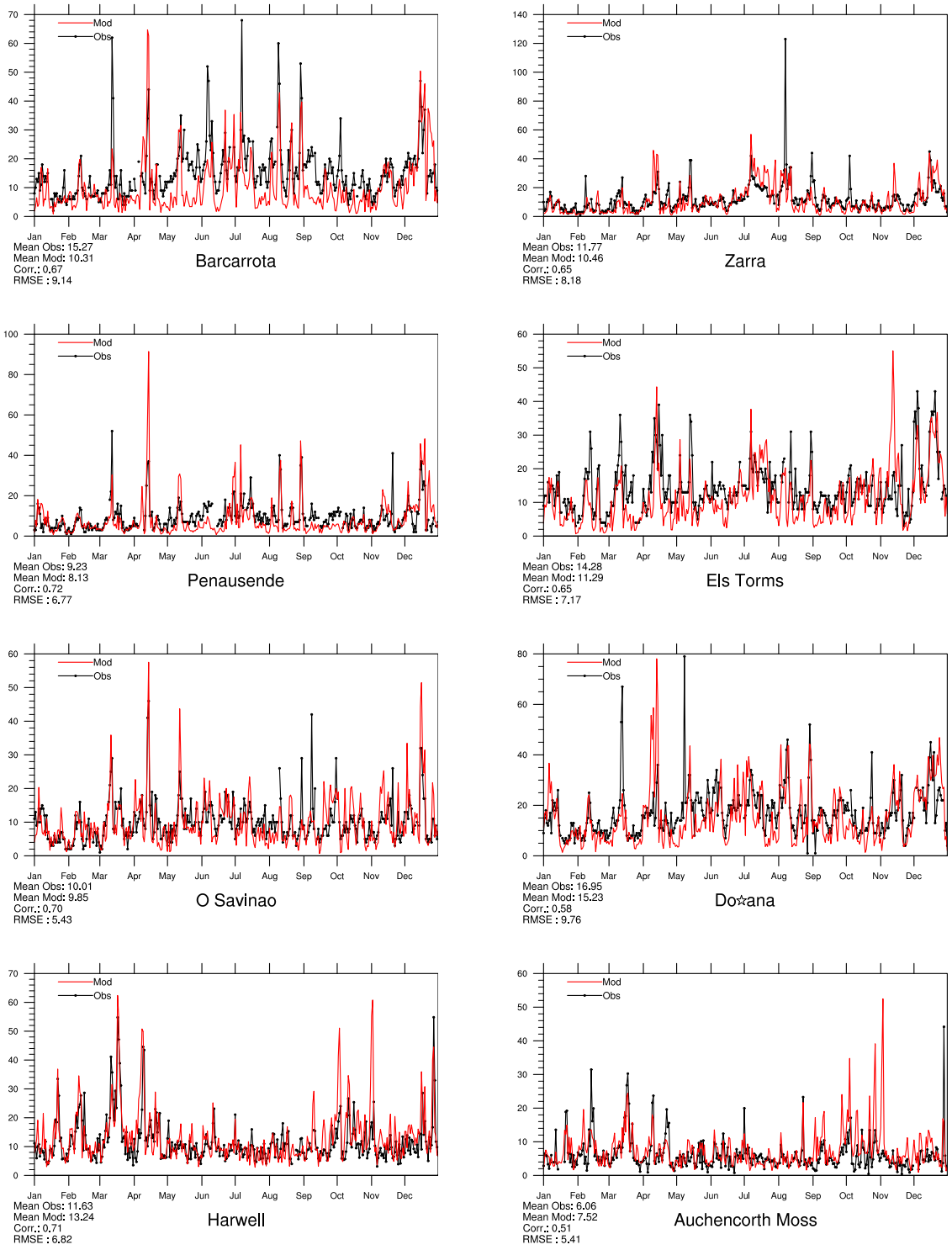

Figure 4.9: Modelled versus Observed Daily PM_{10} [μg m^{-3}] in 2015.

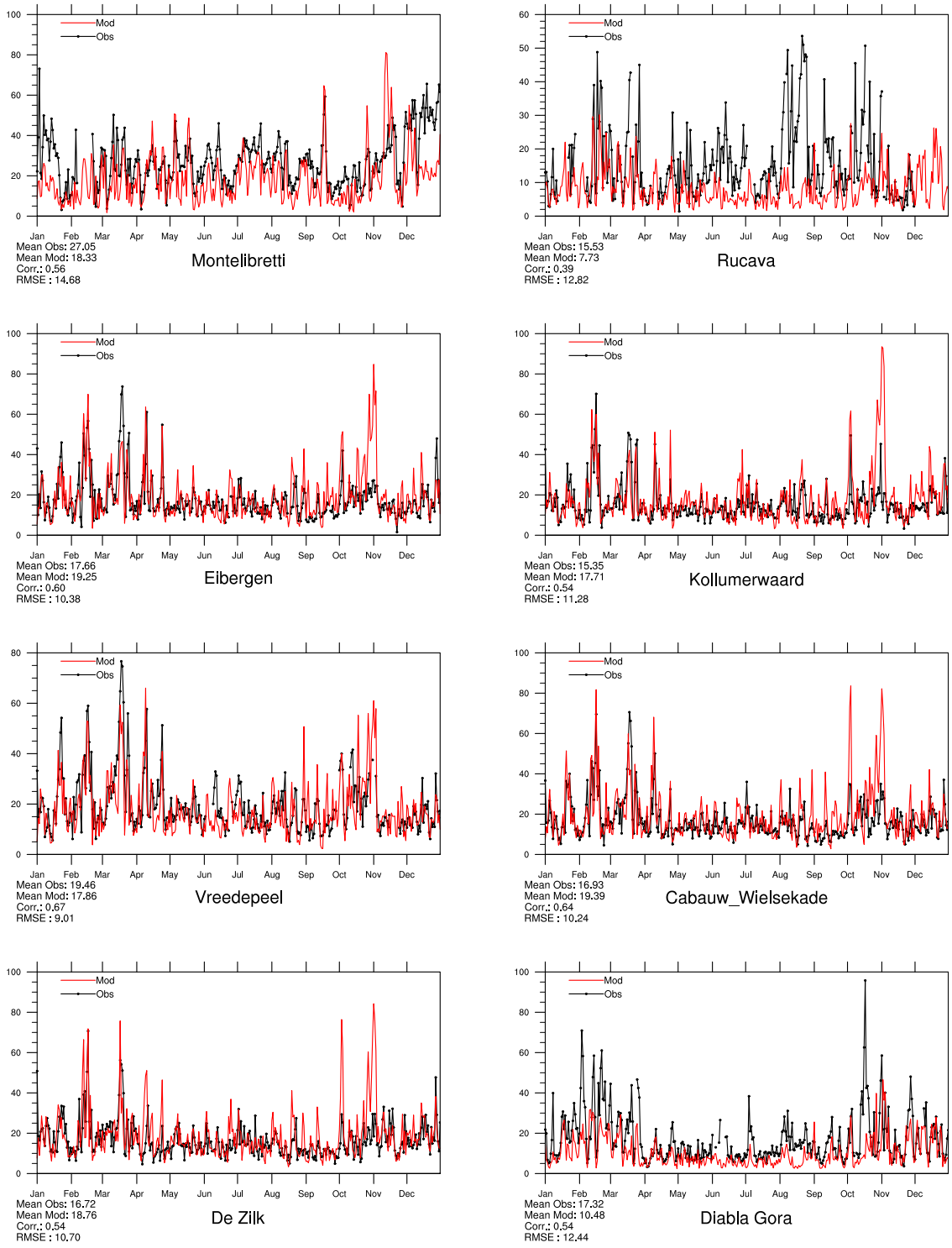

Figure 4.10: Modelled versus Observed Daily PM_{10} [μg m^{-3}] in 2015.

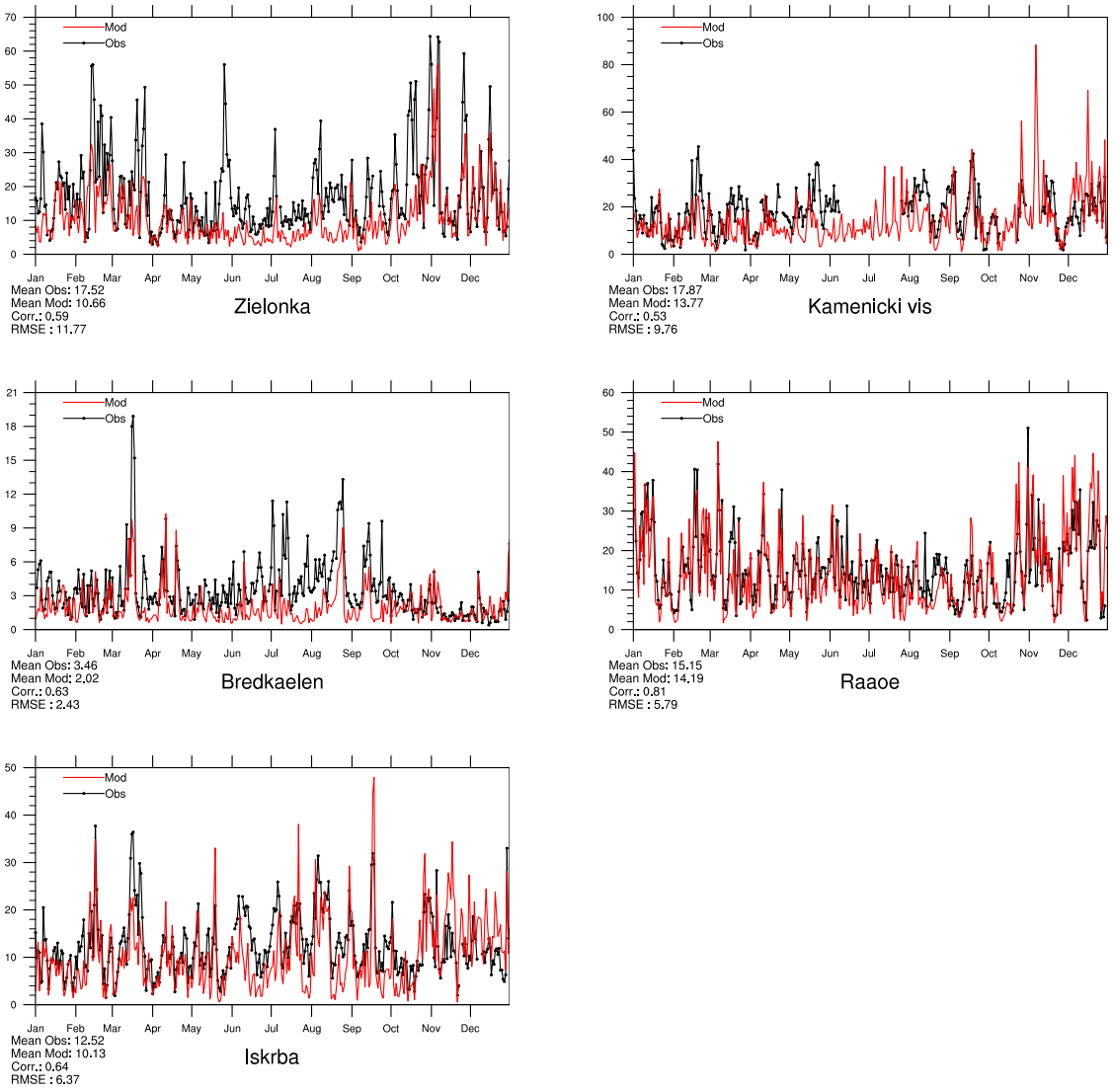

Figure 4.11: Modelled versus Observed Daily PM_{10} [μg m^{-3}] in 2015.

4.3 Combined maps of model results and observations

Combined maps of model results and observations have been produced for nitrogen- and sulphur-containing aerosols only. For details, see Section 2.3 in the chapter on acidifying and eutrophying components.